Synthetic Series-Symbol Data Generation for Time Series Foundation Models

Wenxuan Wang
School of Telecommunications Engineering
Xidian University
whenxuan@ieee.org

Kai Wu*
School of Artificial Intelligence
Xidian Univeristy
kwu@xidian.edu.cn

Yujian Betterest Li
School of Artificial Intelligence
Xidian University
bebetterest@outlook.com

Dan Wang*
School of Telecommunications Engineering
Xidian University
danwang@xidian.edu.cn

Xiaoyu Zhang
School of Cyber Engineering
Xidian University
xiaoyuzhang@xidian.edu.cn

Abstract

Foundation models for time series analysis (TSA) have attracted significant attention. However, challenges such as training data scarcity and imbalance continue to hinder their development. Inspired by complex dynamic system theories, we design a series-symbol data generation mechanism, enabling the unrestricted creation of high-quality time series data paired with corresponding symbolic expressions. To leverage series-symbol data pairs with strong correlations, we develop `SymTime`, a pre-trained foundation model for enhancing time series representation using symbolic information. `SymTime` demonstrates competitive performance across five major TSA tasks when fine-tunes with downstream tasks, rivaling foundation models pre-trained on real-world datasets. This approach underscores the potential of series-symbol data generation and pretraining mechanisms in overcoming data scarcity and enhancing task performance. The code is available at `https://github.com/wwhenxuan/SymTime`.

1 Introduction

In recent years, with the rapid advancement of deep learning, foundation models for time series analysis (TSA) have garnered widespread attention due to their superior generalization capabilities, scalability and advantages in few-shot learning [1, 2]. Coupled with issues of data privacy [3, 4], existing time series datasets are smaller compared to those in the fields of computer vision (CV) and natural language processing (NLP). Besides, current large-scale time series datasets face significant data imbalance issues, with certain types such as finance and healthcare still being relatively scarce (see Appendix B.4). According to scaling laws [5], this can lead to performance bias in the time series foundation models, reducing their generalization capabilities on out-of-distribution data [6, 7].

To mitigate the issue of training data scarcity and imbalance, this paper, starting from Takens' theorem [8, 9], posits that time series are representations of complex dynamical systems [10, 11, 12]. Based on

*Corresponding author

39th Conference on Neural Information Processing Systems (NeurIPS 2025).

symbolic dynamics [13], complex systems can be expressed abstractly using mathematical symbols and formulas [14], with ordinary differential equations (ODE) and partial differential equations (PDE) being the most common methods for modeling complex systems [15, 16]. In an ideal scenario, continuously constructing diverse symbolic expressions allows us to cover a broader range of complex dynamical systems. As a result, the time series generated from these symbolic expressions exhibit rich and varied properties. To this end, we provide a series-symbol (S^2) dual-modality data generation mechanism. Simulation experiments demonstrate that this approach effectively mitigates the problem of training data scarcity. To encapsulate our work, the contributions are as follows:

- **Addressing Data Scarcity:** Our approach overcomes the challenge of limited training data when building foundation models. The observation that the size of the S^2 dataset directly correlates with model performance on downstream tasks validates this point.
- **Introducing SymTime:** We present `SymTime`, a scalable and efficient foundation model for time series analysis that leverages symbolic information to enhance representations. Pretrained on the constructed S^2 dataset, `SymTime` offers broader task generality compared to existing foundation models that are typically limited to zero-shot forecasting.

2 Related Work

Pre-trained foundation models (PTFMs) [17, 18, 19, 20, 21] have been demonstrated to adapt to a variety of downstream tasks after fine-tuning on specific datasets, exhibiting excellent generalization and scalability [22, 23]. Inspired by this, recent years have seen significant progress in PTFMs for TSA [24, 25], with the emergence of various pre-training methods. Moirai, through masked time series modeling (MTM) and reconstruction [26, 27], has been pre-trained on large datasets ($27B$), yielding a universal forecasting model with zero-shot advantages [28]. Timer, after generative pre-training on large datasets ($1B$), has performed well in forecasting [29]. TimeGPT trained a encoder-decoder Transformer with $100B$ data [30]. COMET, using multi-level contrastive learning on a large ECG dataset, has obtained a medical time series PTFMs with few-shot advantages [4].

As discussed in Appendix B.4, these baseline models still face challenges related to data scarcity and data imbalance. In the next section, we introduce the proposed data generation mechanism and the corresponding dual-modality foundation model designed to mitigate these issues. The review of other topics can be found in Appendix D.

3 Main Methods

Definition 1 Time Series Foundation Model. *It is a deep neural network pre-trained in a self-supervised or unsupervised manner on large-scale, diverse time series data. By learning generalizable time series representations, it can then rapidly adapt—via few-shot or transfer learning—to efficiently solve a wide range of downstream time series tasks.*

Theorem 1 Takens' Theorem. *This theorem demonstrates that through phase space reconstruction [31, 32, 16, 33], a univariate time series, as a low-dimensional projection of a high-dimensional complex system, can completely preserve the dynamic topology of the original system, thereby forming an effective external representation of the complex system [8, 9, 34, 35, 36, 37, 38, 39].*

Theorem 2 Symbolic Dynamics. *This theory encodes the evolution of continuous systems into finite symbolic expressions by discretizing the state space of complex systems, establishing an isomorphic relationship between symbolic expressions and system behaviors [13, 41, 42, 43, 44]. This means that any complex system can be modeled using symbolic expressions [45, 46].*

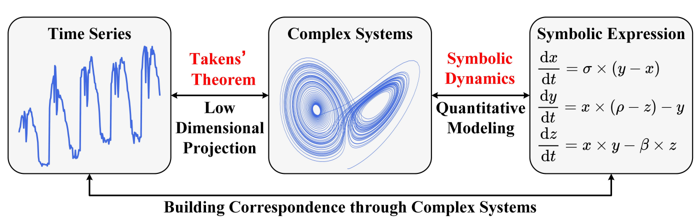

Figure 1: The connection between time series and symbolic expressions (taking the Lorentz system as an example) [40].

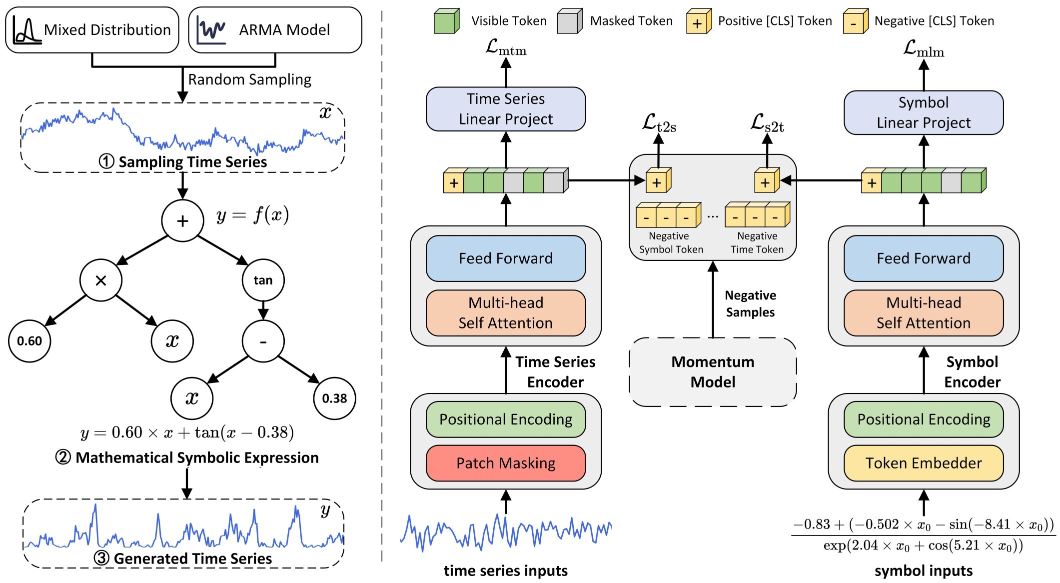

Figure 2: S^2 dataset generation mechanism (**left**) and `SymTime` network architecture (**right**).

As show in Figure 1, the two aforementioned theorems, using complex dynamical systems as a conceptual bridge, fundamentally connect time series and symbolic expressions. They provide rigorous theoretical support for the semantic correspondence between temporal patterns and symbolic representations. Compared with previous time series data generation methods [47, 22], the S^2 data generation mechanism proposed in this paper is more in line with the nature of time series generation.

3.1 Series-Symbol (S^2) Dataset Generation

The pre-training of `SymTime` relies on a large synthetic series-symbol (S^2) dataset[2]. The specific generation process is shown in Figure 2 (**left**). Firstly, we construct a multivariate input-output symbolic expression $f(\cdot)$ through random sampling [48]. Then, we use the randomly generated sampling series $X \in \mathbb{R}^{M \times L}$ to forward propagate through the symbolic expression to obtain the generated series $Y = f(X) \in \mathbb{R}^{N \times L}$, where N and M represent the dimensions of the input and output series respectively, and L is the length of the series. The mathematical symbols and their explanations in this section are shown in Table 9. In Appendix B.3, we present an analysis of the statistical characterization of the S^2 data. In Appendix B.7, we demonstrate that the time complexity of generating the S^2 data scales linearly with the series length L, approximating $\mathcal{O}(L)$.

3.1.1 Sampling of Functions

Mathematical expressions can usually be represented using a tree structure, where constants and variables are the root nodes, binary operators are nodes with two children, and unary operators are nodes with one child. Therefore, we (1) build a binary tree over input variables using binary operators, (2) randomly insert constants and variables into the tree, and (3) add unary operator and perform affine transformation. The three key steps are illustrated in Figure 3.

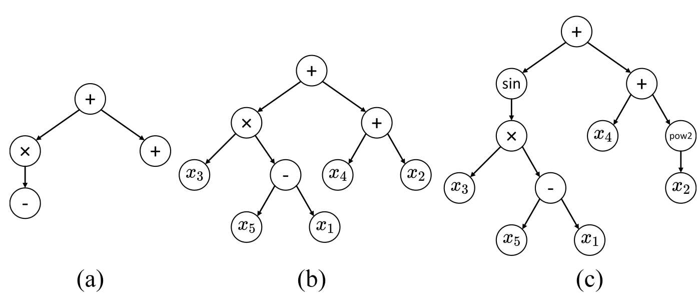

Figure 3: The process of building a binary tree when sampling symbolic expressions. (a) tree construction; (b) variable assignment to leaf nodes; (c) unary operator insertion.

[2]The code for S^2 data generation is available at `https://github.com/wwhenxuan/S2Generator`.

Input/Output Dimension Selection. Instead of randomly sampling input/output dimensions $M \sim \mathcal{U}(1, M_{\max})$ and $N \sim \mathcal{U}(1, N_{\max})$ as in prior work [12, 14, 49], we exhaustively traverse $M \in [1, M_{\max}], N \in [1, N_{\max}]$ (with $M_{\max} = 6$, $N_{\max} = 12$) to fully cover multivariate time series representations. An input dimension M defines M variable nodes $(x_1, \ldots, x_M)$, while the output dimension yields N generated series $y_i = f_i(x_1, \ldots, x_M), i = 1, \ldots, N$ [48].

Binary Operator Selection. We sample the number of binary operators $b \sim \mathcal{U}(b_{\min}, b_{\max})$ to define the root nodes of the expression tree. Each node's operator is then drawn uniformly from $\mathcal{U}\{+, -, \times\}$, enhancing the diversity and complexity of the generated expressions [14, 12, 45, 46].

Tree Construction and Leaf Assignment. We randomly combine the b binary operators to construct a binary tree to form the basic framework of the mathematical expressions (Figure 3a). Then, we randomly select m variables from the M set of variables $[x_1, \ldots, x_M]$ and insert them into the symbolic expression consisting of binary operators, where $m \sim \mathcal{U}(1, M)$ (Figure 3b). If the inserted expression does not form a full binary tree, a random constant node is added to make it full.

Unary Operator Insertion. After inserting the leaf nodes to form a complete binary tree, we select the number of unary operators u from $\mathcal{U}(u_{\min}, u_{\max})$ and insert unary operators at random positions in the binary tree. The available unary operators include $\{\mathrm{inv}, \mathrm{abs}, \mathrm{pow2}, \mathrm{pow3}, \mathrm{sqrt}, \sin, \cos, \tan, \arctan, \log, \exp\}$. This process is shown in Figure 3c. In Appendix B.8 we discussed the choice of unary operators.

Affine Transformation. To further diversify the symbolic expressions, we perform random affine transformations on each random variable x_d and unary operator u_d in the binary tree. Specifically, we replace x_d and u_d with $ax_d + b$ and $au_d + b$, respectively, where a and b are random constants [12, 14]. For example, $x_1 \to ax_1 + b$ and $\tan(\cdot) \to a\tan(\cdot) + b$ with contants a, b sampled randomly.

3.1.2 Generating Inputs and Outputs Series

After obtaining symbolic expressions f_i, we sample $X \in \mathbb{R}^{M \times L}$ from mixed distributions [12, 14, 48] and random-parameter ARMA(p, q) processes [50, 51], then compute $Y \in \mathbb{R}^{N \times L}, y_i = f_i(X)$. The ARMA($p$, q) model consists of moving average (MA) and autoregressive (AR) processes [52], which can be expressed as:

$$Y_t = \phi_1 Y_{t-1} + \phi_2 Y_{t-2} + \cdots + \phi_p Y_{t-p} + e_t - \theta_1 e_{t-1} - \theta_2 e_{t-2} - \cdots - \theta_q e_{t-q}, \tag{1}$$

where p and q represent the orders of the AR and MA models, respectively, ϕ_p and θ_q are the parameters of the AR and MA processes [51], and $e_t \sim \mathcal{N}(0, 1)$ denotes the observed white noise sequence. Since ARMA possess both the temporal correlation of the AR process and the randomness of the MA process, series obtained from mixed distributions and ARMA sampling better reflect the characteristics of time series.

Sampling Strategy. Each input series $X \in \mathbb{R}^{M \times L}$ is drawn either from a mixture of $k \sim \mathcal{U}(1, k_{\max})$ distributions (with weights $w_j \sim \mathcal{U}(0, 1)$ normalized to $\sum_j w_j = 1$, and each component chosen as $\mathcal{N}(\mu_j, \sigma_j^2)$, $\mu_j \sim \mathcal{N}(0, 1)$, $\sigma_j \sim \mathcal{U}(0, 1)$, or $\mathcal{U}(0, \mu_j)$) with probability $P \leq 0.5$, or from an ARMA(p, q) process ($p \sim \mathcal{U}(1, p_{\max})$, $q \sim \mathcal{U}(1, q_{\max})$, parameters $\phi_i, \theta_j \sim \mathcal{U}(-1, 1)$, and stationarity enforced by $\sum_i \phi_i < 1,\ |\phi_p| < 1$) otherwise.

Series Generation and Curation. We normalize each X per channel, compute $Y = f(X)$ via symbolic expressions, and discard any X outside f's domain or $|Y| > 10^4$ [12, 53]. For each random seed, we traverse all input/output channels, sampling each expression once. The resulting S^2 dataset contains $40M$ series–symbol pairs ($50B$ total length); series are patched for the time series encoder [54] and expressions tokenized for the symbolic encoder [55].

3.2 Model Architecture of `SymTime`

As shown in Figure 2 **(right)**, `SymTime` comprises a time series encoder, a symbol encoder, and momentum encoders, each trained with distinct objectives.

Time Series Encoder and Masked Time Series Modeling (MTM). An input time series is first divided into non-overlapping patches P=$\{p_1, p_2, \cdots, p_n\}$ using a sliding window approach [54, 17]. A 6-layer Transformer encodes non-overlapping patches P with random masking and reconstructs them via

$$\mathcal{L}_{\text{mtm}} = \frac{1}{|\mathbf{M}_T|} \sum_{j \in \mathbf{M}_T} \|p_j - \hat{p}_j\|^2, \tag{2}$$

where $\mathbf{M}_T$ is the set of masked patch indices, and $\hat{p}_j$ represents the patch reconstructed by the time series encoder and linear projection [56, 57]. Then, we obtain the corresponding embedded sequence T=$\{t_{\text{cls}}, t_1, t_2, \cdots, t_n\}$, where t_{cls} is the `[CLS]` token added by the time series encoder [58].

Symbolic Encoder and Masked Language Modeling (MLM). We treat symbolic expression data as natural language and use the 6-layer DistilBERT [55] as a symbol encoder to learn the representation of symbol through natural language mask modeling [19]. The loss optimized in this part is

$$\mathcal{L}_{\text{mlm}} = \frac{1}{|\mathbf{M}_S|} \sum_{j \in \mathbf{M}_S} \mathcal{H}\big(y_j,\, p_j^{\text{mask}}\big), \tag{3}$$

where $\mathbf{M}_S$ are masked symbol positions, $\mathcal{H}$ is cross-entropy loss, $p^{\text{mask}}(\hat{s})$ denote the model's predicted probability for the masked token $\hat{s}$, and y_j is a one-hot vocabulary distribution with a probability of **1** for the ground-truth token. Then, we obtain the embedded sequence: $S = \{s_{\text{cls}}, s_1, s_2, \ldots, s_m\}$, where s_{cls} is the `[CLS]` token added by the symbol encoder.

Series–Symbol Contrastive Learning. To leverage series-symbol data pairs with strong correlations (The correspondence between positive and negative samples is shown in Appendix C.2), we employ contrastive learning to enhance time series representation using symbolic information. Using momentum encoders [59], we project `[CLS]` embeddings via linear projections g_t, g_s and define $\text{sim}(t,s) = g_t(t_{\text{cls}})^\top g_s'(s_{\text{cls}}')$, where $g_s'(s_{\text{cls}}')$ is the normalized symbol features generated by the momentum model. Similarly, $\text{sim}(s,t) = g_s(s_{\text{cls}})^{\text{T}} g_t'(t_{\text{cls}}')$. We compute:

$$p^{t2s}(t) = \frac{\exp(\text{sim}(t, s_m)/\tau)}{\sum_m \exp(\text{sim}(t, s_m)/\tau)}, p^{s2t}(s) = \frac{\exp(\text{sim}(s, t_m)/\tau)}{\sum_m \exp(\text{sim}(s, t_m)/\tau)}, \tag{4}$$

where τ is a learnable temperature parameter [4, 59]. Let $y^{t2s}(t)$ and $y^{s2t}(s)$ represent the one-hot similarity, with positive pairs having a probability of **1** and negative pairs having **0** [59]. We optimize

$$\mathcal{L}_{\text{tsc}} = \tfrac{1}{2}\,\mathbb{E}\big[\mathcal{H}(y^{t2s}, p^{t2s}) + \mathcal{H}(y^{s2t}, p^{s2t})\big]. \tag{5}$$

3.3 Momentum Distillation for Masked Data Learning

Inspired by ALBEF [60], we treat random masking as noise and use momentum distillation to align the output representation of our encoder with its momentum counterpart. Let the similarity functions generated by the momentum encoders be $\text{sim}'(t,s) = g_t(t_{\text{cls}}')^{\text{T}} g_s(s_{\text{cls}}')$ and $\text{sim}'(s,t) = g_s(s_{\text{cls}}')^{\text{T}} g_t(t_{\text{cls}}')$. We compute soft pseudo targets $q^{t2s}(t)$ and $q^{s2t}(s)$ by replacing sim with sim$'$ in Equation 4. In addition to the contrastive loss $\mathcal{L}_{\text{tsc}}$ (Equation 5), we compute pseudo-targets q^{t2s}, q^{s2t} from momentum-encoder similarities sim$'$ and optimize

$$\mathcal{L}_{\text{tsc}}^{\text{mod}} = \tfrac{1}{2}\,\mathbb{E}\left[\mathbf{KL}\left(q^{t2s}(t) \| p^{t2s}(t)\right) + \mathbf{KL}\left(q^{s2t}(s) \| p^{s2t}(s)\right)\right]. \tag{6}$$

The total pre-training objective is

$$\mathcal{L} = \mathcal{L}_{\text{mtm}} + \mathcal{L}_{\text{mlm}} + \alpha\mathcal{L}_{\text{tsc}} + (1-\alpha)\mathcal{L}_{\text{tsc}}^{\text{mod}}. \tag{7}$$

3.4 Fine-tuning for Downstream Tasks

We use the pre-trained time series encoder as backbone. After instance normalization [61], we apply the following two strategies:

- **Classification:** patch the series, encode, and classify via a linear head [54, 62].
- **Reconstruction (forecasting, imputation, anomaly detection) [63, 64]:** decompose each series into trend and periodic components; regress trend directly, patch and encode the periodic part, then recombine for the final output.

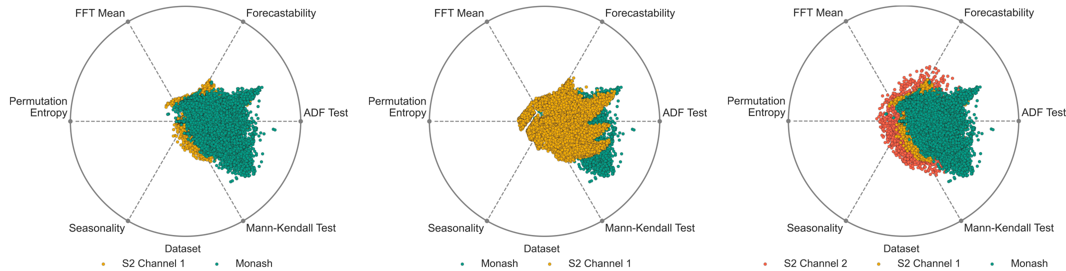

(a) $100K$ single input channel (b) $200K$ single input channel (c) $100K$ single and dual channel

Figure 4: Radviz visualization of S^2 and Monash datasets.

4 Experiments

We explore multiple representation measures and conduct experimental verification on a variety of downstream task datasets to answer the following key questions:

- **RQ1:** Can the unrestrictedly generated S^2 dataset comprehensively cover diverse representation types of time series data?
- **RQ2:** Can `SymTime` pre-trained on the S^2 dataset achieve competitive results across five major TSA tasks (forecasting, classification, imputation and anomaly detection)?
- **RQ3:** Can `SymTime` learn fundamental representations of time series data on the synthetic S^2 dataset to alleviate the data scarcity in TSA?
- **RQ4:** Are the multiple pre-training objectives in `SymTime` effective, and can symbol expressions enhance TSA task performance?
- **RQ5:** How to demonstrate that `SymTime` learns semantic information of symbols?

4.1 Statistical Characterization and Representation Coverage of S^2 Dataset (RQ1)

Target. We quantify the range of representations that the S^2 dataset can cover through statistical metrics (including stationarity (ADF Test) [65], forecastability [66], frequency domain (FFT mean), seasonality [67], trend (Mann-Kendall Test) [68] and prmutation entropy [69]) (See Appendix B.5 for full descriptions).

Setup. We use Radviz [70] to visualize high-dimensional statistical features of 256-length time series segments from our synthetic S^2 and the Monash datasets [71]. From Monash (covering weather, traffic, electricity, tourism, medicine, and energy) we sample $200K$ segments per domain. For S^2, we sample 100K single-channel segments (Figure 4a), then $200K$ single-channel segments (Figure 4b), and finally $100K$ mixed single- and dual-channel segments (Figure 4c).

Results. Radviz visualization confirms that S^2 closely matches the Monash dataset across key statistics (stationarity, predictability, frequency, complexity, seasonality, trend), validating its use for pretraining. Expanding from $100K$ to $200K$ samples further broadens S^2's coverage—surpassing Monash in some regions. Moreover, combining single- and dual-input samples dramatically increases diversity, as multi-variable expressions $f(x_1, \cdots, x_n)$ generate richer dynamics. These findings demonstrate that our infinitely scalable S^2 dataset covers the entire time series representation space.

4.2 Validation of `SymTime` in Five Time Series Analysis Tasks (RQ2)

Setup. We pre-trained `SymTime` on the $50B$-scale S^2 dataset using Equation 7 as the pre-training objective, with the model architecture detailed in Table 16. Then, we evaluate `SymTime` on five TSA tasks: long-term forecasting, short-term forecasting, classification, imputation and anomaly detection, using the TimesNet benchmark [72]. We use mean squared error (MSE) and mean absolute error (MAE) as the metrics for long-term forecasting and imputation tasks; overall weighted average (OWA) for short-term forecasting, which is unique metrics for M4 benchmark [73]; accuracy for classification; precision, recall and F1 score for anomaly detection. Detailed descriptions of datasets

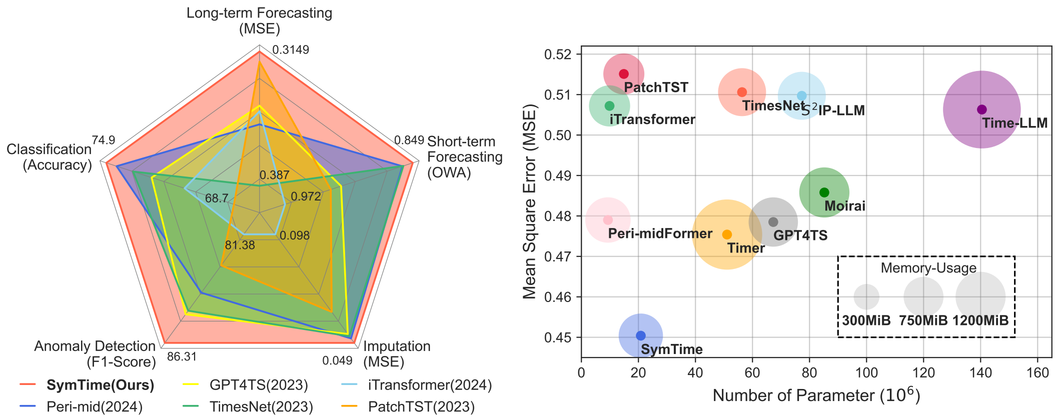

Figure 5: Model performance comparison with the state-of-the-art models in terms of five tasks (**left**). Complexity analysis on long time series forecasting tasks (ETTh1 dataset, forecasting length is 720 with 96 look-back windows) (**right**). Note that since the original backbone of Time-LLM [17] has too many parameters, we replaced it with GPT2 [94].

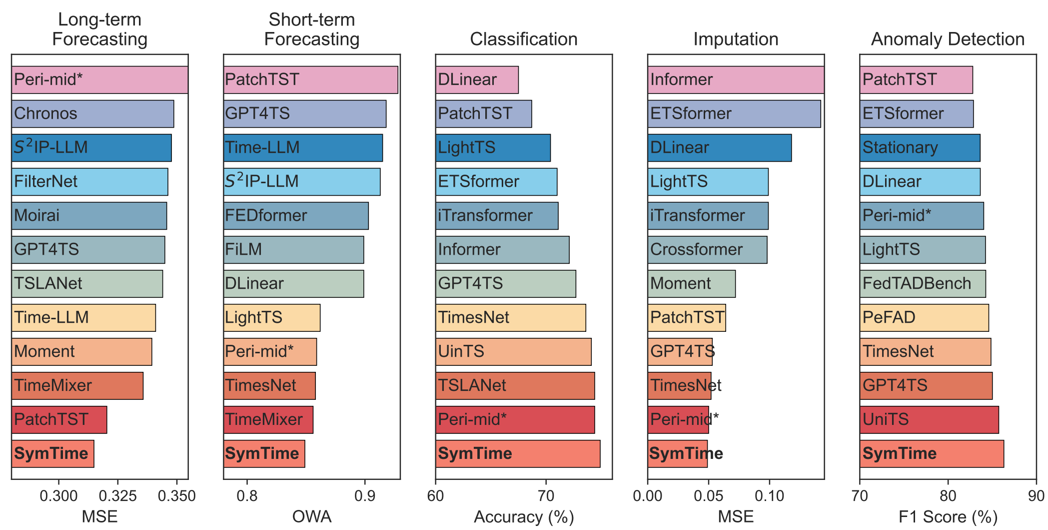

Figure 6: Validation of `SymTime` in 5 time series analysis tasks. We only show the average results of all datasets in this figure. See Appendix A for full results and analysis on different tasks. To ensure fair experimentation, we use the original model hyperparameters. For long-term prediction tasks, when a model is tested at multiple look-back windows, we select the best result.

and metrics for each task are provided in Appendix C.1 and C.3, while the pre-training and fine-tuning configurations for `SymTime` across downstream tasks are outlined in Appendix C.4 and C.5.

Baselines. We compare with various baselines including **Transformer-based models**: PatchTST [54], iTransformer [74], Autoformer [75], ETSformer [76], FEDformer [77], Non-stationary Transformer [78], Crossformer [79], Informer [80], Anomaly Transformer [81], Peri-midFormer [63]; **LLM-based models**: GPT4TS [2], Time-LLM [17], S^2IP-LLM [82]; **CNN-based models**: TimesNet [72], TSLANet [83], Rocket [84], InceptionTime (InTime) [85] and MICN [86]; **MLP-based models**: DLinear [87], LightTS [88], TimeMixer [89], FITS [90] and FilterNet [91]. We alse compare with the **pre-trained foundation models**: Moirai [28], Timer [29], UniTS [92] and Moment [93]. Some models can be applied to all 5 TSA tasks, while others are suitable for only one or some specific tasks. For those pre-trained foundation models, we first load their pre-trained parameters and then fine-tune them in the same way.

Main Results. Figure 5 **(left)** compares `SymTime` with models of the same type, while Figure 6 presents `SymTime`'s performance against additional models across different tasks. These results

Table 1: Fine-tuning results of on long-term forecasting tasks with different pre-training dataset sizes. See Appendix F.8 for full results. The look-back window length for all experiments is **96**. **Red**: best, Blue: second best.

Datasets	ETTm1		ETTm2		ETTh1		ETTh2		Weather		Electricity		Traffic		Exchange		Average	
Metrics	MSE	MAE	MSE	MAE	MSE	MAE	MSE	MAE	MSE	MAE	MSE	MAE	MSE	MAE	MSE	MAE	MSE	MAE
0B	0.401	0.409	0.293	0.339	0.487	0.474	0.376	0.412	0.257	0.289	0.193	0.284	0.471	0.310	0.383	0.415	0.358	0.366
1B	0.376	0.398	0.292	0.331	0.461	0.459	0.403	0.419	0.257	0.282	0.199	0.285	0.473	0.303	0.370	0.410	0.354	0.361
10B	0.376	0.393	0.281	0.329	0.444	0.444	0.376	0.408	0.250	0.279	0.196	0.286	0.473	0.294	0.368	0.407	0.345	0.355
25B	0.378	0.393	0.278	0.325	0.434	0.438	0.371	0.405	0.253	0.282	0.195	0.288	0.467	0.299	**0.357**	**0.401**	0.342	0.354
50B	**0.371**	**0.390**	**0.274**	**0.321**	**0.430**	**0.436**	**0.365**	**0.402**	**0.247**	**0.276**	**0.187**	**0.276**	**0.457**	**0.291**	0.359	**0.401**	**0.336**	**0.349**

Table 2: Fine-tuning results on short-term forecasting and imputation with different pre-training dataset sizes. See Appendix F.9 and F.11 for full results. **Red**: best, Blue: second best.

tasks	Short-term Time Series Forecasting					Time Series Imputation											
Datasets	Yearly	Quartly	Monthly	Others	Avg	ETTm1		ETTm2		ETTh1		ETTh2		ECL		Weather	
Metrics	Overall Weighted Average (OWA)					MSE	MAE	MSE	MAE	MSE	MAE	MSE	MAE	MSE	MAE	MSE	MAE
0B	**0.782**	0.913	0.964	1.097	0.887	0.042	0.122	0.038	0.106	0.112	0.230	0.065	0.160	0.058	0.155	0.036	0.053
1B	0.784	0.911	0.893	1.082	0.861	0.039	0.119	0.031	0.097	0.113	0.217	0.066	0.160	0.057	0.152	0.033	0.050
10B	0.783	0.905	0.896	1.055	0.859	0.038	0.119	0.030	0.095	0.107	0.213	0.063	0.158	0.056	**0.151**	0.033	0.048
25B	0.788	0.909	0.877	1.061	0.856	0.037	0.118	0.028	0.093	0.104	0.207	0.059	0.154	**0.055**	0.152	0.030	0.043
50B	0.786	**0.872**	**0.872**	**1.045**	**0.849**	**0.036**	**0.117**	**0.026**	**0.088**	**0.095**	**0.201**	**0.058**	**0.148**	**0.054**	**0.151**	**0.028**	**0.038**

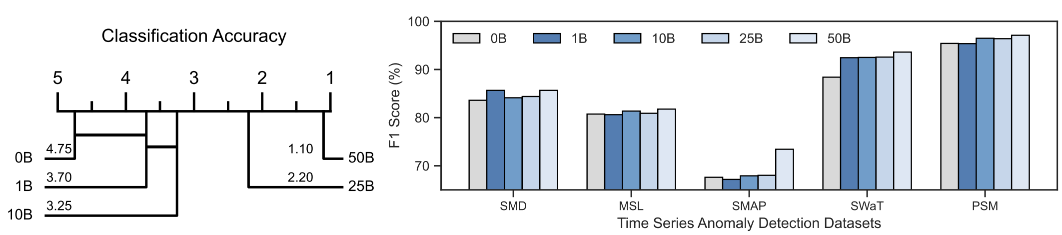

(a) Time Series Classification

(b) Time Series Anomaly Detection

Figure 7: Fine-tuning results of on classification and anomaly detection tasks with different pre-training dataset sizes. We use critical difference diagrams to measure the performance of classification in (a) [95], where the specific values represent the comprehensive ranking of the model on multiple datasets. See Appendix F.10 and F.12 for full results.

demonstrate that SymTime, pre-trained on the S^2 dataset, successfully learns fundamental representations of time series data and achieves competitive results when fine-tuned on downstream tasks. For each different task, the specific experimental settings and results are shown in: **long-term forecasting** (Appendix A.1), **short-term forecasting** (Appendix A.2), **classification** (Appendix A.3), **imputation** (Appendix A.4) and **anomaly detection** (Appendix A.5).

Complexity Analysis. We analyze the complexity of the model on the long-term forecasting ETTh1 dataset, with results shown in Figure 5 **(right)**. We consider the parameter count, the GPU memory required for forward and backward propagation when the batch size is 1, Using MSE as an evaluation metric, we find that SymTime achieves better performance with a smaller model parameter count and memory capacity than existing foundation models in forecasting task.

4.3 The Impact of Pre-training Dataset Size on SymTime Performance (RQ3)

Setup. Following the scaling laws of neural networks [6, 96], a large-scale and representationally comprehensive pre-training dataset is critical for building foundation models. In Section 3.1 and 4.1, we introduce and validate the unrestricted generation capability and comprehensive representational coverage of the S^2 dataset. Building on this, we proportionally divide the generated S^2 dataset into timestamp-based subsets $\{0B, 1B, 10B, 25B, 50B\}$ and pre-train SymTime under identical configurations. To evaluate the effectiveness of pre-training, we fine-tune the models on five major TSA tasks (with $0B$ denoting direct fine-tuning without pre-training). The experimental results are summarized in Tables 1, Table 2 and Figure 7.

Results. The results reveal a clear trend: as the scale of the pre-trained S^2 dataset increases, `SymTime` shows progressively enhanced performance across diverse downstream tasks. Furthermore, pre-trained `SymTime` significantly outperforms its non-pre-trained counterpart. Given the unrestricted generation capability and comprehensive representational coverage of our generation methods, the S^2 dataset can theoretically scale to infinite size, progressively enhancing `SymTime`'s downstream task performance through pre-training. This demonstrates that the proposed S^2 mechanism enables models to learn the representations of time series while effectively mitigating performance degradation caused by data scarcity and imbalanced distributions.

4.4 Ablation Study on Different Pre-training Objectives (RQ4)

Setup. We conduct ablation studies on `SymTime`'s pre-training objectives using the ETTh1 and ETTh2 long-term forecasting datasets [80]. First, we establish 8 different control groups based on whether pre-training is performed, freezing the model and various pre-training losses: (1) Freeze, (2) Real-Data, (3) w/o Pre-train, (4) w/o MTM, (5) w/o MLM, (6) w/o T2S, (7) w/o S2T, (8) w/o Symbol and (9) w/o Distill. Specific explanations for the above control groups are provided in Appendix C.6 (Real-Data means we use real time series data of the same scale to pre-train the time series encoder only through the MTM.). Then, We adopt MSE as the metric, load the pre-trained parameters from each ablation configuration, and conduct multiple fine-tuning trials with varied random seeds on the ETT dataset. The average results with error are shown in Figure 8.

Results. As shown in Figure 8, pre-training with standard configurations through Equation 7 significantly enhances `SymTime`'s long-term forecasting performance compared to control groups, demonstrating the validity of its pre-training objectives and the effectiveness of S^2 data generation. It is worth noting that, whether on real time series data (Real-Data) or on synthetic S^2 data (w/o Symbol), removing the symbol encoder part with contrastive learning and relying solely on MTM loss for temporal representation learning will degrade performance of `SymTime`. This suggests that semantic information provided by the symbolic encoder and series-symbol contrastive learning improves the temporal encoder's capability in long-term forecasting [97]. Similar findings are replicated in short-term forecasting tasks, as detailed in Appendix C.7.

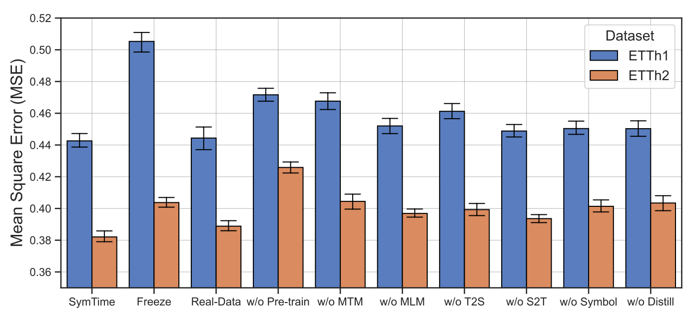

Figure 8: Ablation study on long-term forecasting task.

The Backbone in `SymTime`. There is a time series encoder with a Transformer architecture and a symbol encoder consisting of a pre-trained LLM in `SymTime`. In Appendix C.8, we perform ablation experiments on the model architecture by replacing the backbone of `SymTime`. The results are shown in Figure 18. It is clear that replacing the backbone has no significant impact on downstream tasks. The improvement in model performance mainly comes from the dual-modal pre-training paradigm of time series and symbolic expressions (Equation 7).

4.5 Series-Symbol Representation Learning (RQ5)

We further analyze the data representations learned by `SymTime` through masked modeling and cross-modal contrastive loss. Given that contrastive learning aligns mutually positive samples in the representation space [98, 59], we pre-train `SymTime` on the S^2 dataset and extract its time series encoder and symbol encoder. Using generated univariate time series and unary symbolic expressions, we examine whether the representation spaces of encoders evolve during pre-training. Additionally,

(a) without pre-training (b) with pre-training (c) without pre-training (d) with pre-training

Figure 9: The t-SNE visualization of time series encoder and symbol encoder in `SymTime` representation space with 50 perplexity. (a)(b) time series encoder; (c)(d) symbol encoder.

we specifically evaluate the time series encoder's proficiency in temporal representation learning. Results demonstrate that the time series encoder, pre-trained via large-scale masked modeling [54, 27], achieves zero-shot imputation capability on both the S^2 dataset and real-world time series data. Detailed experimental analyses are provided in Appendix B.6.

4.5.1 Time Series Encoder Representation

Setup. We sample $20K$ single-channels series–symbol pairs from S^2, with each time series labeled by one unary operator (e.g., inv, sin, log). After patching, the time series segments are encoded by time series encoder of `SymTime` with and without series-symbol contrastive pretraining. The output embeddings are reduced via t-SNE [99].

Results. As shown in Figure 9 (a)(b), The untrained encoder produces entangled clusters (aside from outliers like inv, exp), whereas the pretrained encoder forms clear, operator-specific clusters (trigonometric: sin, cos; polynomial: pow2, pow3, sqrt; etc.), confirming that contrastive learning aligns symbolic semantics with series representations. The change in representation space before and after pre-training also proves that the time series encoder has mastered the semantic information of symbolic expressions. Ablations show both contrastive losses are essential.

4.5.2 Symbol Encoder Representation

Setup. We also use $20K$ series-symbol pairs to verify the representation space change of the symbol encoder. First, we tokenize the symbolic expression. Then, we input it into the encoder to obtain its `[CLS]` token [18, 60] and visualize it using the t-SNE [99].

Results. As shown in Figure 9 (c)(d), similar to the time series encoder, the pre-trained DistilBERT-based symbol encoder initially struggles to distinguish between different types of symbol [55]. However, after pre-training with MLM and contrastive learning, the encoder forms distinct clusters in the representation space for symbolic expressions of the same type [12]. Furthermore, the paired time-series data and their corresponding symbolic expression exhibit similar clustering characteristics, as shown in Figure 9 (b) and (d). This demonstrates that cross-modal representation learning effectively brings semantically related data points closer together in the representation space.

5 Conclusion

To mitigate the challenges of data scarcity and distribution imbalance in time series analysis, we introduce a dual-modality series-symbol (S^2) data generation mechanism that enables the unrestricted creation of high-quality time series data, along with corresponding symbolic representations. Leveraging this large-scale series-symbol synthetic dataset, we propose `SymTime`, a pre-trained foundation model that integrates both time series representations and symbolic semantic information through masked modeling and contrastive learning. Our pre-trained model demonstrates exceptional performance across five major TSA tasks, highlighting the effectiveness of both our data generation strategy and pre-training methodology. Looking ahead, we aim to scale up our approach by training larger models on synthetic datasets, further boosting performance on downstream tasks.

Acknowledgement

This work was supported in part by Natural Science Basic Research Program of Shaanxi under Grant 2025JC-QYCX-060, in part by the National Natural Science Foundation of China under Grant 62206205, 62201419, 62472345, and 62471371, in part by the Young Talent Fund of Association for Science and Technology in Shaanxi, China under Grant 20230129, in part by the Guangdong High-level Innovation Research Institution Project under Grant 2021B0909050008, in part by the Guangzhou Key Research and Development Program under Grant 202206030003, and in part by the Fundamental Research Funds for the Central Universities under Grant QTZX25111. This research was supported by Huawei's Al Hundred Schools Program and was carried out using the Huawei Ascend AI technology stack.

References

[1] Shiyu Wang, Jiawei LI, Xiaoming Shi, Zhou Ye, Baichuan Mo, Wenze Lin, Ju Shengtong, Zhixuan Chu, and Ming Jin. Timemixer++: A general time series pattern machine for universal predictive analysis. In *The Thirteenth International Conference on Learning Representations*, 2025.

[2] Tian Zhou, Peisong Niu, Xue Wang, Liang Sun, and Rong Jin. One fits all: Power general time series analysis by pretrained LM. In *Thirty-seventh Conference on Neural Information Processing Systems*, 2023.

[3] Oluwatoyin Ajoke Farayola, Oluwabukunmi Latifat Olorunfemi, and Philip Olaseni Shoetan. Data privacy and security in it: a review of techniques and challenges. *Computer Science & IT Research Journal*, 5(3):606–615, 2024.

[4] Yihe Wang, Yu Han, Haishuai Wang, and Xiang Zhang. Contrast everything: A hierarchical contrastive framework for medical time-series. In *Thirty-seventh Conference on Neural Information Processing Systems*, 2023.

[5] Yasaman Bahri, Ethan Dyer, Jared Kaplan, Jaehoon Lee, and Utkarsh Sharma. Explaining neural scaling laws. *Proceedings of the National Academy of Sciences*, 121(27):e2311878121, 2024.

[6] Qingren Yao, Chao-Han Huck Yang, Renhe Jiang, Yuxuan Liang, Ming Jin, and Shirui Pan. Towards neural scaling laws for time series foundation models. In *The Thirteenth International Conference on Learning Representations*, 2025.

[7] Xiaoming Shi, Shiyu Wang, Yuqi Nie, Dianqi Li, Zhou Ye, Qingsong Wen, and Ming Jin. Time-moe: Billion-scale time series foundation models with mixture of experts. In *The Thirteenth International Conference on Learning Representations*, 2025.

[8] Floris Takens. Detecting strange attractors in turbulence. In David Rand and Lai-Sang Young, editors, *Dynamical Systems and Turbulence, Warwick 1980*, pages 366–381, Berlin, Heidelberg, 1981. Springer Berlin Heidelberg.

[9] Liangyue Cao. Practical method for determining the minimum embedding dimension of a scalar time series. *Physica D: Nonlinear Phenomena*, 110(1):43–50, 1997.

[10] Leo Torres, Ann S Blevins, Danielle Bassett, and Tina Eliassi-Rad. The why, how, and when of representations for complex systems. *SIAM Review*, 63(3):435–485, 2021.

[11] Yuanyuan Li, Kai Wu, and Jing Liu. Discover governing differential equations from evolving systems. *Physical Review Research*, 5:023126, May 2023.

[12] Kazem Meidani, Parshin Shojaee, Chandan Reddy, and Amir Barati Farimani. SNIP: Bridging mathematical symbolic and numeric realms with unified pre-training. In *NeurIPS 2023 AI for Science Workshop*, 2023.

[13] Bai lin Hao. Symbolic dynamics and characterization of complexity. *Physica D: Nonlinear Phenomena*, 51(1):161–176, 1991.

[14] Pierre-Alexandre Kamienny, Stéphane d'Ascoli, Guillaume Lample, and Francois Charton. End-to-end symbolic regression with transformers. In Alice H. Oh, Alekh Agarwal, Danielle Belgrave, and Kyunghyun Cho, editors, *Advances in Neural Information Processing Systems*, 2022.

[15] Charles R Doering. Modeling complex systems: Stochastic processes, stochastic differential equations, and fokker-planck equations. In *1990 Lectures in Complex Systems*, pages 3–52. CRC Press, 2018.

[16] Dirk Aeyels. Generic observability of differentiable systems. *SIAM Journal on Control and Optimization*, 19(5):595–603, 1981.

[17] Ming Jin, Shiyu Wang, Lintao Ma, Zhixuan Chu, James Y. Zhang, Xiaoming Shi, Pin-Yu Chen, Yuxuan Liang, Yuan-Fang Li, Shirui Pan, and Qingsong Wen. Time-LLM: Time series forecasting by reprogramming large language models. In *The Twelfth International Conference on Learning Representations*, 2024.

[18] Alec Radford, Jong Wook Kim, Chris Hallacy, Aditya Ramesh, Gabriel Goh, Sandhini Agarwal, Girish Sastry, Amanda Askell, Pamela Mishkin, Jack Clark, et al. Learning transferable visual models from natural language supervision. In *International conference on machine learning*, pages 8748–8763. PMLR, 2021.

[19] Jacob Devlin, Ming-Wei Chang, Kenton Lee, and Kristina Toutanova. Bert: Pre-training of deep bidirectional transformers for language understanding, 2019.

[20] Wenhui Wang, Hangbo Bao, Li Dong, Johan Bjorck, Zhiliang Peng, Qiang Liu, Kriti Aggarwal, Owais Khan Mohammed, Saksham Singhal, Subhojit Som, et al. Image as a foreign language: Beit pretraining for vision and vision-language tasks. In *Proceedings of the IEEE/CVF Conference on Computer Vision and Pattern Recognition*, pages 19175–19186, 2023.

[21] Kangning Cui, Rongkun Zhu, Manqi Wang, Wei Tang, Gregory D. Larsen, Victor P. Pauca, Sarra Alqahtani, Fan Yang, David Segurado, David A. Lutz, Jean-Michel Morel, and Miles R. Silman. Detection and geographic localization of natural objects in the wild: A case study on palms. In James Kwok, editor, *Proceedings of the Thirty-Fourth International Joint Conference on Artificial Intelligence, IJCAI-25*, pages 9601–9609. International Joint Conferences on Artificial Intelligence Organization, 8 2025. AI and Social Good.

[22] Abdul Fatir Ansari, Lorenzo Stella, Ali Caner Turkmen, Xiyuan Zhang, Pedro Mercado, Huibin Shen, Oleksandr Shchur, Syama Sundar Rangapuram, Sebastian Pineda Arango, Shubham Kapoor, Jasper Zschiegner, Danielle C. Maddix, Hao Wang, Michael W. Mahoney, Kari Torkkola, Andrew Gordon Wilson, Michael Bohlke-Schneider, and Bernie Wang. Chronos: Learning the language of time series. *Transactions on Machine Learning Research*, 2024. Expert Certification.

[23] Xiwen Chen, Peijie Qiu, Wenhui Zhu, Huayu Li, Hao Wang, Aristeidis Sotiras, Yalin Wang, and Abolfazl Razi. TimeMIL: Advancing multivariate time series classification via a time-aware multiple instance learning. In *Forty-first International Conference on Machine Learning*, 2024.

[24] Sabeen Ahmed, Ian E Nielsen, Aakash Tripathi, Shamoon Siddiqui, Ravi P Ramachandran, and Ghulam Rasool. Transformers in time-series analysis: A tutorial. *Circuits, Systems, and Signal Processing*, 42(12):7433–7466, 2023.

[25] Yuxuan Liang, Haomin Wen, Yuqi Nie, Yushan Jiang, Ming Jin, Dongjin Song, Shirui Pan, and Qingsong Wen. Foundation models for time series analysis: A tutorial and survey. In *Proceedings of the 30th ACM SIGKDD Conference on Knowledge Discovery and Data Mining*, pages 6555–6565, 2024.

[26] Shubao Zhao, Ming Jin, Zhaoxiang Hou, Chengyi Yang, Zengxiang Li, Qingsong Wen, and Yi Wang. Himtm: Hierarchical multi-scale masked time series modeling with self-distillation for long-term forecasting. In *Proceedings of the 33rd ACM International Conference on Information and Knowledge Management*, pages 3352–3362, 2024.

[27] Jiaxiang Dong, Haixu Wu, Haoran Zhang, Li Zhang, Jianmin Wang, and Mingsheng Long. SimMTM: A simple pre-training framework for masked time-series modeling. In *Thirty-seventh Conference on Neural Information Processing Systems*, 2023.

[28] Gerald Woo, Chenghao Liu, Akshat Kumar, Caiming Xiong, Silvio Savarese, and Doyen Sahoo. Unified training of universal time series forecasting transformers. In *Forty-first International Conference on Machine Learning*, 2024.

[29] Yong Liu, Haoran Zhang, Chenyu Li, Xiangdong Huang, Jianmin Wang, and Mingsheng Long. Timer: Generative pre-trained transformers are large time series models. In *Forty-first International Conference on Machine Learning*, 2024.

[30] Azul Garza, Cristian Challu, and Max Mergenthaler-Canseco. Timegpt-1, 2024.

[31] Matthew B. Kennel, Reggie Brown, and Henry D. I. Abarbanel. Determining embedding dimension for phase-space reconstruction using a geometrical construction. *Phys. Rev. A*, 45:3403–3411, Mar 1992.

[32] Khaled Sayed, Mahmoud Kamel, Mohammed Alhaddad, Hussein M. Malibary, and Yasser M. Kadah. Characterization of phase space trajectories for brain-computer interface. *Biomedical Signal Processing and Control*, 38:55–66, 2017.

[33] N. H. Packard, J. P. Crutchfield, J. D. Farmer, and R. S. Shaw. Geometry from a time series. *Phys. Rev. Lett.*, 45:712–716, Sep 1980.

[34] Andrew M. Fraser and Harry L. Swinney. Independent coordinates for strange attractors from mutual information. *Phys. Rev. A*, 33:1134–1140, Feb 1986.

[35] Sara P. Garcia and Jonas S. Almeida. Nearest neighbor embedding with different time delays. *Phys. Rev. E*, 71:037204, Mar 2005.

[36] Tao Wu, Xiangyun Gao, Feng An, Xiaotian Sun, Haizhong An, Zhen Su, Shraddha Gupta, Jianxi Gao, and Jürgen Kurths. Predicting multiple observations in complex systems through low-dimensional embeddings. *Nature Communications*, 15(1):2242, 2024.

[37] Zeyu Li, Wang Han, Yue Zhang, Qingfei Fu, Jingxuan Li, Lizi Qin, Ruoyu Dong, Hao Sun, Yue Deng, and Lijun Yang. Learning spatiotemporal dynamics with a pretrained generative model. *Nature Machine Intelligence*, 6(12):1566–1579, 2024.

[38] Cosma Rohilla Shalizi. *Methods and Techniques of Complex Systems Science: An Overview*, pages 33–114. Springer US, Boston, MA, 2006.

[39] Krzysztof Barański, Yonatan Gutman, and Adam Śpiewak. A probabilistic takens theorem. *Nonlinearity*, 33(9):4940, jul 2020.

[40] N. V. Kuznetsov, T. N. Mokaev, O. A. Kuznetsova, et al. The lorenz system: hidden boundary of practical stability and the lyapunov dimension. *Nonlinear Dynamics*, 102:713–732, 2020.

[41] George Sugihara and Robert M. May. Nonlinear forecasting as a way of distinguishing chaos from measurement error in time series. *Nature*, 344:734–741, 1990.

[42] B. R. R. Boaretto, R. C. Budzinski, K. L. Rossi, et al. Discriminating chaotic and stochastic time series using permutation entropy and artificial neural networks. *Scientific Reports*, 11:15789, 2021.

[43] E. Tan, S. D. Algar, D. Corrêa, et al. Network representations of attractors for change point detection. *Communications Physics*, 6:340, 2023.

[44] B.-W. Shen. Nonlinear feedback in a six-dimensional lorenz model: impact of an additional heating term. *Nonlinear Processes in Geophysics*, 22(6):749–764, 2015.

[45] Marco Virgolin, Tanja Alderliesten, Cees Witteveen, and Peter AN Bosman. Improving model-based genetic programming for symbolic regression of small expressions. *Evolutionary computation*, 29(2):211–237, 2021.

[46] F. O. de Franca and G. S. I. Aldeia. Interaction–transformation evolutionary algorithm for symbolic regression. *Evolutionary Computation*, 29(3):367–390, 09 2021.

[47] Samuel Dooley, Gurnoor Singh Khurana, Chirag Mohapatra, Siddartha Venkat Naidu, and Colin White. ForecastPFN: Synthetically-trained zero-shot forecasting. In *Thirty-seventh Conference on Neural Information Processing Systems*, 2023.

[48] Guillaume Lample and François Charton. Deep learning for symbolic mathematics. In *International Conference on Learning Representations*, 2020.

[49] Uri Alon, Frank F. Xu, Junxian He, Sudipta Sengupta, Dan Roth, and Graham Neubig. Neuro-symbolic language modeling with automaton-augmented retrieval. In *ICML 2022 Workshop on Knowledge Retrieval and Language Models*, 2022.

[50] Robert Lund and. Time series analysis and its applications: With r examples. *Journal of the American Statistical Association*, 102(479):1079–1079, 2007.

[51] Pasapitch Chujai, Nittaya Kerdprasop, and Kittisak Kerdprasop. Time series analysis of household electric consumption with arima and arma models. In *Proceedings of the international multiconference of engineers and computer scientists*, volume 1, pages 295–300, 2013.

[52] Paul Newbold. Arima model building and the time series analysis approach to forecasting. *Journal of forecasting*, 2(1):23–35, 1983.

[53] Chen Xu, Hanyang Jiang, and Yao Xie. Conformal prediction for multi-dimensional time series by ellipsoidal sets. In *Forty-first International Conference on Machine Learning*, 2024.

[54] Yuqi Nie, Nam H Nguyen, Phanwadee Sinthong, and Jayant Kalagnanam. A time series is worth 64 words: Long-term forecasting with transformers. In *The Eleventh International Conference on Learning Representations*, 2023.

[55] Victor Sanh, Lysandre Debut, Julien Chaumond, and Thomas Wolf. Distilbert, a distilled version of bert: smaller, faster, cheaper and lighter, 2020.

[56] Shengsheng Lin, Weiwei Lin, Wentai Wu, Haojun Chen, and Junjie Yang. SparseTSF: Modeling long-term time series forecasting with *1k* parameters. In *Forty-first International Conference on Machine Learning*, 2024.

[57] Wenzhen Yue, Yong Liu, Haoxuan Li, Hao Wang, Xianghua Ying, Ruohao Guo, Bowei Xing, and Ji Shi. Olinear: A linear model for time series forecasting in orthogonally transformed domain, 2025.

[58] Alexey Dosovitskiy, Lucas Beyer, Alexander Kolesnikov, Dirk Weissenborn, Xiaohua Zhai, Thomas Unterthiner, Mostafa Dehghani, Matthias Minderer, Georg Heigold, Sylvain Gelly, Jakob Uszkoreit, and Neil Houlsby. An image is worth 16x16 words: Transformers for image recognition at scale. In *International Conference on Learning Representations*, 2021.

[59] Kaiming He, Haoqi Fan, Yuxin Wu, Saining Xie, and Ross Girshick. Momentum contrast for unsupervised visual representation learning. In *Proceedings of the IEEE/CVF conference on computer vision and pattern recognition*, pages 9729–9738, 2020.

[60] Junnan Li, Ramprasaath R. Selvaraju, Akhilesh Deepak Gotmare, Shafiq Joty, Caiming Xiong, and Steven Hoi. Align before fuse: Vision and language representation learning with momentum distillation. In A. Beygelzimer, Y. Dauphin, P. Liang, and J. Wortman Vaughan, editors, *Advances in Neural Information Processing Systems*, 2021.

[61] Taesung Kim, Jinhee Kim, Yunwon Tae, Cheonbok Park, Jang-Ho Choi, and Jaegul Choo. Reversible instance normalization for accurate time-series forecasting against distribution shift. In *International Conference on Learning Representations*, 2022.

[62] Yuxuan Wang, Haixu Wu, Jiaxiang Dong, Guo Qin, Haoran Zhang, Yong Liu, Yun-Zhong Qiu, Jianmin Wang, and Mingsheng Long. Timexer: Empowering transformers for time series forecasting with exogenous variables. In *The Thirty-eighth Annual Conference on Neural Information Processing Systems*, 2024.

[63] Qiang Wu, Gechang Yao, Zhixi Feng, and Shuyuan Yang. Peri-midformer: Periodic pyramid transformer for time series analysis. In *The Thirty-eighth Annual Conference on Neural Information Processing Systems*, 2024.

[64] Wenzhen Yue, Xianghua Ying, Ruohao Guo, DongDong Chen, Ji Shi, Bowei Xing, Yuqing Zhu, and Taiyan Chen. Sub-adjacent transformer: Improving time series anomaly detection with reconstruction error from sub-adjacent neighborhoods, 2024.

[65] Graham Elliott, Thomas J Rothenberg, and James H Stock. Efficient tests for an autoregressive unit root, 1992.

[66] Georg Goerg. Forecastable component analysis. In Sanjoy Dasgupta and David McAllester, editors, *Proceedings of the 30th International Conference on Machine Learning*, volume 28 of *Proceedings of Machine Learning Research*, pages 64–72, Atlanta, Georgia, USA, 17–19 Jun 2013. PMLR.

[67] Robert B Cleveland, William S Cleveland, Jean E McRae, Irma Terpenning, et al. Stl: A seasonal-trend decomposition. *J. off. Stat*, 6(1):3–73, 1990.

[68] Sylvia R Esterby. Review of methods for the detection and estimation of trends with emphasis on water quality applications. *Hydrological processes*, 10(2):127–149, 1996.

[69] Yinhe Cao, Wen-wen Tung, J. B. Gao, V. A. Protopopescu, and L. M. Hively. Detecting dynamical changes in time series using the permutation entropy. *Physical Review E*, 70(4):046217, 2004.

[70] Fangfang Zhou, Minghui Chen, Zeyu Wang, Feng Luo, Xiaobo Luo, Wei Huang, Yi Chen, and Ying Zhao. A radviz-based visualization for understanding fuzzy clustering results. In *Proceedings of the 10th International Symposium on Visual Information Communication and Interaction*, VINCI '17, page 9–15, New York, NY, USA, 2017. Association for Computing Machinery.

[71] Rakshitha Wathsadini Godahewa, Christoph Bergmeir, Geoffrey I. Webb, Rob Hyndman, and Pablo Montero-Manso. Monash time series forecasting archive. In *Thirty-fifth Conference on Neural Information Processing Systems Datasets and Benchmarks Track (Round 2)*, 2021.

[72] Haixu Wu, Tengge Hu, Yong Liu, Hang Zhou, Jianmin Wang, and Mingsheng Long. Timesnet: Temporal 2d-variation modeling for general time series analysis. In *The Eleventh International Conference on Learning Representations*, 2023.

[73] Spyros Makridakis. M4 dataset, 2018.

[74] Yong Liu, Tengge Hu, Haoran Zhang, Haixu Wu, Shiyu Wang, Lintao Ma, and Mingsheng Long. itransformer: Inverted transformers are effective for time series forecasting. In *The Twelfth International Conference on Learning Representations*, 2024.

[75] Haixu Wu, Jiehui Xu, Jianmin Wang, and Mingsheng Long. Autoformer: Decomposition transformers with auto-correlation for long-term series forecasting. In A. Beygelzimer, Y. Dauphin, P. Liang, and J. Wortman Vaughan, editors, *Advances in Neural Information Processing Systems*, 2021.

[76] Gerald Woo, Chenghao Liu, Doyen Sahoo, Akshat Kumar, and Steven Hoi. ETSformer: Exponential smoothing transformers for time-series forecasting, 2023.

[77] Tian Zhou, Ziqing Ma, Qingsong Wen, Xue Wang, Liang Sun, and Rong Jin. Fedformer: Frequency enhanced decomposed transformer for long-term series forecasting. In *International conference on machine learning*, pages 27268–27286. PMLR, 2022.

[78] Yong Liu, Haixu Wu, Jianmin Wang, and Mingsheng Long. Non-stationary transformers: Exploring the stationarity in time series forecasting. In Alice H. Oh, Alekh Agarwal, Danielle Belgrave, and Kyunghyun Cho, editors, *Advances in Neural Information Processing Systems*, 2022.

[79] Yunhao Zhang and Junchi Yan. Crossformer: Transformer utilizing cross-dimension dependency for multivariate time series forecasting. In *The Eleventh International Conference on Learning Representations*, 2023.

[80] Haoyi Zhou, Shanghang Zhang, Jieqi Peng, Shuai Zhang, Jianxin Li, Hui Xiong, and Wancai Zhang. Informer: Beyond efficient transformer for long sequence time-series forecasting. In *Proceedings of the AAAI conference on artificial intelligence*, volume 35, pages 11106–11115, 2021.

[81] Jiehui Xu, Haixu Wu, Jianmin Wang, and Mingsheng Long. Anomaly transformer: Time series anomaly detection with association discrepancy, 2022.

[82] Zijie Pan, Yushan Jiang, Sahil Garg, Anderson Schneider, Yuriy Nevmyvaka, and Dongjin Song. s^2IP-LLM: Semantic space informed prompt learning with LLM for time series forecasting. In *Forty-first International Conference on Machine Learning*, 2024.

[83] Emadeldeen Eldele, Mohamed Ragab, Zhenghua Chen, Min Wu, and Xiaoli Li. Tslanet: Rethinking transformers for time series representation learning. In *ICML*, 2024.

[84] Angus Dempster, François Petitjean, and Geoffrey I Webb. Rocket: exceptionally fast and accurate time series classification using random convolutional kernels. *Data Mining and Knowledge Discovery*, 34(5):1454–1495, 2020.

[85] Hassan Ismail Fawaz, Benjamin Lucas, Germain Forestier, Charlotte Pelletier, Daniel F Schmidt, Jonathan Weber, Geoffrey I Webb, Lhassane Idoumghar, Pierre-Alain Muller, and François Petitjean. Inceptiontime: Finding alexnet for time series classification. *Data Mining and Knowledge Discovery*, 34(6):1936–1962, 2020.

[86] Huiqiang Wang, Jian Peng, Feihu Huang, Jince Wang, Junhui Chen, and Yifei Xiao. MICN: Multi-scale local and global context modeling for long-term series forecasting. In *The Eleventh International Conference on Learning Representations*, 2023.

[87] Ailing Zeng, Muxi Chen, Lei Zhang, and Qiang Xu. Are transformers effective for time series forecasting? In *Proceedings of the Thirty-Seventh AAAI Conference on Artificial Intelligence*, AAAI'23/IAAI'23/EAAI'23. AAAI Press, 2023.

[88] Tianping Zhang, Yizhuo Zhang, Wei Cao, Jiang Bian, Xiaohan Yi, Shun Zheng, and Jian Li. Less is more: Fast multivariate time series forecasting with light sampling-oriented mlp structures, 2022.

[89] Shiyu Wang, Haixu Wu, Xiaoming Shi, Tengge Hu, Huakun Luo, Lintao Ma, James Y. Zhang, and JUN ZHOU. Timemixer: Decomposable multiscale mixing for time series forecasting. In *The Twelfth International Conference on Learning Representations*, 2024.

[90] Zhijian Xu, Ailing Zeng, and Qiang Xu. FITS: Modeling time series with $10k$ parameters. In *The Twelfth International Conference on Learning Representations*, 2024.

[91] Kun Yi, Jingru Fei, Qi Zhang, Hui He, Shufeng Hao, Defu Lian, and Wei Fan. Filternet: Harnessing frequency filters for time series forecasting. In *The Thirty-eighth Annual Conference on Neural Information Processing Systems*, 2024.

[92] Shanghua Gao, Teddy Koker, Owen Queen, Thomas Hartvigsen, Theodoros Tsiligkaridis, and Marinka Zitnik. UniTS: A unified multi-task time series model. In *The Thirty-eighth Annual Conference on Neural Information Processing Systems*, 2024.

[93] Mononito Goswami, Konrad Szafer, Arjun Choudhry, Yifu Cai, Shuo Li, and Artur Dubrawski. MOMENT: A family of open time-series foundation models. In *Forty-first International Conference on Machine Learning*, 2024.

[94] Alec Radford, Jeffrey Wu, Rewon Child, David Luan, Dario Amodei, Ilya Sutskever, et al. Language models are unsupervised multitask learners. *OpenAI blog*, 1(8):9, 2019.

[95] Hassan Ismail Fawaz, Germain Forestier, Jonathan Weber, Lhassane Idoumghar, and Pierre-Alain Muller. Deep learning for time series classification: a review. *Data mining and knowledge discovery*, 33(4):917–963, 2019.

[96] Jared Kaplan, Sam McCandlish, Tom Henighan, Tom B. Brown, Benjamin Chess, Rewon Child, Scott Gray, Alec Radford, Jeffrey Wu, and Dario Amodei. Scaling laws for neural language models, 2020.

[97] Yong Liu, Guo Qin, Xiangdong Huang, Jianmin Wang, and Mingsheng Long. Autotimes: Autoregressive time series forecasters via large language models. In *The Thirty-eighth Annual Conference on Neural Information Processing Systems*, 2024.

[98] Ting Chen, Simon Kornblith, Mohammad Norouzi, and Geoffrey Hinton. A simple framework for contrastive learning of visual representations. In *Proceedings of the 37th International Conference on Machine Learning*, ICML'20, 2020.

[99] Martin Wattenberg, Fernanda Viégas, and Ian Johnson. How to use t-sne effectively. *Distill*, 2016.

[100] Yong Liu, Guo Qin, Xiangdong Huang, Jianmin Wang, and Mingsheng Long. Timer-xl: Long-context transformers for unified time series forecasting. In *The Thirteenth International Conference on Learning Representations*, 2025.

[101] Wetterstation. Weather. `https://www.bgc-jena.mpg.de/wetter/`.

[102] UCI. Electricity. `https://archive.ics.uci.edu/ml/datasets/ElectricityLoadDiagrams20112014`.

[103] PeMS. Traffic. `http://pems.dot.ca.gov/`.

[104] Guokun Lai, Wei-Cheng Chang, Yiming Yang, and Hanxiao Liu. Modeling long- and short-term temporal patterns with deep neural networks. In *The 41st International ACM SIGIR Conference on Research & Development in Information Retrieval*, SIGIR '18, page 95–104, New York, NY, USA, 2018. Association for Computing Machinery.

[105] Anthony Bagnall, Hoang Anh Dau, Jason Lines, Michael Flynn, James Large, Aaron Bostrom, Paul Southam, and Eamonn Keogh. The uea multivariate time series classification archive, 2018, 2018.

[106] Ya Su, Youjian Zhao, Chenhao Niu, Rong Liu, Wei Sun, and Dan Pei. Robust anomaly detection for multivariate time series through stochastic recurrent neural network. KDD '19, page 2828–2837, New York, NY, USA, 2019. Association for Computing Machinery.

[107] Kyle Hundman, Valentino Constantinou, Christopher Laporte, Ian Colwell, and Tom Soderstrom. Detecting spacecraft anomalies using lstms and nonparametric dynamic thresholding. KDD '18, page 387–395, New York, NY, USA, 2018. Association for Computing Machinery.

[108] Aditya P. Mathur and Nils Ole Tippenhauer. Swat: a water treatment testbed for research and training on ics security. In *2016 International Workshop on Cyber-physical Systems for Smart Water Networks (CySWater)*, pages 31–36, 2016.

[109] Ahmed Abdulaal, Zhuanghua Liu, and Tomer Lancewicki. Practical approach to asynchronous multivariate time series anomaly detection and localization. In *Proceedings of the 27th ACM SIGKDD Conference on Knowledge Discovery & Data Mining*, KDD '21, page 2485–2494, New York, NY, USA, 2021. Association for Computing Machinery.

[110] Javier Selva, Anders S Johansen, Sergio Escalera, Kamal Nasrollahi, Thomas B Moeslund, and Albert Clapés. Video transformers: A survey. *IEEE Transactions on Pattern Analysis and Machine Intelligence*, 45(11):12922–12943, 2023.

[111] Chengsen Wang, Qi Qi, Jingyu Wang, Haifeng Sun, Zirui Zhuang, Jinming Wu, Lei Zhang, and Jianxin Liao. Chattime: A unified multimodal time series foundation model bridging numerical and textual data, 2024.

[112] Kaiming He, Xinlei Chen, Saining Xie, Yanghao Li, Piotr Dollár, and Ross Girshick. Masked autoencoders are scalable vision learners. In *Proceedings of the IEEE/CVF conference on computer vision and pattern recognition*, pages 16000–16009, 2022.

[113] Kai Wu, Yujian Betterest Li, Jian Lou, Xiaoyu Zhang, Handing Wang, and Jing Liu. Rapid plug-in defenders. In *The Thirty-eighth Annual Conference on Neural Information Processing Systems*, 2024.

[114] Armen Aghajanyan, Lili Yu, Alexis Conneau, Wei-Ning Hsu, Karen Hambardzumyan, Susan Zhang, Stephen Roller, Naman Goyal, Omer Levy, and Luke Zettlemoyer. Scaling laws for generative mixed-modal language models. In Andreas Krause, Emma Brunskill, Kyunghyun Cho, Barbara Engelhardt, Sivan Sabato, and Jonathan Scarlett, editors, *Proceedings of the 40th International Conference on Machine Learning*, volume 202 of *Proceedings of Machine Learning Research*, pages 265–279. PMLR, 23–29 Jul 2023.

[115] Yi Xiao, LEI BAI, Wei Xue, Hao Chen, Kun Chen, kang chen, Tao Han, and Wanli Ouyang. Towards a self-contained data-driven global weather forecasting framework. In *Forty-first International Conference on Machine Learning*, 2024.

[116] Che Liu, Zhongwei Wan, Cheng Ouyang, Anand Shah, Wenjia Bai, and Rossella Arcucci. Zero-shot ECG classification with multimodal learning and test-time clinical knowledge enhancement. In *Forty-first International Conference on Machine Learning*, 2024.

[117] Carmen Martin Turrero, Maxence Bouvier, Manuel Breitenstein, Pietro Zanuttigh, and Vincent Parret. ALERT-transformer: Bridging asynchronous and synchronous machine learning for real-time event-based spatio-temporal data. In *Forty-first International Conference on Machine Learning*, 2024.

[118] Andrea Cini, Danilo Mandic, and Cesare Alippi. Graph-based time series clustering for end-to-end hierarchical forecasting. In *Forty-first International Conference on Machine Learning*, 2024.

[119] Jiaxiang Dong, Haixu Wu, Yuxuan Wang, Yun-Zhong Qiu, Li Zhang, Jianmin Wang, and Mingsheng Long. Timesiam: A pre-training framework for siamese time-series modeling. In *Forty-first International Conference on Machine Learning*, 2024.

[120] Abhimanyu Das, Weihao Kong, Rajat Sen, and Yichen Zhou. A decoder-only foundation model for time-series forecasting. In *Forty-first International Conference on Machine Learning*, 2024.

[121] Romain Ilbert, Ambroise Odonnat, Vasilii Feofanov, Aladin Virmaux, Giuseppe Paolo, Themis Palpanas, and Ievgen Redko. SAMformer: Unlocking the potential of transformers in time series forecasting with sharpness-aware minimization and channel-wise attention. In *Forty-first International Conference on Machine Learning*, 2024.

[122] Sumanth Varambally, Yian Ma, and Rose Yu. Discovering mixtures of structural causal models from time series data. In *Forty-first International Conference on Machine Learning*, 2024.

[123] George Zerveas, Srideepika Jayaraman, Dhaval Patel, Anuradha Bhamidipaty, and Carsten Eickhoff. A transformer-based framework for multivariate time series representation learning. In *Proceedings of the 27th ACM SIGKDD conference on knowledge discovery & data mining*, pages 2114–2124, 2021.

[124] Ronghao Lin and Haifeng Hu. Multi-task momentum distillation for multimodal sentiment analysis. *IEEE Transactions on Affective Computing*, 15(2):549–565, 2024.

[125] Diederik P. Kingma and Jimmy Ba. Adam: A method for stochastic optimization, 2017.

[126] Ilya Loshchilov and Frank Hutter. Decoupled weight decay regularization. In *International Conference on Learning Representations*, 2019.

[127] Ashish Vaswani, Noam Shazeer, Niki Parmar, Jakob Uszkoreit, Llion Jones, Aidan N Gomez, Ł ukasz Kaiser, and Illia Polosukhin. Attention is all you need. In I. Guyon, U. Von Luxburg, S. Bengio, H. Wallach, R. Fergus, S. Vishwanathan, and R. Garnett, editors, *Advances in Neural Information Processing Systems*, volume 30. Curran Associates, Inc., 2017.

[128] Lu Han, Han-Jia Ye, and De-Chuan Zhan. SIN: Selective and interpretable normalization for long-term time series forecasting. In *Forty-first International Conference on Machine Learning*, 2024.

[129] junxin lu and Shiliang Sun. CaudiTS: Causal disentangled domain adaptation of multivariate time series. In *Forty-first International Conference on Machine Learning*, 2024.

[130] Shizhan Liu, Hang Yu, Cong Liao, Jianguo Li, Weiyao Lin, Alex X. Liu, and Schahram Dustdar. Pyraformer: Low-complexity pyramidal attention for long-range time series modeling and forecasting. In *International Conference on Learning Representations*, 2022.

[131] Mingtao Feng, Chenbo Yan, Zijie Wu, Weisheng Dong, Yaonan Wang, and Ajmal Mian. Hyperrectangle embedding for debiased 3d scene graph prediction from rgb sequences. *IEEE Transactions on Pattern Analysis and Machine Intelligence*, 47(8):6410–6426, 2025.

[132] Kendong Liu, Mingtao Feng, Wei Zhao, Jingtao Sun, Weisheng Dong, Yaonan Wang, and Ajmal Mian. Pixel-level noise mining for weakly supervised salient object detection. *IEEE Transactions on Neural Networks and Learning Systems*, 36(10):18815–18829, 2025.

[133] Defu Cao, Wen Ye, and Yan Liu. Timedit: General-purpose diffusion transformers for time series foundation model. In *ICML 2024 Workshop on Foundation Models in the Wild*, 2024.

[134] Wenzhen Yue, Yong Liu, Xianghua Ying, Bowei Xing, Ruohao Guo, and Ji Shi. Freeformer: Frequency enhanced transformer for multivariate time series forecasting, 2025.

[135] Silviu-Marian Udrescu and Max Tegmark. Ai feynman: A physics-inspired method for symbolic regression. *Science Advances*, 6(16):eaay2631, 2020.

[136] Deaglan J. Bartlett, Harry Desmond, and Pedro G. Ferreira. Exhaustive symbolic regression. *IEEE Transactions on Evolutionary Computation*, 28(4):950–964, 2024.

[137] Samuel Müller, Noah Hollmann, Sebastian Pineda Arango, Josif Grabocka, and Frank Hutter. Transformers can do bayesian inference. In *International Conference on Learning Representations*, 2022.

[138] Thomas Nagler. Statistical foundations of prior-data fitted networks. In Andreas Krause, Emma Brunskill, Kyunghyun Cho, Barbara Engelhardt, Sivan Sabato, and Jonathan Scarlett, editors, *Proceedings of the 40th International Conference on Machine Learning*, volume 202 of *Proceedings of Machine Learning Research*, pages 25660–25676. PMLR, 23–29 Jul 2023.

[139] Jinghao Bian, Mingtao Feng, Weisheng Dong, Zijie Wu, Jianqiao Luo, Fangfang Wu, Yaonan Wang, and Guangming Shi. Locally aware visual state space for small defect segmentation in complex component images. *IEEE Transactions on Industrial Informatics*, 21(8):5965–5976, 2025.

[140] Ege Onur Taga, Muhammed Emrullah Ildiz, and Samet Oymak. TimePFN: Effective multivariate time series forecasting with synthetic data. In *NeurIPS Workshop on Time Series in the Age of Large Models*, 2024.

[141] Zhe Li, Shiyi Qi, Yiduo Li, and Zenglin Xu. Revisiting long-term time series forecasting: An investigation on linear mapping, 2023.

[142] Tian Zhou, Ziqing Ma, xue wang, Qingsong Wen, Liang Sun, Tao Yao, Wotao Yin, and Rong Jin. FiLM: Frequency improved legendre memory model for long-term time series forecasting. In Alice H. Oh, Alekh Agarwal, Danielle Belgrave, and Kyunghyun Cho, editors, *Advances in Neural Information Processing Systems*, 2022.

[143] Nikita Kitaev, Lukasz Kaiser, and Anselm Levskaya. Reformer: The efficient transformer. In *International Conference on Learning Representations*, 2020.

[144] Donald J. Berndt and James Clifford. Using dynamic time warping to find patterns in time series. In *Proceedings of the 3rd International Conference on Knowledge Discovery and Data Mining*, AAAIWS'94, page 359–370. AAAI Press, 1994.

[145] Tianqi Chen and Carlos Guestrin. Xgboost: A scalable tree boosting system. In *Proceedings of the 22nd ACM SIGKDD International Conference on Knowledge Discovery and Data Mining*, KDD '16, page 785–794, New York, NY, USA, 2016. Association for Computing Machinery.

[146] Sepp Hochreiter and Jürgen Schmidhuber. Long short-term memory. *Neural Computation*, 9(8):1735–1780, 11 1997.

[147] Albert Gu, Karan Goel, and Christopher Re. Efficiently modeling long sequences with structured state spaces. In *International Conference on Learning Representations*, 2022.

[148] Jean-Yves Franceschi, Aymeric Dieuleveut, and Martin Jaggi. Unsupervised scalable representation learning for multivariate time series. In H. Wallach, H. Larochelle, A. Beygelzimer, F. d'Alché-Buc, E. Fox, and R. Garnett, editors, *Advances in Neural Information Processing Systems*, volume 32. Curran Associates, Inc., 2019.

[149] Fanxing Liu, Cheng Zeng, Le Zhang, Yingjie Zhou, Qing Mu, Yanru Zhang, Ling Zhang, and Ce Zhu. Fedtadbench: Federated time-series anomaly detection benchmark. In *2022 IEEE 24th Int Conf on High Performance Computing & Communications; 8th Int Conf on Data Science & Systems; 20th Int Conf on Smart City; 8th Int Conf on Dependability in Sensor, Cloud & Big Data Systems & Application (HPCC/DSS/SmartCity/DependSys)*, pages 303–310, 2022.

[150] Ronghui Xu, Hao Miao, Senzhang Wang, Philip S. Yu, and Jianxin Wang. Pefad: A parameter-efficient federated framework for time series anomaly detection. In *Proceedings of the 30th ACM SIGKDD Conference on Knowledge Discovery and Data Mining*, KDD '24, page 3621–3632, New York, NY, USA, 2024. Association for Computing Machinery.

[151] Zhihan Li, Youjian Zhao, Jiaqi Han, Ya Su, Rui Jiao, Xidao Wen, and Dan Pei. Multivariate time series anomaly detection and interpretation using hierarchical inter-metric and temporal embedding. In *Proceedings of the 27th ACM SIGKDD Conference on Knowledge Discovery & Data Mining*, KDD '21, page 3220–3230, New York, NY, USA, 2021. Association for Computing Machinery.

A Main Results and Conclusions of the Five Tasks in Time Series Analysis

A.1 Long-term Forecasting

Setup. Time series forecasting, which analyzes historical data patterns to predict future trends, is crucial for financial market analysis, inventory management, energy demand and other fields [1, 100]. We adopt 8 real-world benchmark datasets for long-term forecasting, including ETTm1, ETTm2, ETTh1, ETTh2 [80], Weather [101], ECL [102], Traffic [103] and Exchange [104]. The forecasting lengths are set to $\{96, 192, 336, 720\}$. To ensure the fairness of the experiment, we set up three different look-back windows $\{96, 336, 512\}$ for the experiment, except Moirai and Timer are 672. For different models, we try our best to ensure that they are tested according to their original experimental configuration. For foundation models that can perform zero-shot forecasting and have been pre-trained, such as Moirai [28], Timer [29], Moment [93] and Chronos [22], we first load the pre-trained parameters of the model, and then perform supervised fine-tuning on it in the same way.

Table 3: Long-term forecasting task with **96** look-back windows. The results are averaged from four different series length $\{96, 192, 336, 720\}$. (* means former.) See Appendix F.1 for full results. **Red**: best, Blue: second best. The standard deviation is within 1%.

Model	`SymTime` **(Ours)**		Peri-mid* [63]		Moirai [28]		Timer [29]		Time-LLM [17]		TSLANet [83]		S^2IP-LLM [82]		GPT4TS [2]		TimeMixer [89]	
Metrics	MSE	MAE	MSE	MAE	MSE	MAE	MSE	MAE	MSE	MAE	MSE	MAE	MSE	MAE	MSE	MAE	MSE	MAE
ETTm1	0.371	**0.387**	0.409	0.410	0.398	0.417	0.388	0.402	**0.369**	0.394	0.377	0.397	0.374	0.404	0.369	0.395	0.382	0.397
ETTm2	0.274	**0.321**	0.290	0.328	0.296	0.348	0.405	0.408	0.275	0.324	0.283	0.327	0.266	0.325	**0.264**	0.328	0.279	0.325
ETTh1	**0.430**	**0.436**	0.455	0.446	0.441	0.454	0.434	0.444	0.438	0.445	0.448	0.441	0.456	0.454	0.434	0.440	0.453	0.441
ETTh2	0.365	0.402	0.400	0.416	0.402	0.411	0.428	0.441	0.369	0.407	**0.355**	**0.391**	0.362	0.405	0.359	0.403	0.388	0.408
Weather	0.247	0.276	0.262	0.283	0.265	0.299	0.329	0.358	0.247	**0.269**	0.259	0.352	**0.243**	0.274	0.265	0.285	0.253	0.280
ECL	0.187	0.276	0.178	0.267	**0.167**	**0.252**	0.177	0.267	0.180	0.269	0.199	0.283	0.191	0.283	0.206	0.291	0.185	0.274
Traffic	0.457	0.291	0.458	0.295	0.424	0.289	0.436	**0.284**	0.471	0.334	0.463	0.310	**0.417**	0.306	0.491	0.320	0.499	0.306
Exchange	**0.359**	**0.401**	0.388	0.417	0.373	0.417	0.382	0.425	0.376	0.414	0.368	0.414	0.472	0.478	0.370	0.411	0.403	0.423
Average	**0.336**	**0.349**	0.355	0.358	0.346	0.361	0.372	0.378	0.341	0.357	0.344	0.364	0.348	0.366	0.345	0.359	0.355	0.357

Table 4: Long-term forecasting task with **336** look-back windows. The results are averaged from four different series length $\{96, 192, 336, 720\}$. See Appendix F.2 for full results. **Red**: best, Blue: second best. The standard deviation is within 1%.

Model	`SymTime` **(Ours)**		PatchTST [54]		TimeMixer [89]		TimesNet [72]		Autoformer [75]		DLinear [87]		iTransformer [74]		TimeXer [62]		FEDformer [77]	
Metrics	MSE	MAE	MSE	MAE	MSE	MAE	MSE	MAE	MSE	MAE	MSE	MAE	MSE	MAE	MSE	MAE	MSE	MAE
ETTm1	**0.350**	0.382	0.352	0.382	0.368	0.392	0.421	0.423	0.618	0.539	0.357	**0.379**	0.368	0.395	0.372	0.395	0.441	0.452
ETTm2	**0.256**	0.316	0.258	**0.315**	0.262	0.318	0.282	0.334	0.400	0.420	0.291	0.353	0.272	0.329	0.262	0.317	0.325	0.377
ETTh1	**0.413**	0.432	0.419	**0.432**	0.430	0.437	0.485	0.480	0.580	0.539	0.425	0.440	0.450	0.457	0.493	0.483	0.450	0.472
ETTh2	0.341	0.390	**0.331**	**0.379**	0.396	0.425	0.409	0.440	0.663	0.604	0.490	0.476	0.390	0.416	0.375	0.410	0.430	0.467
Weather	0.238	0.273	0.258	0.292	**0.235**	0.273	0.250	0.286	0.441	0.450	0.245	0.298	0.238	**0.272**	0.287	0.290	0.313	0.363
ECL	0.164	0.258	0.165	0.294	0.169	0.260	0.197	0.297	0.236	0.346	0.170	0.269	**0.163**	**0.257**	0.172	0.267	0.214	0.327
Traffic	**0.391**	**0.267**	0.396	0.268	0.411	0.271	0.615	0.331	0.676	0.413	0.465	0.320	0.401	0.283	0.452	0.281	0.610	0.376
Exchange	**0.367**	**0.406**	0.385	0.420	0.415	0.438	0.548	0.532	1.053	0.807	0.448	0.462	0.392	0.427	0.409	0.500	0.376	0.427
Average	**0.315**	**0.341**	0.320	0.348	0.336	0.352	0.401	0.390	0.583	0.515	0.361	0.375	0.347	0.355	0.353	0.368	0.395	0.408

Results. Tables 3, Table 4, and Table 5 respectively show the results of `SymTime` with look-back windows of length $\{96, 336, 512\}$. It can be seen that `SymTime` demonstrates excellent performance in time series long-term forecasting tasks. Our model surpasses Peri-midFormer, GPT4TS and TimesNet, which are foundation models for the five major tasks, as well as Moirai and Timer, two general forecasting models. Compared with Time-LLM and S^2IP-LLM, which use pre-trained large language models as backbone, `SymTime` achieves better results with a more lightweight Transformer encoder.

Table 5: Long-term forecasting task with **512** look-back windows. The results are averaged from four different series length $\{96, 192, 336, 720\}$. See Appendix F.3 for full results. **Red**: best, Blue: second best. The standard deviation is within 1%.

Models	SymTime Ours		PatchTST [54]		TimeMixer [89]		TimesNet [72]		Autoformer [75]		DLinear [87]		iTransformer [74]		TimeXer [62]		FITS [90]	
Metrics	MSE	MAE	MSE	MAE	MSE	MAE	MSE	MAE	MSE	MAE	MSE	MAE	MSE	MAE	MSE	MAE	MSE	MAE
ETTm1	0.356	**0.380**	**0.352**	0.382	0.371	0.392	0.425	0.430	0.556	0.518	0.358	0.380	0.367	0.397	0.378	0.401	0.374	0.384
ETTm2	0.265	0.320	0.256	0.317	0.263	0.323	0.294	0.344	0.371	0.416	0.275	0.340	0.273	0.331	0.274	0.329	**0.254**	**0.313**
ETTh1	0.414	**0.432**	**0.413**	0.434	0.429	0.444	0.481	0.486	0.627	0.579	0.418	0.438	0.446	0.460	0.475	0.479	0.418	0.441
ETTh2	0.365	0.405	0.357	0.409	0.373	0.410	0.397	0.432	0.687	0.609	0.499	0.478	0.388	0.417	**0.354**	**0.400**	0.363	0.408
weather	0.234	0.273	0.245	0.284	**0.231**	**0.271**	0.251	0.288	0.489	0.486	0.241	0.292	0.249	0.280	0.282	0.284	0.244	0.281
ECL	0.163	0.267	0.169	0.269	0.177	0.274	0.201	0.302	0.353	0.393	0.167	0.267	**0.162**	**0.257**	0.171	0.270	0.169	0.265
Traffic	0.395	**0.268**	0.399	0.272	0.410	0.270	0.624	0.334	0.705	0.435	0.433	0.305	**0.383**	0.273	0.466	0.287	0.420	0.287
Exchange	**0.384**	**0.412**	0.398	0.423	0.517	0.497	0.718	0.608	0.944	0.768	0.500	0.494	0.427	0.467	0.514	0.506	0.393	0.439
Average	**0.322**	**0.345**	0.324	0.349	0.346	0.360	0.424	0.403	0.591	0.525	0.361	0.374	0.337	0.360	0.364	0.369	0.329	0.352

A.2 Short-term Forecasting

Setup. We adopt M4 benchmark [73] for short-term forecasting, which contains the yearly, quarterly and monthly collected univariate marketing data. Then, we use symmetric mean absolute error (SMAPE), mean absolute scaled error (MASE) and overall weighted average (OWA) to measure the forecasting performance, which are calculated as detailed in Appendix C.3.

Results. Table 6 indicates that SymTime after pre-training, surpasses TimeMixer, Peri-midFormer and TimesNet on the short-term forecasting tasks in terms of SMAPE, MASE and OWA metrics, achieving state-of-the-art performance. Specifically, SymTime performs well on Yearly, Quarterly and Monthly datasets, demonstrating its capability to capture not only the trends of annual variations but also the cyclic characteristics of seasonal and monthly encoding.

Table 6: Short-term forecasting task on M4. The prediction lenghs are $\{6, 48\}$ and results are weighted averaged from several datasets under different sample intervals. (* means former, TMixer is TimeMixer, S-LLM is S^2IP-LLM, T-LLM is Time-LLM). See Appendix F.4 for full results. **Red**: best, Blue: second best. The standard deviation is within 1%.

Models	SymTime **(Ours)**	Peri-mid* [63]	S-LLM [82]	T-LLM [17]	GPT4TS [2]	TMixer [89]	PatchTST [54]	iTrans* [74]	TimesNet [72]	DLinear [87]	LightTS [88]	FED* [77]	In* [80]
SMAPE	**11.785**	11.897	12.514	12.584	12.367	11.885	12.866	13.233	11.888	12.500	11.962	12.605	15.018
MASE	**1.584**	1.607	1.726	1.763	1.767	1.598	1.734	1.850	1.607	1.678	1.609	1.677	2.096
OWA	**0.849**	0.859	0.913	0.915	0.918	0.856	0.928	0.972	0.858	0.899	0.862	0.903	1.102

A.3 Classification

Setup. Time series classification is crucial for the identification and diagnosis of patterns in complex systems and plays a significant role in various fields such as financial analysis, medical diagnosis and industrial monitoring [95]. Using the experimental setup from TimesNet [72], we test SymTime's discriminative ability on 10 UEA multivariate time series classification datasets [105], including categories such as Industry, Face Detection, ECG, Voice and Transportation.

Results. As shown in Figure 10, SymTime achieves an average accuracy of 74.9%, surpassing all baselines, indicating that SymTime is competitive in classification tasks.

A.4 Imputation

Setup. Sensors monitoring complex systems in the real world may experience distortions or malfunctions, leading to partial missing data in the collected time series. Therefore, time series imputation is crucial for the recovery of complete datasets. We verify SymTime's imputation capabilities on 6

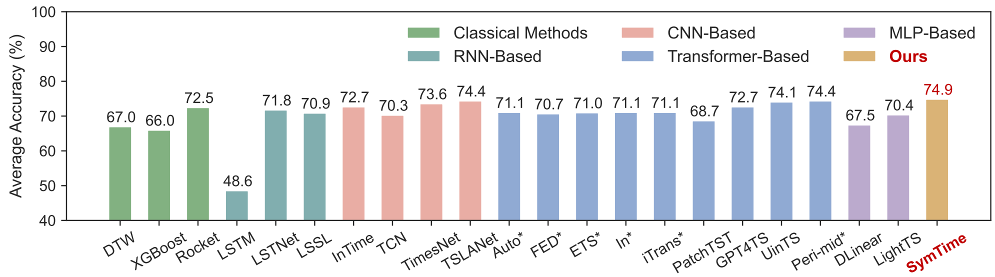

Figure 10: Comparison of the average accuracy of `SymTime` and other baselines on 10 UEA datasets. See Appendix F.5 for full results.

datasets: ETTm1, ETTm2, ETTh1, ETTh2 [80], Weather [101] and ECL [102]. To test the model's imputation ability under varying degrees of missing data, we add random masks at proportions of $\{12.5\%, 25\%, 37.5\%, 50\%\}$ in point level on time series of length 96. Since `SymTime` was pre-trained by randomly masking patches level for series reconstruction and masks are added randomly in point level in the imputation task. Considering the differences between these masking approaches and the potential disruption of the series's original trends and periodic features at higher mask rates, we adopt per-interpolation for the masked series from [63]. Analysis and ablation experiments regarding this method are presented in Appendix C.9. The results demonstrate that per-interpolation can be used as a model-independent feature engineering to improve the performance of downstream tasks.

Table 7: Imputation task, where we randomly mask {12.5%, 25%, 37.5%, 50%} time points of length-96 time series. The reuslts averaged from 4 different mask ratios. (* means former.) See Appendix F.6 for full results. **Red**: best, Blue: second best.

Model	SymTime (Ours)		GPT4TS [2]		TimesNet [72]		Peri-mid* [63]		Moment [93]		iTrans* [74]		PatchTST [54]		DLinear [87]		LightTS [88]	
Metric	MSE	MAE	MSE	MAE	MSE	MAE	MSE	MAE	MSE	MAE	MSE	MAE	MSE	MAE	MSE	MAE	MSE	MAE
ETTm1	0.036	0.116	0.028	0.109	**0.027**	**0.107**	0.036	0.116	0.074	0.168	0.072	0.185	0.049	0.143	0.090	0.204	0.068	0.182
ETTm2	0.026	0.088	**0.022**	**0.088**	**0.022**	0.089	0.026	0.087	0.031	0.108	0.082	0.191	0.030	0.101	0.102	0.212	0.068	0.176
ETTh1	0.095	0.201	0.093	0.200	**0.089**	0.199	0.091	**0.196**	0.139	0.234	0.148	0.269	0.126	0.231	0.169	0.283	0.159	0.278
ETTh2	0.058	0.148	0.052	**0.147**	**0.050**	0.148	0.057	**0.147**	0.061	0.159	0.139	0.254	0.066	0.164	0.163	0.273	0.143	0.258
ECL	**0.054**	**0.151**	0.093	0.212	0.094	0.211	0.063	0.169	0.094	0.211	0.099	0.224	0.078	0.192	0.128	0.256	0.108	0.238
Weather	**0.028**	**0.038**	0.032	0.058	0.030	0.056	0.029	0.041	0.035	0.075	0.052	0.114	0.033	0.057	0.053	0.116	0.047	0.106
Average	**0.049**	**0.124**	0.053	0.136	0.052	0.135	0.050	0.126	0.072	0.159	0.099	0.206	0.064	0.148	0.118	0.224	0.099	0.206

Results. Table 7 shows that `SymTime` outperforms Peri-midFormer, GPT4TS and TimesNet in overall performance establishing `SymTime` as the latest state-of-the-art approach. Although `SymTime`'s performance on the ETT series of datasets is not as strong as GPT4TS, it achieves more significant effects on datasets with a higher number of channels, such as ECL and Weather.

A.5 Anomaly Detection

Setup. Time series anomaly detection is crucial for rapidly identifying anomalies in critical areas, aiding in risk prevention and decision optimization. Due to the difficulty in annotating time series anomalies, we focus primarily on unsupervised anomaly detection. We conduct experiments on 5 widely used anomaly detection datasets: SMD and SMAP [106], MSL [107], SWaT [108], PSM [109], encompassing service monitoring, space & earth exploration, and water treatment applications. We adopt the same data preprocessing method as the Anomaly Transformer [81], dividing the data into non-overlapping segments of length 100 for reconstruction. Specifically, normal data is used for model training and we employ a simple reconstruction loss to help the model learn the distribution of normal data [63]. In subsequent testing phases, reconstructed outputs exceeding a specified threshold are considered anomalies.

Table 8: Anomaly detection task, where we calculate the F1-score (as %) for each dataset. (* means former, TNet is TimesNet, PTST is PatchTST.) A higher value of F1-score indicates a better performance. See Appendix F.7 for full results. **Red**: best, Blue: second best.

Model	SymTime **(Ours)**	UniTS [92]	Peri-mid* [63]	GPT4TS [2]	TNet [72]	PTST [54]	LightTS [88]	DLinear [87]	iTrans* [74]	Anomaly [81]	Stationary [78]	Cross* [79]	In* [80]	Auto* [75]
SMD	**85.66**	83.69	84.08	84.49	84.37	84.62	82.53	79.76	80.19	85.49	82.97	77.22	77.88	71.17
MSL	81.77	81.16	80.68	82.03	81.14	78.70	78.95	81.87	72.47	**83.31**	76.68	80.59	81.07	82.22
SMAP	73.43	**74.00**	67.53	68.85	69.05	68.82	69.21	67.30	66.72	71.18	69.02	67.12	73.26	73.97
SWaT	**93.61**	92.51	91.64	92.60	92.61	85.72	93.33	92.66	92.64	83.10	92.24	90.22	80.35	79.19
PSM	97.10	**97.31**	96.21	97.09	97.06	96.08	97.15	96.64	94.88	79.40	97.23	92.52	90.43	88.24
Avg F1	**86.31**	85.73	84.03	85.01	84.85	82.79	84.23	83.64	81.38	80.50	83.63	81.53	80.60	78.96

Results. The results in Table 8 show that SymTime surpasses all previous models such as TimesNet and GPT4TS in the time series anomaly detection task and becomes the latest SOTA model. Compared with UniTS [92] pre-trained on real time series data, SymTime is pre-trained on synthetic datasets and achieves better model performance.

B Analysis of Series-Symbol (S^2) Dataset and Model Pre-training

Table 9: Some symbols used in data generation and their explanations.

Symbols	Explanation	Symbols	Explanation
X	sampling series	Y	generated series
$f(\cdot)$	symbolic expression	e_t	white noise sequence
M	the input channels number	N	the output channels number
$\mathcal{U}$	uniform distribution	$\mathcal{N}$	normal distribution
P	probability of selecting sampling methods	k	total number of mixed distributions
p	the order of the AR process	q	the order of the MA process
ϕ_p	the parameters of AR process	θ_q	the parameter of MA process

Based on the viewpoint of complex dynamic system modeling, this paper proposes a bimodal series-symbol (S^2) generation mechanism to alleviate the problem of shortage of training data in the field of time series analysis. Table 9 shows the specific symbols we used in constructing symbolic expressions in Section 3.1. This part is mainly divided into the following sections:

- B.1 Series-Symbol Data Display: This section shows the symbolic expressions and time series data that can be generated through the S^2 data generation mechanism.
- B.2 Composition and Usage of the Series-Symbol Dataset: This section introduces the specific composition of the S^2 dataset and how to use it when training SymTime.
- B.3 Statistics Analysis: This section examines and analyzes the basic statistical representation of the S^2 data.
- B.4 Analysis of Existing Large-scale Datasets for Time Series Pre-training: This section analyzes the data shortage and distribution imbalance faced by large-scale time series pre-training datasets in TSA.
- B.5 S^2 Dataset Statistical Characterization Coverage Experiments: This section details the specific configuration of the characterization coverage experiments in the Section 4.1.
- B.6 Masked Time Series Modeling and Zero-shot Imputation for Representation Learning:
- B.7 Time Complexity Analysis of S^2 Data Generation Mechanism: In this section we analyze in detail the time complexity of the S^2 data generation mechanism.
- B.8 The Selection of the Unary Operators: In this section we analyze the unary operators used in S^2 data generation.
- B.9 The Limitations of S^2 Generation Mechanism.

B.1 Series-Symbol Data Display

In Figure 11, we show the visualization of the generated series from 1 input channel and 1 output channel to 4 input channels and 4 output channels. We show two sets of cases for each input and output channel. The symbolic expressions $f(\cdot)$ for the generated series in (a), (c), (e) and (g) in Figure 11 are shown above.

The symbolic expressions with text format are shown as follow:

Symbolic expression of Figure 11 (a)

y_1 = (-0.795 add ((-0.675 mul ((0.999 add (-6.7 mul x_1)))**2) add ((-0.798 mul inv((-5.99 add (-0.751 mul x_1)))) sub (9.68 mul sqrt((-7.37 add (0.756 mul x_1)))))))

Symbolic expression of Figure 11 (c)

y_1 = (-3.39 add (((0.56 mul (inv((-98.9 add (58.2 mul x_2))) mul ((-19.7000 mul x_1) sub (31.9000 mul x_2)))) sub (40.4000 mul x_1)) add (0.71 mul (((7.13 mul x_2) sub (-1.68 mul (x_1 mul sqrt((-92.8000 add (0.054 mul (x_2 mul ((0.327 mul x_2) sub (2.3 mul x_2))))))))) mul x_1))))

y_2 = (1.0 add ((68.9 mul x_2) sub (((80.9 mul (x_1 mul (x_1 mul ((6.1000 mul x_2) sub ((34.2 mul sqrt((64.4 add (29.2000 mul x_1)))) add (-5.24 mul x_1)))))) add (6.78 mul x_2)) sub (((0.5730 mul x_1) sub ((2.34 mul x_2) sub (-6.72 mul x_1))) add (0.966 mul sqrt((76.8000 add (-7.79 mul x_1))))))))

Symbolic expression of Figure 11 (e)

y_1 = (0.795 add ((0.42 mul x_3) sub ((4.39 mul x_1) add (((0.1430 mul x_2) sub ((-5.28 mul x_3) add (((-0.028 mul ((((1.27 mul x_3) sub (((0.331 mul x_2) sub ((2.99 mul x_3) add (-0.932 mul (((0.606 mul x_1) sub (0.967 mul x_3)) mul x_3)))) sub (-0.609 mul x_3))) add (-1.25 mul x_1)) mul x_1)) sub (77.3000 mul x_1)) sub (1.93 mul x_3)))) sub (16.7 mul x_3)))))

y_2 = (-9.2900 add ((0.398 mul ((((-49.7 mul x_1) sub ((5.93 mul sin((6.54 add (-0.045 mul x_1)))) add ((62.3000 mul inv(((0.138 mul x_2) add (29.0 mul x_1)))) add (8.75 mul x_2)))) add ((-0.9500 mul x_3) add (-8.1 mul x_1))) mul x_3)) add ((-9.74 mul x_3) add ((((-0.9 mul x_3) sub (4.45 mul sqrt((-0.373 add (-0.151 mul x_3))))) add (-54.6 mul x_3)) sub (-0.758 mul ((85.3000 add (8.74 mul x_3)))**2)))))

y_3 = (-0.975 add ((-54.4000 mul sqrt((-0.722 add (-9.33 mul x_2)))) sub (1.45 mul ((66.4 add (-9.65 mul x_1)))**2)))

Symbolic expression of Figure 11 (g)

y_1 = (-7.17 add (0.537 mul x_1))

y_2 = (-0.843 add (48.8000 mul x_1))

y_3 = (57.3000 add (((-0.449 mul x_2) add (-1.32 mul x_3)) add ((-0.9400 mul x_4) add (0.51 mul x_1))))

y_4 = (-0.2040 add (((-6.6000 mul inv((0.88 add (58.1 mul x_4)))) sub ((-23.0 mul x_4) add ((-91.0 mul x_3) sub (-93.6000 mul x_2)))) sub ((-6.6000 mul x_4) sub (0.9580 mul ((x_3 mul x_3) mul ((-0.45 mul x_2) sub ((((-9.09 mul x_4) sub ((8.93 mul sqrt(((-26.6 mul x_4) add (-0.907 mul x_1)))) add (-6.2 mul x_4))) sub (-0.078 mul x_4)) sub (-16.5 mul x_2))))))))

B.2 Composition and Usage of the Series-Symbol Dataset

We set the maximum number of input channels and the maximum number of output channels to 6 and 12 respectively to generate symbolic expressions and series. Each symbolic expression is sampled only once. We generated a total of 40M pairs of series and symbols. The cumulative series length is 50B. The data number of each input channel and output channel in the dataset is shown in Figure 12.

When pre-training `SymTime` with S^2 dataset, we start by combining the sampled and generated series and then segmenting them into patches using a sliding window [54, 17]. The sliding window's kernel size and step size are both set to 16. Due to the requirement for mask time series modeling (MTM) [27, 26], there is no overlap between adjacent patches. Given the varying number of input and output channels in the data, the series from the maximum input and output channels can be segmented into up to 288 patches ($18 \times 256/16$) [110]. For series with fewer than 288 patches, we pad them with zeros

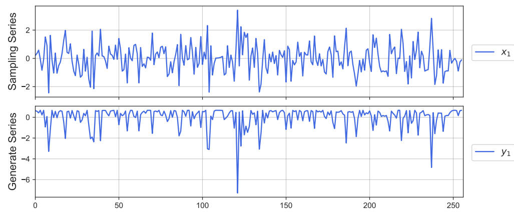

(a) 1 input channel 1 output channel data example 1

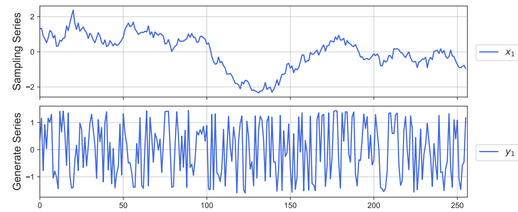

(b) 1 input channel 1 output channel data example 2

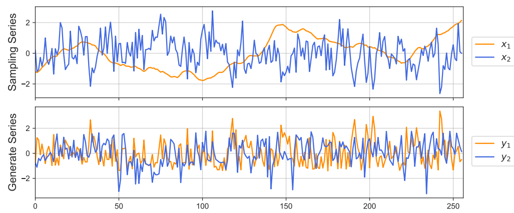

(c) 2 input channels 2 output channels data example 1

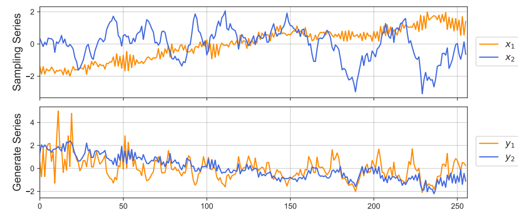

(d) 2 input channels 2 output channels data example 2

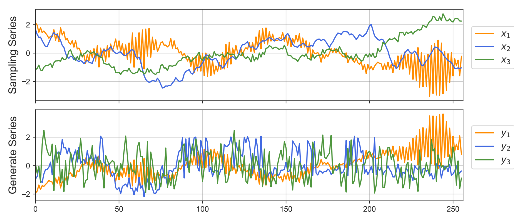

(e) 3 input channels 3 output channels data example 1

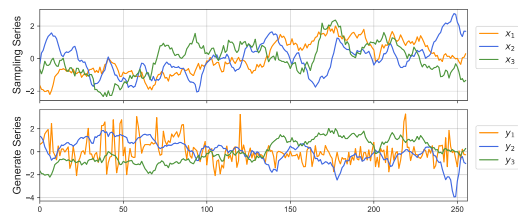

(f) 3 input channels 3 output channels data example 2

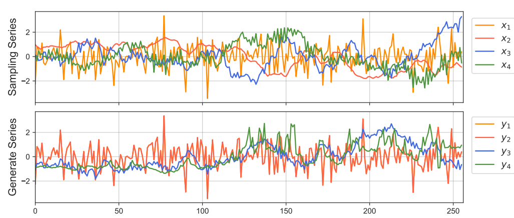

(g) 4 input channels 4 output channels data example 1

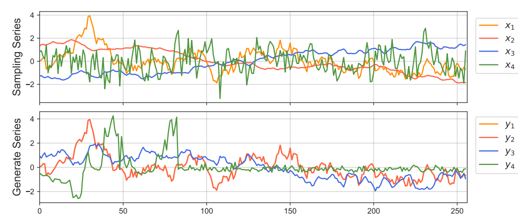

(h) 4 input channels 4 output channels data example 2

Figure 11: Visualization of series from 1 input channel 1 output channel to 4 input channels 4 output channels.

to align the length. Next, for symbolic expressions in natural language form [19, 12, 82, 75, 111], we set a maximum length of 512 characters and perform tokenization. Ultimately, the time series patches and natural language tokens are fed into the time series encoder and the LLM of the Transformer architecture, respectively.

B.3 Statistics Analysis

Setup. In Section B.2, we provide a detailed introduction to the generation process, composition and usage of the S^2 dataset [12, 14, 48]. In this section, we first conduct a random sampling analysis of the statistical characteristics of the S^2 dataset, including stationarity [65] and predictability [66, 29].

Stationarity. Stationarity is one of the fundamental properties of time series [50, 51]. This attribute ensures that the statistical characteristics of time series data remain consistent across different time points, which is crucial for building effective predictive models and making reliable statistical inferences. To this end, we employ the Augmented Dickey-Fuller (ADF) [65] test to examine the stationarity of the data, thereby determining whether the generated S^2 dataset is suitable for deep neural networks (DNNs) to learn representations of time series.

Forecastability. The forecastability of a time series refers to the ability and accuracy to forecast future values based on historical data and statistical models [52, 29]. For certain specific time series and complex systems, such as stock markets, it is often challenging to predict their subsequent developments. Therefore, it is necessary to test whether the S^2 dataset is non-chaotic and learnable. Forecastability is calculated by subtracting the entropy of the series' Fourier decomposition as adopted from [66] and [29], where a higher forecastability value indicates better predictability. Please note that since the method provided by [66] is only applicable to multivariate time series, we merge the input channels and output channels together for calculation.

Test Methods and Results. For the multiple input-output channels presented in the Table 10, we randomly selected 1,000 samples to calculate their average ADF statistics, p-values, and Forecastability metrics. The results indicate that the average p-value from the ADF test across all samples is greater than 0.05, suggesting that the majority of the generated series in the S^2 dataset are non-stationary time series, posing a challenge in modeling and learning [65]. However, the Forecastability metric, which is greater than 0.3 for all tested samples, indicates that the generated series Y is not produced by a chaotic system and is, overall, predictable.

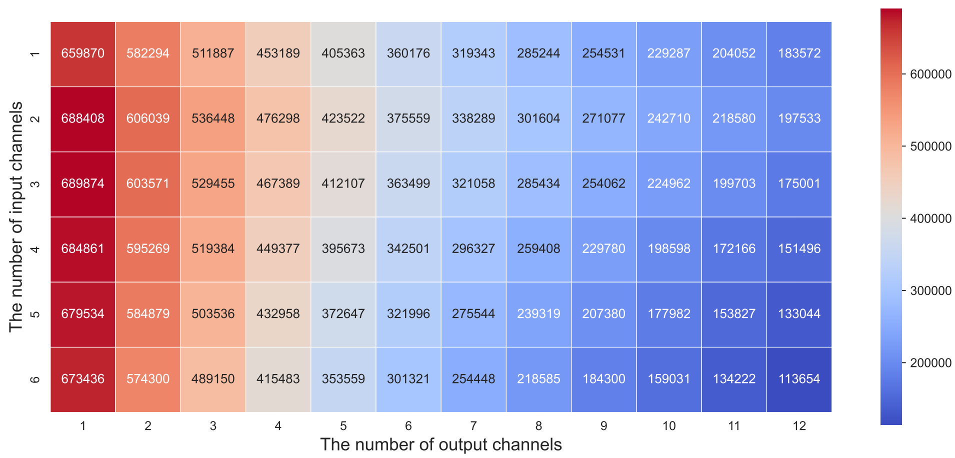

Figure 12: The number of samples in each part of the S^2 dataset.

Table 10: Results of the stationarity and forecastability tests for the S^2 dataset.

inputs	outputs	ADF	p value	forecast	inputs	outputs	ADF	p value	Forecastability
1	1	-12.77	0.0538	0.3155	1	6	-11.48	0.0619	0.3375
2	2	-11.89	0.0568	0.3199	2	6	-11.46	0.0733	0.3218
3	3	-12.40	0.0544	0.3328	3	6	-11.43	0.0625	0.3244
4	4	-11.66	0.0617	0.3491	4	6	-11.53	0.0640	0.3428
5	5	-11.38	0.0628	0.3140	5	6	-12.32	0.0597	0.3284
6	6	-12.43	0.0625	0.3262	6	8	-11.52	0.0555	0.3246
6	10	-11.65	0.0619	0.3287	6	12	-11.66	0.0520	0.3310

B.4 Analysis of Existing Large-scale Datasets for Time Series Pre-training

Large-scale datasets are crucial for building foundation models. Almost all deep learning models today are data-driven, relying on training data [80, 85, 112, 113]. Therefore, when constructing a pre-trained foundation model for time series, a large-scale and comprehensively representative pre-training dataset is indispensable [28, 29, 20, 18, 98]. The scaling laws of neural networks indicate that the learning effectiveness of deep neural networks is primarily influenced by three factors: the number of model parameters, the size of the training dataset, and the amount of computational resources [5, 6, 96, 114]. Expanding the scale of the pre-training dataset can effectively improve the model's generalization capability and performance, and the performance gains from increasing data volume

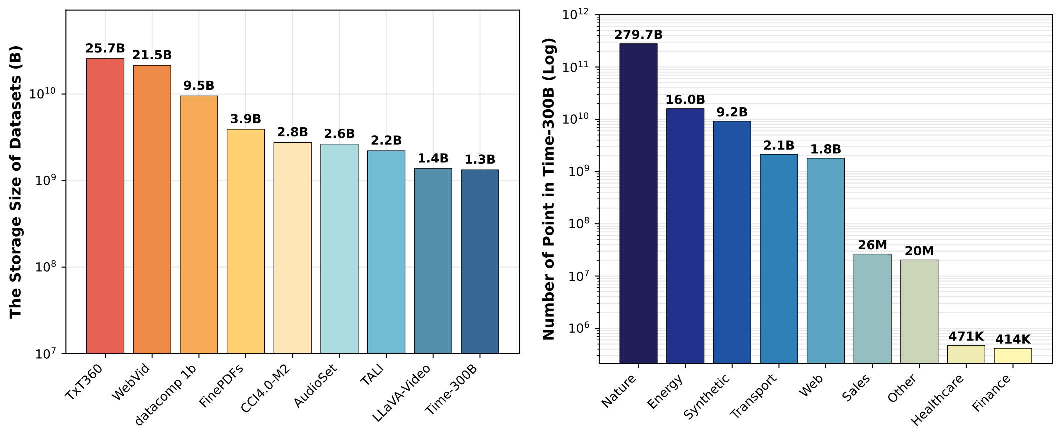

(a) data scarcity

(b) data imbalance

Figure 13: The scarcity and imbalance of time series pre-training dataset (taking the largest open-source time series dataset Time-300B as an example [7]). (a) time series datasets are data-scarce compared to text datasets in natural language processing and video understanding datasets in computer vision. (b) Large-scale time series pre-training datasets face serious distribution imbalance problems.

Table 11: Time-300B time series dataset from Time-MoE [7].

	Energy	**Finance**	**Health**	**Nature**	**Sales**	**Synthetic**	**Transport**	**Web**	**Other**	**Total**
# Obs.	15.98B	413.70K	471.04K	279.72B	26.38M	9.22B	2.13B	1.80B	20.32M	309.09B
%	5.17%	5.17%	0.0001%	90.50%	0.008%	2.98%	0.69%	0.58%	0.006%	100%

Table 12: UTSD time series dataset from Timer [29], where Mise. means Multiple Sources.

	Energy	**Environment**	**Health**	**IoT**	**Nature**	**Transport**	**Web**	**Cloud**	**Sales**	**Finance**	**Mise.**
# Obs.	16.86B	70.45M	233.M	165M	201B	4.9B	157M	2.15B	198M	0.33M	56.52M
%	7.461%	0.031%	0.103%	0.073%	89%	2.17%	0.07%	0.95%	0.088%	0.00%	0.025%

Table 13: LOTSA time series dataset from Moirai [28].

	Energy	**Transport**	**Climate**	**CloudOps**	**Web**	**Sales**	**Nature**	**Finance**	**Health**	**Total**
# Obs.	16.36B	4.90B	4.19B	1.52B	428M	198M	28.55M	24.92M	1.59M	27.65B
%	59.17%	17.73%	15.15%	5.49%	1.55%	0.72%	0.09%	0.10%	0.01%	100%

Table 14: Time series datasets from neural scaling laws [6]

	Transport	**Climate**	**Energy**	**CloudOps**	**Health**	**Sales**	**Web**	**Total**
# Obs.	4.82B	4.73B	2.34B	2.15B	240M	140M	600M	14.46B
%	33.31%	32.71%	16.15%	14.86%	1.61%	0.96%	0.40%	100%

are independent of the model architecture and training methods [6, 115, 116, 117]. Consequently, an increasing number of models are adopting the approach of training larger-scale models on large-scale pre-training datasets to achieve better performance [118]. This paper surveys the pre-training datasets used by the three current mainstream pre-trained foundation models—Time-MoE [7], Moirai [28], and Timer [29]—as well as the datasets utilized in the study of time series scaling laws [6], which are shown in Tables 11, 12, 13 and 14. In Figure 13 (a) we demonstrate that the current largest time series datasets are still smaller than those in CV and NLP.

Imbalanced domain distribution issues in large-scale time series datasets. The distribution of data across various domains indicates that the four large-scale time series pre-training datasets all face issues with imbalanced domain data distribution. For instance, domains such as Nature, Energy and Transport have the most datasets [80], while others like Sales, IoT, Web, Finance and Multiple Sources suffer from extremely low data volumes due to difficulties in data collection or data privacy concerns as shown in Figure 13 (b). According to the scaling laws of neural networks, the imbalance in the pre-training dataset distribution can lead to significant performance biases in in-domain and out-of-domain forecasting tasks for the trained foundation models [6, 118], meaning there is a considerable performance gap between domains with less data and those with more data. To address this, this paper proposes an unrestricted method for generating high-quality time series data to alleviate the scarcity and imbalanced distribution of data in time series analysis domains.

B.5 S^2 Dataset Statistical Characterization Coverage Experiments

Metric. To further examine the diversity of the artificially synthesized data in the S^2 dataset, we conduct a sampling assessment from six dimensions: stationarity, predictability, frequency domain characteristics, complexity, seasonality intensity, and trend characteristics. For each dimension, we select corresponding statistical indicators for dataset evaluation and quantification, as detailed below:

1. **Augmented Dickey-Fuller (ADF) Test:** Consistent with section B.3, we employ the ADF test to assess the stationarity of time series, using its test statistic as an indicator of time series stationarity [65, 29].
2. **Forecastability:** Based on [66] method, we determine whether a time series is chaotic or can be accurately predicted through machine learning models by using Fourier decomposition and entropy [29]. Note that since the method provided by [66] is only applicable to multivariate time series, we invert the sampled single-channel time series to form a dual-channel series to calculate the indicator.
3. **FFT Mean:** We utilize the average of the Fourier transform power spectrum to evaluate the frequency domain characteristics of time series. This indicator can be used to measure the overall intensity of time series and assess the energy distribution.
4. **Permutation Entropy:** This indicator assesses the dynamic complexity of a time series by analyzing its permutation patterns [69]. We set the embedding dimension $m = 3$ and time delay $\tau = 1$, and calculate its specific value using Shannon Entropy in Equation 8. See [69] for more detailed calculation.
5. **Seasonality:** We decompose the time series into trend, seasonal and residual components using the Seasonal-Trend Decomposition using LOESS (STL) algorithm [67]. Then, we calculate the intensity of the seasonal component in the time series according to Equation 9.
6. **Mann-Kendall Test:** This is a non-parametric statistical method used to detect monotonic trends in time series [68]. The basic principle is to compare the size relationship between each data point and other data points in the time series. Therefore, this method does not rely on a specific distribution of data and is not affected by outliers. We use the statistical test results of this method as the evaluation indicator, where -1 indicates a downward trend, 1 indicates an upward trend, and 0 indicates no obvious trend.

$$\text{Permutation} = -\sum_{j=1}^{K} P_j \times \ln P_j, \tag{8}$$

$$\begin{cases} Y_t = T_t + S_t + R_t \\ \text{Seasonality} = \max\left\{0, 1 - \frac{\text{Var}(R_t)}{\text{Var}(S_t + R_t)}\right\} \end{cases}, \tag{9}$$

where, P_i represents the frequency of the i-th permutation model in the permutation entropy, and $K = m!$ is the total number of permutation patterns [69]. Y_t represents the original time series, T_t, S_t and R_t are the trend, seasonal and residual components decomposed by the STL algorithm [67] respectively. $\text{Var}(\cdot)$ means calculating the variance of a series.

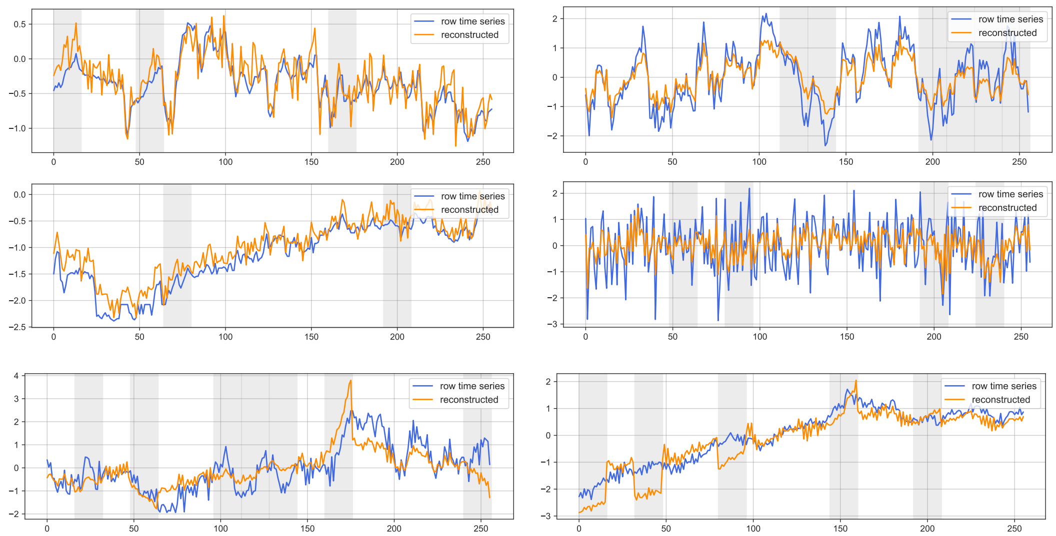

Figure 14: Zero-shot time series imputation in S² out-of-domain data.

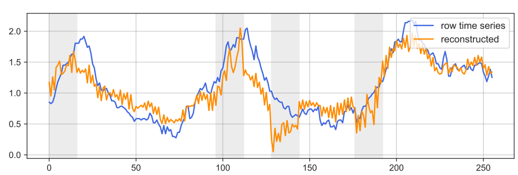

(a) ETTm1

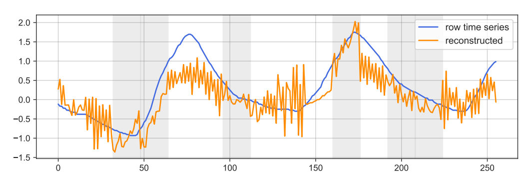

(b) ETTm2

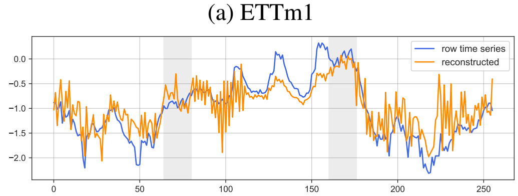

(c) ETTh1

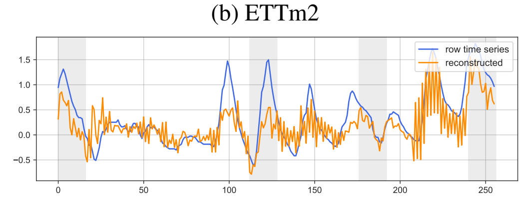

(d) ETTh2

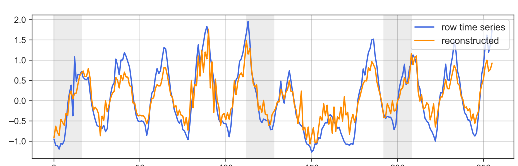

(e) Electricity

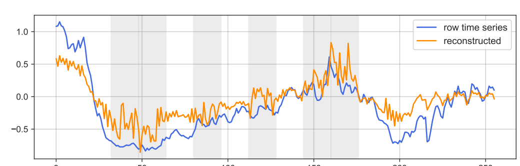

(f) Weather

Figure 15: Zero-shot time series imputation in real world time series dataset in ETTm1, ETTm2, ETTh1, ETTh2 [80], Electricity [102] and Weather [101].

B.6 Masked Time Series Modeling and Zero-shot Imputation for Representation Learning

Setup. Since we incorporate MTM loss in the pre-training process of `SymTime`, in this section, we assess the specific learning effects of the time series encoder in `SymTime` through masked modeling [54, 27, 119, 89]. We test the model's performance using both pre-trained synthetic data not in the S² dataset and real datasets from time series imputation tasks [12, 14, 48]. As `SymTime` adds masks in units of patches of length 16 during pre-training, we also add masks in the form of 16-length patches. The reconstruction effect of the masked parts by the time series encoder is shown in Figure 14 and 15.

S^2 Dataset Out-of-Domain Data. In Figure 14, we generate new data using the method from the S^2 dataset and add masks to test the reconstruction ability of the time series encoder [12, 14, 48]. The gray sections represent the masked segments, while blue and orange represent the original and reconstructed series, respectively. We input time series outside the gray parts in patches and have the model reconstruct the gray sections based on the remaining information. Since we only calculate the MTM loss on the masked parts [27, 119], the visible reconstruction does not overlap with the original input series [29, 120, 93]. From the Figure 14, it can be observed that the time series encoder in `SymTime` performs well in fitting the fluctuations and trends of time series, demonstrating that our encoder successfully learned the fundamental representations of time series during pre-training [28, 121, 122].

Real-world Time Series Data. In Figure 15, we conduct representation learning tests on 6 real datasets: ETTm1, ETTm2, ETTh1, ETTh2 [80], Electricity [102], and Weather [101]. Since no real data are used for model pre-training, these datasets are also considered as out of domain data. We similarly add masks in patch units (gray sections). It can be observed that the time series encoder in `SymTime` also performs well in zero-shot reconstruction on real-world data [27, 123].

B.7 Time Complexity Analysis of S^2 Data Generation Mechanism

We define the specific symbol and its explanation in Table 9. Then, we use the divide-and-conquer approach to anaylze the complexity of the S^2 data generation mechanism.

1. **Symbolic Expression Generation:** We construct symbolic expressions using a tree structure as a medium. When we have b binary operators, we further insert $(b+1)$ leaf nodes (the process from (a) to (b) in Figure 3 in our paper). Therefore, after inserting u unary operators (Figure 3 (c)), the total number of nodes in the tree is $n = 2b + u + 1$. Because there are many ways to construct a tree, we consider the time complexity of constructing a balanced tree. Therefore, for N symbols constructed, the specific complexity of this process is $\mathcal{O}(N \times n\text{log}n)$.
2. **Sampling series generation:** When we want to generate a sampling time series with M channels, each channel has a probability of P to be sampled using a mixture distribution and a probability of $(1-P)$ to be sampled using an ARMA model. When the sampling length of the series is L, the complexity of generating k mixture distribution and ARMA (p, q) series is $O(kL)$ and $O(L(p+q))$. Therefore, the time complexity of this process can be quantified as $\mathcal{O}\left(ML \times [Pk + (1-P)(p+q)]\right)$.
3. **Sampling through symbolic expressions and series:** We simplify the specific operational details of this process and only consider the time complexity of operations with variables. For a series of length L, we have N symbolic expressions to be sampled, and each symbol has an average of $\frac{M+1}{2}$ variables (Each symbolic expression may contain any number of variables from 1 to M, so here we take $\frac{M+1}{2} = \frac{(1+2+\cdots+M)}{M}$ as the average probability). Then the process can be quantified as $\mathcal{O}(N \cdot \frac{M+1}{2} \cdot L)$.

To sum up, the symbolic expressions we construct and the parameters used in the sampling process are typically smaller than the length of the time series L. Therefore, we ignore the symbolic expression generation process and consider only the two processes of generating the sampling series and sampling using the symbolic expression. Since the number of channels, M and N, as well as k, p and q are all smaller than L, we can intuitively assume that the time complexity of the S^2 data generation mechanism is linearly related to the length of the series L.

B.8 The Selection of the Unary Operators

From the perspective of constructing symbolic expressions in the current S^2 data generation mechanism, binary operators primarily serve to connect multiple variables, while unary operators can increase the diversity of numerical values through specific operations. However, we choose not to use all symbolic and linear operations, but only use the unary operators $\{\text{inv}, \text{abs}, \text{pow2}, \text{pow3}, \text{sqrt}, \sin, \cos, \tan, \arctan, \log, \exp\}$ for generation.

Although ignoring certain mathematical symbols will reduce the diversity of symbolic expressions, we have found in numerous experiments and tests that differential $\frac{\mathrm{d}y}{\mathrm{d}x}$, integral $\int$, power operations

x^n, and exponential operations with various bases n^x will seriously affect our data generation to a certain extent. The specific reasons are as follows:

1. **Value explosion:** To maintain quality, we cap large magnitudes (Section 3.1). Integration, exponential and high-order powers readily cause overflow, so they were dropped; exp alone is retained for diversity.
2. **Numerical differentiation:** Symbolic differentiation introduces truncation/round-off trade-offs. Combined with reciprocal and absolute-value operators, functions such as $|x|$ or $\sin\left(\frac{1}{x}\right)$ because non-smooth or high-frequency vibration at $x = 0$, breaking differentiation.
3. **Numerical integration:** Randomly built expression trees often yield integrands with singularities (e.g., $\int_0^1 \frac{1}{\sqrt{x}} \mathrm{d}x$) or force costly oscillatory integrals (e.g., $\int_0^{100} sin(100x) \mathrm{d}x$); interval selection is non-trivial.
4. **Symbolic cost:** Differentiation and integration are slow and can trigger exponential memory growth. Many elementary functions lack closed-form antiderivatives (e.g., $\int \exp(-x^2)\mathrm{d}x$).

Considering factors like numerical stability, symbolic complexity, computational efficiency, and sampling success rate, we selectively omitted some symbolic operations. Nevertheless, the data generation framework proposed is essentially a complete theory. It already incorporates the vast majority of symbolic operations, and new operators or user-defined symbolic operations can be easily added. The omission of some operations due to the above factors does not undermine the validity of this framework.

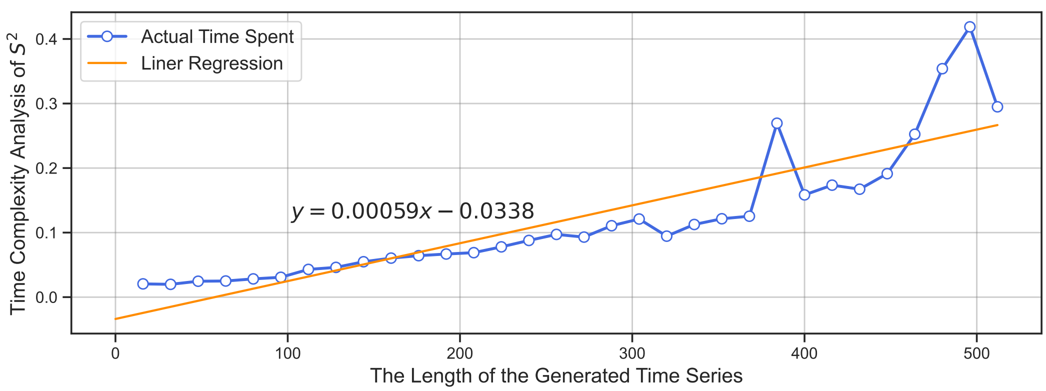

Figure 16: The time complexity analysis of S^2 Generation

To further demonstrate that the time complexity of the S^2 data generation mechanism is linearly related $\mathcal{O}(L)$ to the length of the generated time series, we start with a time series of length 16 and generate it every 16 lengths until 512. We switch to a different random seed for each generation and repeat the experiment 1280 times. The average time of each data generation is shown in Figure 16. The linear fit line of the result shows that the time complexity of data generation is linearly related to the sequence length when sampling failure is not considered.

B.9 The Limitations of S^2 Generation Mechanism

As outlined in the abstract and introduction, to address the scarcity of training data for time series foundation models, this work proposes a dual-modal data generation mechanism grounded in complex dynamical systems theory (detailed in Section 3.1). This mechanism enables comprehensive coverage of time series representation spaces through unrestricted, high-quality generation. However, generating symbolic expressions (complex systems) via randomized binary tree algorithms occasionally results in oversized trees, leading to overly intricate symbolic systems. This issue narrows the domain of symbolic functions $f(\cdot)$, hinders sampling of stimulus-driven time series X, and reduces sampling efficiency. Notably, differential and integral operations—complex linear transformations—severely degrade sampling speed. Consequently, these operations are excluded from the current S^2 dataset generation. Future work will explore integrating ordinary and partial differential equations into the

S^2 framework to enrich symbolic expression diversity (complex systems) and further enhance the representational capacity of generated time series data.

C Implementation Details

In this section, we first provide a detailed introduction to the datasets and evaluation metrics used for the five TSA tasks. Subsequently, we elaborate on the training details of our experiments, including how we pre-trained `SymTime` on the S^2 dataset and how we fine-tuned it on downstream task datasets. All experiments and deep neural networks training are implemented in PyTorch on 8 NVIDIA A6000 48GB GPU.

C.1 Downstream Tasks Datasets Details

We conduct experiments using the TimesNet benchmark [72], with a detailed description of the dataset provided in Table 15. Specifically, we utilize 8 datasets including ETTh1, ETTh2, ETTm1, ETTm2 [80], Electricity [102], Traffic [103], Weather [101], and Exchange [104] to conduct long-term time series forecasting experiments. Our model, `SymTime`, employ input series of lookback lengths 96 and 512, with forecast horizons of 96, 192, 336, and 720. For short-term forecasting experiments, we employ the M4 benchmark dataset, predicting data of various frequencies [73]. In the time series imputation task, we test on 6 datasets—ETTh1, ETTh2, ETTm1, ETTm2 [80], Electricity [102], and Weather [101]—with mask rates of 12.5%, 25%, 37.5%, and 50%. For time series classification, we utilize ten UEA multivariate time series classification benchmark datasets [105]. For anomaly detection in time series, we experiment with five datasets: SMD [106], MSL [107], SMAP [107], SWaT [108], and PSM [109].

C.2 Correspondence between Positive and Negative Samples in `SymTime`

In our S^2 data generation mechanism, we randomly construct a symbolic expression $f(\cdot)$ and an input stimulus time series X, and then forward propagate the symbolic expression to obtain the complex system's response time series Y. Therefore, the generated time series Y has a natural generating-being relationship with the symbolic expression $f(\cdot)$. Since symbolic expressions can model complex systems, and different symbolic expressions can correspond to different symbolic systems, the generated time series can also reflect the corresponding complex system's representation. When performing contrastive learning, we consider the time series and the symbolic expression that generated it as positive samples, and other unrelated symbols as negative samples.

C.3 Metrics

We assess the five TSA tasks using various metrics. For long-term forecasting and imputation tasks, we employ mean squared error (MSE) and mean absolute error (MAE). For short-term forecasting, we utilize symmetric mean absolute percentage error (SMAPE), mean absolute scaled Error (MASE), and overall weighted average (OWA), with OWA being a metric unique to the M4 competition. For time series classification tasks, we use classification accuracy as the metric. For anomaly detection tasks, we adopt precision, recall, and F1-score as our evaluation metrics. The calculations for these metrics are as follows.

$$\mathrm{MSE} = \sum_{i=1}^{n} \left(y_i - \hat{y}_i\right)^2, \tag{10}$$

$$\mathrm{MAE} = \sum_{i=1}^{n} \left|y_i - \hat{y}_i\right|, \tag{11}$$

$$\mathrm{SMAPE} = \frac{200}{T} \sum_{i=1}^{T} \frac{\left|\mathbf{X}_i - \hat{\mathbf{Y}}_i\right|}{\left|\mathbf{X}_i\right| + \left|\hat{\mathbf{Y}}_i\right|}, \tag{12}$$

$$\mathrm{MAPE} = \frac{100}{T} \sum_{i=1}^{T} \frac{\left|\mathbf{X}_i - \hat{\mathbf{Y}}_i\right|}{\left|\mathbf{X}_i\right|}, \tag{13}$$

Table 15: Dataset descriptions. The dataset size is organized in (Train, Validation, Test).

Tasks	Dataset	Dim	Series Length	Dataset Size	Information (Frequency)
Forecasting (Long-term)	ETTm1, ETTm2	7	{96, 192, 336, 720}	(34465, 11521, 11521)	Electricity (15 mins)
	ETTh1, ETTh2	7	{96, 192, 336, 720}	(8545, 2881, 2881)	Electricity (15 mins)
	Electricity	321	{96, 192, 336, 720}	(18317, 2633, 5261)	Electricity (Hourly)
	Traffic	862	{96, 192, 336, 720}	(12185, 1757, 3509)	Transportation (Hourly)
	Weather	21	{96, 192, 336, 720}	(36792, 5271, 10540)	Weather (10 mins)
	Exchange	8	{96, 192, 336, 720}	(5120, 665, 1422)	Exchange rate (Daily)
Forecasting (short-term)	M4-Yearly	1	6	(23000, 0, 23000)	Demographic
	M4-Quarterly	1	8	(24000, 0, 24000)	Finance
	M4-Monthly	1	18	(48000, 0, 48000)	Industry
	M4-Weakly	1	13	(359, 0, 359)	Macro
	M4-Daily	1	14	(4227, 0, 4227)	Micro
	M4-Hourly	1	48	(414, 0, 414)	Other
Imputation	ETTm1, ETTm2	7	96	(34465, 11521, 11521)	Electricity (15 mins)
	ETTh1, ETTh2	7	96	(8545, 2881, 2881)	Electricity (15 mins)
	Electricity	321	96	(18317, 2633, 5261)	Electricity (15 mins)
	Weather	21	96	(36792, 5271, 10540)	Weather (10 mins)
Classification (UEA)	EthanolConcentration	3	1751	(261, 0, 263)	Alcohol Industry
	FaceDetection	144	62	(5890, 0, 3524)	Face (250Hz)
	Handwriting	3	152	(150, 0, 850)	Handwriting
	Heartbeat	61	405	(204, 0, 205)	Heart Beat
	JapaneseVowels	12	29	(270, 0, 370)	Voice
	PEMS-SF	963	144	(267, 0, 173)	Transportation (Daily)
	SelfRegulationSCP1	6	896	(268, 0, 293)	Health (256Hz)
	SelfRegulationSCP2	7	1152	(200, 0, 180)	Health (256Hz)
	SpokenArabicDigits	13	93	(6599, 0, 2199)	Voice (11025Hz)
	UWaveGestureLibrary	3	315	(120, 0, 320)	Gesture
Anomaly Detection	SMD	38	100	(566724, 141681, 708420)	Server Machine
	MSL	55	100	(44653, 11664, 73729)	Spacecraft
	SMAP	25	100	(108146, 27037, 427617)	Spacecraft
	SWaT	51	100	(396000, 99000, 449919)	Infrastructure
	PSM	25	100	(105984, 26497, 87841)	Server Machine

$$\mathrm{MASE} = \frac{1}{T}\sum_{i=1}^{T}\frac{\left|\mathbf{X}_i - \hat{\mathbf{Y}}_i\right|}{\frac{1}{T-q}\sum_{j=q+1}^{T}\left|\mathbf{X}_j - \mathbf{X}_{j-q}\right|}, \tag{14}$$

$$\mathrm{OWA} = \frac{1}{2}\left[\frac{\mathrm{SMAPE}}{\mathrm{SMAPE}_{\text{Naïve2}}} + \frac{\mathrm{MASE}}{\mathrm{MASE}_{\text{Naïve2}}}\right], \tag{15}$$

Table 16: The model architecture of the time series and symbolic encoders in `SymTime`.

Encoder	Layers	d_{model}	d_{ff}	Heads	Params
Time Series	6	512	2048	8	19M
Symbol	6	768	3072	12	67M

where, y_i is the ground true value, $\hat{y}_i$ is the model prediction, q is the peridoicity of the time series data. $\mathbf{X}, \hat{\mathbf{Y}} \in \mathbb{R}^{T \times C}$ are the ground truth and prediction results of the future with T time points and C dimensions. $\mathbf{X}_i$ means the i-th future time point.

C.4 Pre-training

Model Architecture. The model architecture of the time series and symbolic encoders in `SymTime` are shown in Table 16.

Model Hyper-parameter. The parameter configurations for the time series encoder and symbol encoder in `SymTime` are shown in Table 16. During model pre-training, we primarily set three hyperparameters: (1) the masking ratio of time series patches, (2) the masking ratio for natural language symbols, and (3) the proportion factor α used to balance pseudo-targets in momentum distillation. Based on the masked time series modeling pre-training experimental configuration of PatchTST [54] and SimMTM [27], we set the masking ratio for time series to 40%. Following the experimental configuration of BERT in masked language modeling [19, 55], we set the masking ratio for symbolic data to 15%. Based on the experimental configuration of momentum distillation in ALBEF [60, 124, 59], we set α to 0.6.

Training Configurations. During the pre-training of `SymTime`, we employ AdamW [125, 126] as the optimizer with the defult hyperparameter configuration for (β_1, β_2) as (0.9, 0.999). Then, we utilize the OneCycle policy to dynamically adjust the learning rate. We set the warmup epochs to 10, during which the learning rate gradually grows up to an initial value of 5×10^{-5}, and then adjust it dynamically using a cosine annealing schedule, with the minimum learning rate set at 1×10^{-7}. We conduct pre-training using data parallelism on a hardware setup consisting of 8 NVIDIA RTX A6000 GPUs with 48GB of memory each. We set the batch size to 128 and trained for a total of 85 epochs. Unlike SNIP [12], we do not generate data on-the-fly during training for pre-training. Instead, we prepare the data in advance and then load it into the device for pre-training. Due to the large size of our generat S^2 dataset, we load data into the GPU in batches during each epoch for pre-training.

C.5 Fine-tuning

For the five major tasks in TSA, we conduct downstream task fine-tuning experiments using the configurations in Table 17. For all downstream task fine-tuning experiments, we employ the Adam optimizer [125, 126] with hyperparameters (β_1, β_2) set to $(0.9, 0.999)$. The LR in the table represents the initial learning rate and we utilize the dynamic learning rate adjustment strategy from TimesNet [72].

Table 17: Experiment configuration of `SymTime` fine-tuning.

Tasks / Configurations	**Model Parameter**			**Training Configurations**			
	d_{model}	d_{ff}	Layers	LR	Loss	Batch Size	Epochs
Long-term Forecasting	512	2048	3, 6	$10^{-4} - 5 \times 10^{-4}$	MSE	4-64	20
Short-term Forecasting			2, 3	$10^{-4} - 2 \times 10^{-4}$	SMAPE	8-32	16
Classification			1-6	$10^{-4} - 5 \times 10^{-3}$	Cross Entropy	4-64	64
Imputation			2, 3, 6	$10^{-4} - 5 \times 10^{-4}$	MSE	4-64	32
Anomaly Detection			3, 6	$10^{-4} - 5 \times 10^{-4}$	MSE	4-64	12

C.6 Ablation Experiments Details

Ablation study on pre-training strategies and objectives. To further verify the effectiveness of our series-symbol pre-training strategy and objectives, we establish 8 distinct ablation experiment groups and a control group. The specific configurations of these 8 ablation experiment groups are as follows.

1. **Freeze**: All parameters in the pre-trained time series encoder are frozen, with only the linear projection layer for outputting prediction results fine-tuned.
2. **Read-Data**: Since real time series data does not have matching symbolic expression information, we temporarily discarded the symbolic encoder and momentum model in this ablation experiment and only used real time series data for pre-training using the MTM method.
3. **w/o Pretrain**: No series-symbol pre-training is conducted; the time series encoder with initialized parameters is used for downstream task experiments.
4. **w/o MTM**: The masked time series modeling (MTM) is removed from the pre-training objectives.
5. **w/o MLM**: The masked language modeling (MLM) is removed from the pre-training objectives.
6. **w/o T2S**: The contrastive loss from time series to symbols is removed from the pre-training objectives.
7. **w/o S2T**: The contrastive loss from symbols to time series is removed from the pre-training objectives.
8. **w/o Symbol**: Only time series data from the S^2 dataset are used to pre-train the time series encoder via MTM, disregarding the correspondence with symbols.
9. **w/o Distill**: The contrastive loss in pre-training does not use the pseudo objective of momentum distillation.

C.7 Ablation Experiments on Short-term Forecasting

Setup. We adopt the same experimental setup as in Section 4.4 to conduct ablation studies on short-term time series forecasting tasks. We first select the Yearly and Monthly sub-datasets from the M4 benchmark dataset [73] to perform ablation experiments on SymTime's pre-training objectives. We choose SMAPE as the evaluation metric and the average results with error bars are shown in Figure 17.

Results. Figure 17 (a) indicates that SymTime's performance drops sharply when the backbone encoder is frozen and no pre-training is conducted. When some pre-training objectives are removed, the model's performance in short-term time series forecasting also declines, but the sensitivity of performance degradation is not as pronounced as in long-term forecasting experiments. Figure 17 (a) shows that as the size of the pre-training dataset increases, SymTime's performance on the Quarterly dataset improves significantly.

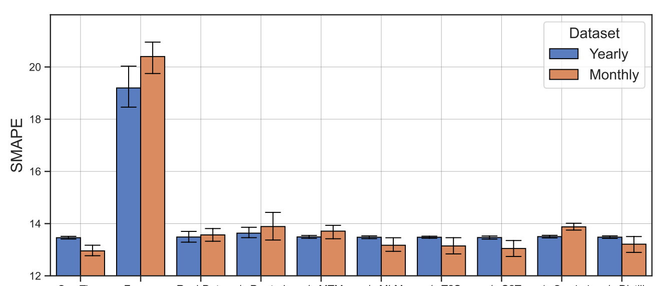

Figure 17: Ablation study on short-term forecasting task.

C.8 The Ablation of Backbone in `SymTime`

Setup. `SymTime` is composed of two encoders with Transformer architectures [127]. The time series encoder is composed of a multi-layer Transformer encoder architecture. The symbolic expression encoder is pre-trained with a large language model. We conducted an ablation experiment on the

SymTime model architecture by changing the encoder structure through control variables. Specifically, we adjusted the number of parameters (d_{model} and d_{ff}) of the time series encoder and the type of pre-trained LLM used by the symbolic encoder to set different control groups:

- **SymTime:** The original model architecture in Table 16 uses the DistilBERT [55].
- **SymTime$_{small}$:** Change the time series encoder to a 3-layer Transformer model with $d_{\mathrm{model}} = 386$ and $d_{\mathrm{ff}} = 1536$.
- **SymTime$_{large}$:** Change the time series encoder to a 6-layer Transformer model with $d_{\mathrm{model}} = 768$ and $d_{\mathrm{ff}} = 3072$.
- **BERT-base$_{110M}$:** Replace the pre-trained LLM with BERT-base$_{110M}$ [19].
- **BERT-large$_{340M}$:** Replace the pre-trained LLM with BERT-large$_{340M}$ [19].
- **GPT2-small$_{124M}$:** Replace the pre-trained LLM with GPT2-small$_{124M}$ [94].
- **GPT2-medium$_{335M}$:** Replace the pre-trained LLM with GPT2-medium$_{335M}$ [94].

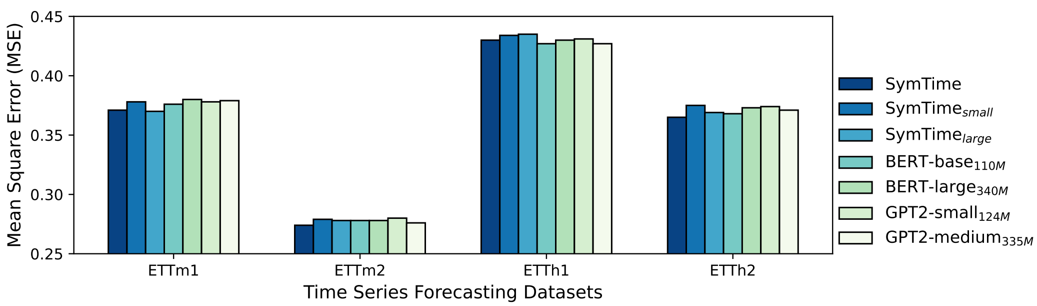

Figure 18: The ablation results of backbone in `SymTime`. We choose to conduct experimental verification on four ETT datasets [80] for long-term time series prediction.

Results. As shown in Figure 18, changing the backbone of `SymTime` does not significantly affect the experimental results in long-term time series forecasting tasks. Ablation experiments on pre-training objectives (Equation 7) reveal that the performance gains achieved during pre-training are primarily due to the pre-training paradigm of masked modeling of time series and symbolic expressions and contrastive learning. This pre-training approach is independent of the model backbone. Therefore, if the basic pre-training requirements are met (pre-training loss can be successfully optimized), a more lightweight model can be used for fine-tuning on downstream tasks.

C.9 The Impact and Ablation of Pre-interpolation on Time Series Imputation Task

`SymTime` adds masks randomly at the patch level during pre-training for time series reconstruction. While in the imputation task, masks are added randomly at the data point level. Additionally, high masking rates may disrupt the original trend and periodic features of the time series. Therefore, we use Peri-midFormer's method to apply per-interpolation to the masked time series to restore the disrupted periodic features [63, 72, 89, 1, 128, 129]. It is important to note that this method is general and independent of deep learning models. The use of this method aims to further enhance the potential of deep learning models. To further verify the effectiveness and impact of the per-interpolation method, we conduct experiments on the ECL time series imputation dataset, with results shown in Table 18. Taking the ECL time series dataset 0.5 mask ratio as an example, the effect of pre-interpolation is shown in Figure 19. We perform experiments with masking rate of $\{0.125, 0.25, 0.375, 0.50\}$ and compare models such as Peri-midFormer [63], TimesNet [72], PatchTST [54], DLinear [87] and Pyraformer [130]. Per-interpolation represents the experimental results obtained using only linear interpolation. For a missing time series x_t at time t, the method can be described as:

$$x_t = \begin{cases} \frac{x_{t-1}+x_{t+1}}{2}, & if\ (x_{t-1}) \neq \text{None}\ \&\ (x_{t+1} \neq \text{None}) \\ x_{t+1}, & if\ (x_{t-1}) = \text{None}\ \&\ (x_{t+1} \neq \text{None}) \\ x_{t-1}, & if\ (x_{t-1}) \neq \text{None}\ \&\ (x_{t+1} = \text{None}) \end{cases}, \tag{16}$$

Table 18: Ablation Experiments of pre-interpolation in inputation task on ECL dataset. The per-interpolation results for Peri-midFormer, TimesNet, PatchTST, DLinear and Pyraformer are copied from [63].

Methods	Metric	w/o per-interpolation				with per-interpolation			
		0.125	0.25	0.375	0.5	0.125	0.25	0.375	0.5
Per-interpolation	MSE	-	-	-	-	0.086	0.110	0.149	0.206
	MAE	-	-	-	-	0.188	0.213	0.251	0.301
SymTime (Ours)	MSE	0.050	0.064	0.074	0.092	0.037	0.047	0.060	0.075
	MAE	0.145	0.169	0.181	0.206	0.122	0.139	0.160	0.181
Peri-midFormer [63]	MSE	0.073	0.092	0.107	0.122	0.047	0.053	0.067	0.085
	MAE	0.187	0.214	0.231	0.248	0.140	0.162	0.179	0.195
TimesNet [72]	MSE	0.088	0.092	0.096	0.102	0.081	0.083	0.086	0.091
	MAE	0.203	0.208	0.214	0.221	0.196	0.198	0.201	0.207
PatchTST [54]	MSE	0.061	0.072	0.082	0.097	0.050	0.059	0.070	0.087
	MAE	0.170	0.185	0.198	0.216	0.148	0.164	0.181	0.202
DLinear [87]	MSE	0.084	0.113	0.141	0.173	0.050	0.062	0.789	0.105
	MAE	0.206	0.243	0.273	0.303	0.144	0.164	0.189	0.225
Pyraformer [130]	MSE	0.297	0.294	0.296	0.299	0.165	0.165	0.171	0.173
	MAE	0.383	0.380	0.381	0.383	0.290	0.291	0.293	0.295

where, x_{t-1} and x_{t+1} represent the values at the previous and next time points, respectively, while None indicates a missing value. The results in Table 18 show that this method significantly improves the performance of all models in a model-independent manner.

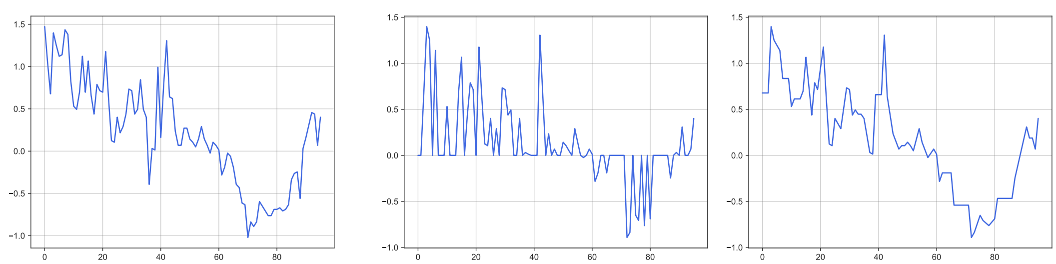

(a) Original data (b) Data with 50% missing values (c) Per-interpolated data

Figure 19: Visualization of original data, data with 50% missing values and pre-interpolated data of ECL dataset.

D Related Work

D.1 Time Series Foundation Models

In CV and NLP [18, 131, 132], PTFMs have been demonstrated to adapt to a variety of downstream tasks after fine-tuning on specific datasets, exhibiting excellent generalization and scalability. Inspired by this, recent years have seen significant progress in PTFMs for TSA [24, 25, 133, 134], with the emergence of various pre-training methods. MOIRAI, through MTM and reconstruction, has been pre-trained on large datasets (27B), yielding a universal forecasting model with significant zero-shot advantages [28]. Timer, after generative pre-training on large datasets (1B), has performed well in forecasting [29]. TimeGPT trained a encoder-decoder Transformer with 100B data [30]. COMET, using multi-level contrastive learning on a large ECG dataset, has obtained a medical time series PTFMs with few-shot advantages [4].

As discussed in Appendix Section B.4, these baseline models still face challenges related to data scarcity and data imbalance. In the next section, we introduce the proposed data generation mechanism and the corresponding dual-modality foundation model designed to address these issues.

D.2 Deep Learning and Symbolic Regression

The central thesis of this paper is to regard time series as representations of complex dynamical systems [135]. Traditionally, complex systems are modeled by observing time series utilizing ODE and PDE [15]. With the advancement of machine learning, symbolic regression (SR) [136], as a supervised learning method, can discover hidden mathematical expressions from numerical series. Although genetic algorithms (GAs) are the mainstream approach for SR [45, 46], deep learning-based methods have also made significant progress. [14] constructed an end-to-end SR model using Transformers, while SNIP built a large-scale pre-trained model through contrastive learning on symbolic expressions and numerical observations [12]. Both methods treat symbolic expressions as nature language and use deep neural networks to learn their features. Therefore, this paper employs a pre-trained LLM as a symbol encoder to learn the features of symbolic expressions and jointly trains a time series foundation model imbued with semantic information through contrastive learning [129].

D.3 Time Series Forecasting Models Based on Synthetic Data

Unlike the representation pre-training conducted on the large synthetic S^2 dataset in this paper, previous TSA models trained on synthetic data were mainly based on Prior-data Fitted Networks (PFN) [137, 138, 139]. This model learns prior distributions from synthetic data using Bayesian methods, enabling zero-shot inference. ForecastPFN generated a large number of synthetic time series by separately modeling the seasonal trend, global trend and noise based on given constraint expressions [47]. Although PFN trained in this way offered certain zero-shot and few-shot advantages, this approach was limited to generating time series through sampling fixed expressions and performing linear combinations. In contrast, the S^2 data generation mechanism proposed in this paper can sample an infinite variety of symbolic expressions [12, 14, 48, 129]. TimePFN constructed synthetic datasets by filtering real time series with linear and periodic convolution kernels, training PFN for zero-shot inference [140]. However, this method depends on real-world time series for filtering and linear transformations between channels. Compared to the S^2 data generation mechanism, it can not create large-scale and fully representative synthetic datasets for model pre-training.

E Visualization

E.1 Long-term Time Series Forecasting with 96 Prediction on ETTh1 (Figure 20) and ECL (Figure 21)

E.2 Short-term Time Series Forecasting on M4 Weekly (Figure 22) and Monthly (Figure 23)

E.3 Time Series Imputation with 50% mask rate on ETTh1 (Figure 24) and ETTm1 (Figure 25)

F Full Results

For the five downstream TSA tasks results, we use (1) Peri-midFormer for Peri-midFormer [63], (2) uni2ts for Moirai [28], (3) Large-Time-Series-Model for Timer [29], (4) Time-LLM for Time-LLM [17], (5) TSLANet for TSLANet [83], (6) S2IP-LLM for S2IP-LLM [82], (7) NeurIPS²023-One-Fits-All for GPT4TS [2], (8) UniTS for UniTS [92], (9) moment for Moment [93], (10) FilterNet for FilterNet [91], (11) RTSF for RLinear [141], and (12) Time-Series-Library for other models, such as TimesNet [72], PatchTST [54], TimeMixer [89], iTransformer [74], DLinear [87], Autoformer [75] and Informer [80], TimeXer [62], Chronos-forecasting for Chronos [22]. To ensure a fair comparison, we use the original experimental configuration in the project scripts.

F.1 Time Series Long-term Forecasting with 96 look-back windows (Table 19, Table 20 and Table 21)

F.2 Time Series Long-term Forecasting with 336 look-back windows (Table 22)

F.3 Time Series Long-term Forecasting with 512 look-back windows (Table 23)

F.4 Time Series Short-term Forecasting (Table 24 and Table 25)

F.5 Time Series Classification (Table 26 and Table 27)

F.6 Time Series Imputation (Table 28 and Table 29)

F.7 Time Series Anomaly Detection (Table 30)

F.8 Pre-training and Fine-tuning Results of Long-term Forecasting (Table 31)

F.9 Pre-training and Fine-tuning Results of Short-term Forecasting (Table 32)

F.10 Pre-training and Fine-tuning Results of classification (Table 33)

F.11 Pre-training and Fine-tuning Results of Imputation (Table 34)

F.12 Pre-training and Fine-tuning Results of Anomaly Detection (Table 35)

G Impact Statement

The potential value of this work lies in its ability to mitigate fundamental challenges in TSA, such as the lack of sufficient labeled data and the issue of imbalanced datasets. By generating rich, diverse, and high-quality synthetic data, our approach not only addresses these issues but also opens new avenues for improving model generalization across a wide range of applications. Furthermore, the dual-modality framework, which combines time series data with symbolic semantics, introduces a novel way of enriching the representation power of models, allowing them to better understand complex temporal dynamics and their underlying patterns.

We foresee that pre-training models on synthetic datasets, especially those that combine structured symbolic information with time series data, will become a key development trend in the TSA field. This could pave the way for more robust and scalable solutions in a variety of domains, including finance, healthcare, and climate modeling, where time series data is abundant, but labeled data is often scarce or hard to obtain.

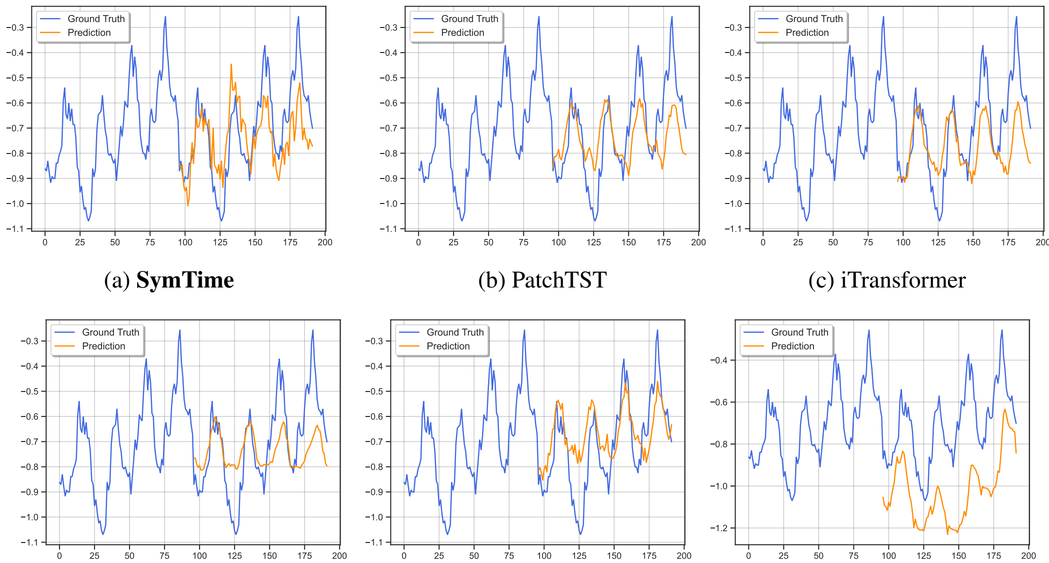

(a) **SymTime** (b) PatchTST (c) iTransformer

(d) TimesNet (e) DLinear (f) Autoformer

Figure 20: Visualization of long-term forecasting with 96 prediction length of ETTh1 dataset.

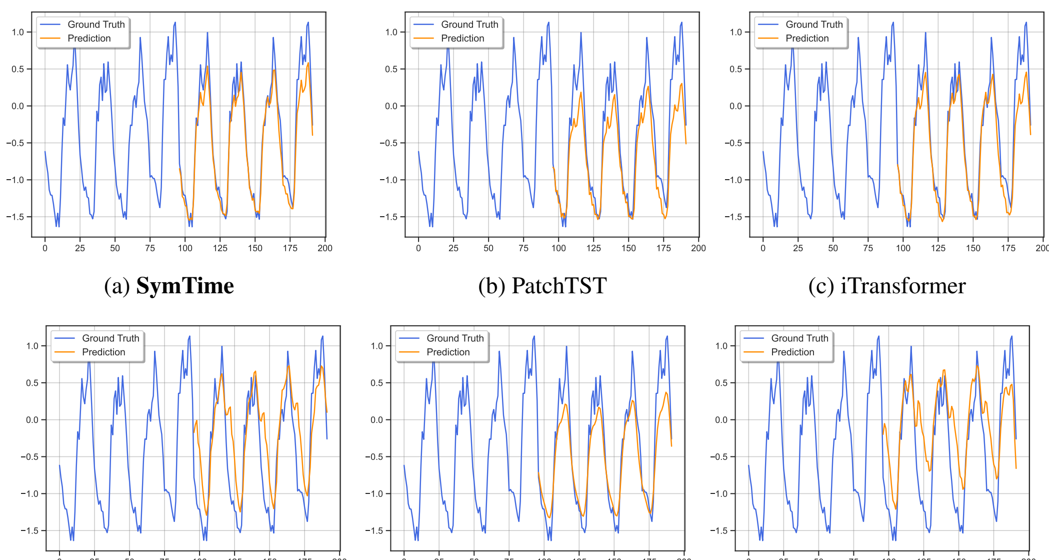

(a) **SymTime** (b) PatchTST (c) iTransformer

(d) TimesNet (e) DLinear (f) Autoformer

Figure 21: Visualization of long-term forecasting with 96 prediction length of Electricity dataset.

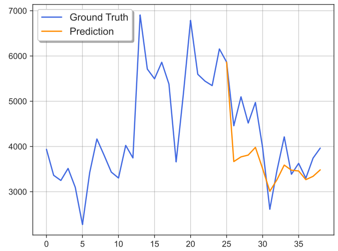

(a) **SymTime**

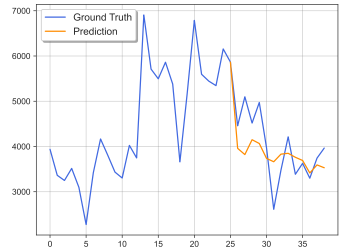

(b) PatchTST

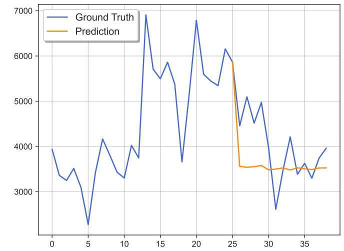

(c) iTransformer

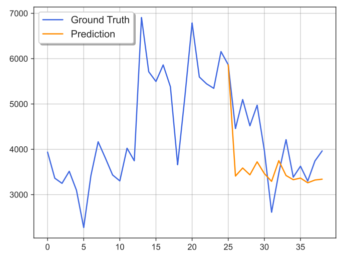

(d) TimesNet

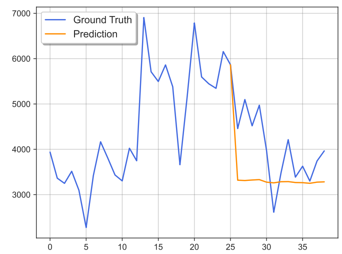

(e) DLinear

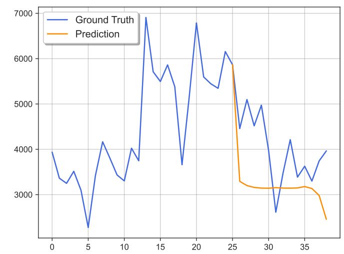

(f) Autoformer

Figure 22: Visualization of time series short-term forecasting in M4 dataset Weekly.

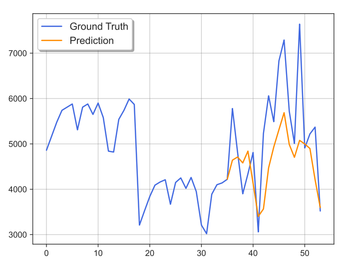

(a) **SymTime**

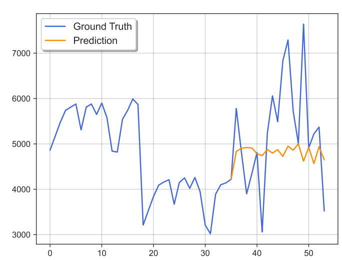

(b) PatchTST

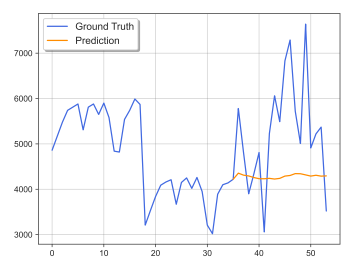

(c) iTransformer

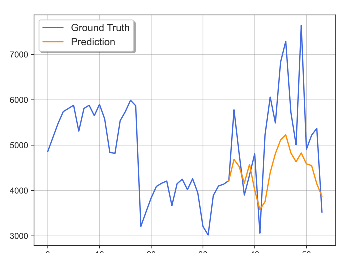

(d) TimesNet

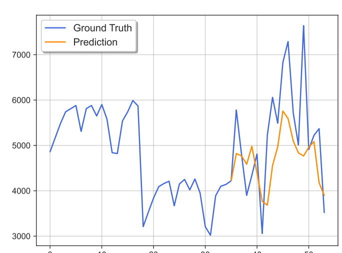

(e) DLinear

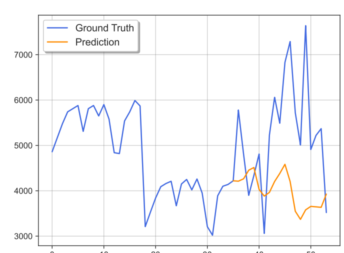

(f) Autoformer

Figure 23: Visualization of time series short-term forecasting in M4 dataset Monthly.

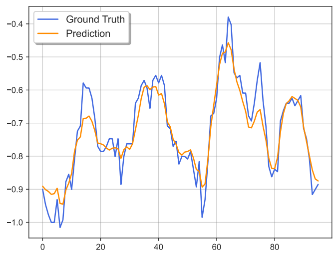

(a) **SymTime**

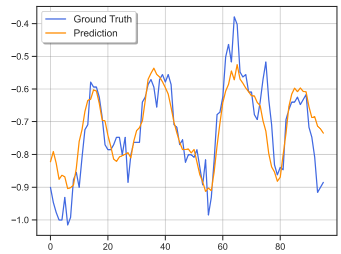

(b) PatchTST

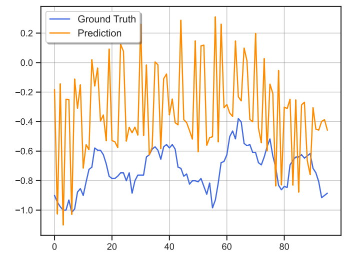

(c) iTransformer

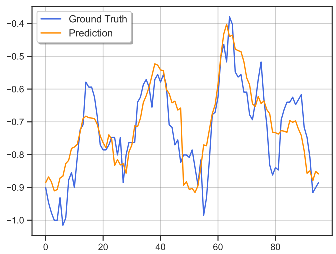

(d) TimesNet

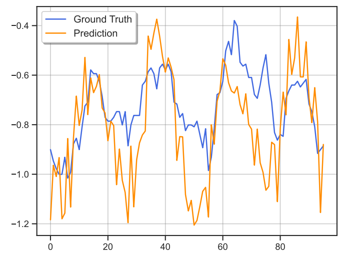

(e) DLinear

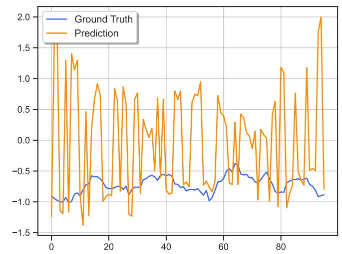

(f) Autoformer

Figure 24: Visualization of time series imputation with 50% mask rate of ETTh1 dataset.

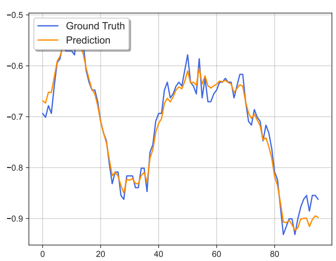

(a) **SymTime**

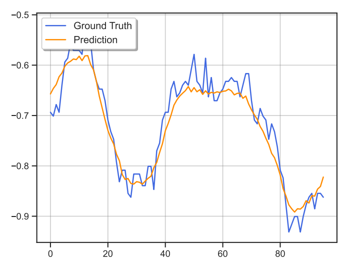

(b) PatchTST

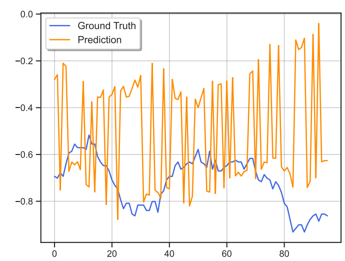

(c) iTransformer

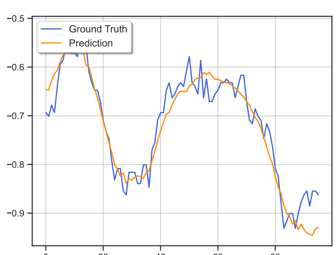

(d) TimesNet

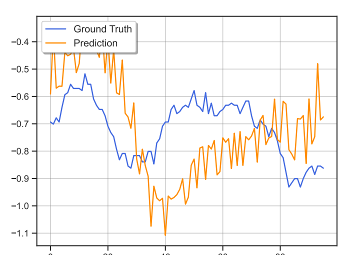

(e) DLinear

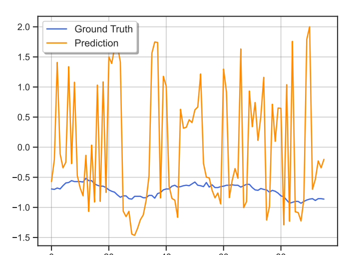

(f) Autoformer

Figure 25: Visualization of time series imputation with 50% mask rate of ETTm1 dataset.

Table 19: Full results for the long-term forecasting task compared with Peri-midFormer [63], Moirai [28], Timer [29], Moment [93], Time-LLM [17], TSLANet [83], S^2IP-LLM [82] and GPT4TS [2]. (* means former, T-LLM is Time-LLM, S-LLM is S^2IP-LLM.) To ensure fairness in the comparison, we set the look-back window length of all models to **96**. Since the Timer and Moirai need to input a longer series to build a token, their windows are **672**. S^2IP-LLM has a gradient explosion when the window is **96**, so its look-back window is **512**. The standard deviation is within 0.5%. **Red**: best, Blue: second best.

Methods		`SymTime` **(Ours)**		Peri-mid* [63]		Moirai [28]		Timer [29]		Moment [93]		T-LLM [17]		TSLANet [83]		S-LLM [82]		GPT4TS [2]	
Metrics		MSE	MAE	MSE	MAE	MSE	MAE	MSE	MAE	MSE	MAE	MSE	MAE	MSE	MAE	MSE	MAE	MSE	MAE
ETTm1	96	0.318	0.353	0.334	0.370	0.311	0.358	0.315	0.354	0.305	0.353	0.304	0.359	0.321	0.362	0.325	0.371	0.293	0.362
	192	0.362	0.380	0.382	0.391	0.381	0.402	0.369	0.378	0.369	0.386	0.368	0.396	0.361	0.383	0.361	0.397	0.374	0.392
	336	0.386	0.402	0.417	0.418	0.436	0.432	0.425	0.428	0.392	0.404	0.383	0.393	0.383	0.404	0.385	0.403	0.389	0.404
	720	0.419	0.423	0.501	0.461	0.466	0.476	0.442	0.447	0.425	0.436	0.420	0.429	0.445	0.437	0.426	0.446	0.421	0.423
	Avg	0.371	**0.390**	0.409	0.410	0.398	0.417	0.388	0.402	0.373	0.395	**0.369**	0.394	0.377	0.397	0.374	0.404	0.369	0.395
ETTm2	96	0.174	0.257	0.174	0.255	0.179	0.267	0.168	0.254	0.170	0.264	0.177	0.269	0.179	0.261	0.174	0.263	0.171	0.265
	192	0.238	0.299	0.249	0.305	0.244	0.311	0.429	0.425	0.285	0.294	0.239	0.305	0.243	0.303	0.232	0.306	0.226	0.304
	336	0.295	0.337	0.319	0.349	0.335	0.371	0.476	0.457	0.275	0.329	0.301	0.340	0.308	0.345	0.300	0.344	0.288	0.345
	720	0.390	0.392	0.418	0.405	0.425	0.444	0.545	0.497	0.383	0.397	0.382	0.381	0.403	0.401	0.359	0.386	0.372	0.398
	Avg	0.274	**0.321**	0.290	0.328	0.296	0.348	0.405	0.408	0.278	0.321	0.275	0.324	0.283	0.327	0.266	0.325	**0.264**	0.328
ETTh1	96	0.376	0.400	0.382	0.403	0.369	0.408	0.374	0.404	0.385	0.402	0.386	0.395	0.387	0.405	0.380	0.403	0.388	0.399
	192	0.428	0.431	0.436	0.435	0.441	0.450	0.430	0.438	0.449	0.450	0.421	0.424	0.448	0.436	0.410	0.427	0.425	0.429
	336	0.463	0.456	0.492	0.455	0.469	0.469	0.458	0.453	0.455	0.472	0.438	0.450	0.451	0.437	0.426	0.442	0.444	0.455
	720	0.450	0.458	0.508	0.490	0.486	0.490	0.475	0.480	0.480	0.503	0.506	0.510	0.505	0.485	0.610	0.543	0.479	0.477
	Avg	**0.430**	**0.436**	0.455	0.446	0.441	0.454	0.434	0.444	0.442	0.457	0.438	0.445	0.448	0.441	0.456	0.454	0.434	0.440
ETTh2	96	0.293	0.347	0.312	0.358	0.288	0.350	0.315	0.360	0.285	0.343	0.307	0.369	0.289	0.345	0.292	0.353	0.292	0.351
	192	0.364	0.397	0.388	0.403	0.390	0.426	0.411	0.423	0.368	0.403	0.349	0.384	0.362	0.391	0.355	0.388	0.351	0.394
	336	0.385	0.423	0.443	0.443	0.441	0.435	0.465	0.467	0.380	0.421	0.394	0.420	0.350	0.389	0.368	0.417	0.380	0.421
	720	0.420	0.441	0.455	0.459	0.487	0.435	0.521	0.515	0.423	0.466	0.426	0.454	0.418	0.439	0.434	0.460	0.424	0.446
	Avg	0.365	0.402	0.400	0.416	0.402	0.411	0.428	0.441	0.364	0.408	0.369	0.407	**0.355**	**0.391**	0.362	0.405	0.359	0.403
Weather	96	0.166	0.213	0.157	0.201	0.156	0.206	0.289	0.331	0.168	0.228	0.172	0.221	0.177	0.216	0.162	0.213	0.184	0.224
	192	0.212	0.254	0.244	0.273	0.229	0.274	0.314	0.349	0.226	0.262	0.194	0.241	0.226	0.258	0.197	0.246	0.230	0.263
	336	0.267	0.294	0.283	0.303	0.282	0.316	0.339	0.363	0.257	0.303	0.286	0.282	0.279	0.588	0.281	0.299	0.285	0.302
	720	0.342	0.344	0.364	0.355	0.395	0.401	0.375	0.388	0.331	0.355	0.337	0.332	0.355	0.346	0.333	0.339	0.362	0.352
	Avg	0.247	0.276	0.262	0.283	0.265	0.299	0.329	0.358	0.245	0.287	0.247	**0.269**	0.259	0.352	**0.243**	0.274	0.265	0.285
ECL	96	0.162	0.253	0.151	0.245	0.137	0.221	0.150	0.244	0.153	0.247	0.149	0.242	0.176	0.261	0.149	0.251	0.186	0.272
	192	0.173	0.264	0.168	0.259	0.158	0.243	0.159	0.252	0.166	0.252	0.167	0.261	0.182	0.268	0.171	0.269	0.190	0.277
	336	0.194	0.285	0.184	0.268	0.167	0.255	0.190	0.271	0.172	0.269	0.188	0.270	0.199	0.285	0.199	0.291	0.205	0.292
	720	0.220	0.304	0.207	0.297	0.207	0.290	0.210	0.300	0.213	0.311	0.214	0.301	0.240	0.317	0.244	0.319	0.245	0.323
	Avg	0.187	0.276	0.178	0.267	**0.167**	**0.252**	0.177	0.267	0.176	0.270	0.180	0.269	0.199	0.283	0.191	0.283	0.206	0.291
Traffic	96	0.432	0.280	0.426	0.277	0.376	0.264	0.391	0.260	0.442	0.295	0.424	0.295	0.398	0.291	0.385	0.289	0.471	0.312
	192	0.444	0.287	0.440	0.283	0.410	0.279	0.426	0.271	0.452	0.301	0.455	0.315	0.430	0.307	0.403	0.308	0.478	0.312
	336	0.458	0.293	0.477	0.311	0.442	0.287	0.451	0.297	0.467	0.309	0.494	0.335	0.494	0.312	0.425	0.299	0.493	0.319
	720	0.492	0.303	0.487	0.308	0.470	0.328	0.475	0.307	0.489	0.316	0.513	0.394	0.528	0.332	0.454	0.326	0.523	0.335
	Avg	0.457	0.291	0.458	0.295	0.424	0.289	0.436	**0.284**	0.463	0.305	0.471	0.334	0.463	0.310	**0.417**	0.306	0.491	0.320
Exchange	96	0.084	0.201	0.083	0.199	0.089	0.211	0.098	0.228	0.091	0.214	0.090	0.209	0.082	0.200	0.147	0.279	0.087	0.218
	192	0.174	0.295	0.190	0.307	0.175	0.289	0.196	0.325	0.185	0.307	0.188	0.310	0.172	0.295	0.234	0.354	0.171	0.294
	336	0.331	0.416	0.401	0.458	0.345	0.423	0.359	0.433	0.345	0.414	0.342	0.427	0.329	0.415	0.403	0.474	0.349	0.418
	720	0.847	0.694	0.879	0.702	0.882	0.744	0.875	0.713	0.874	0.729	0.885	0.707	0.889	0.747	1.103	0.804	0.873	0.713
	Avg	**0.359**	**0.401**	0.388	0.417	0.373	0.417	0.382	0.425	0.374	0.416	0.376	0.414	0.368	0.414	0.472	0.478	0.370	0.411
Average		**0.336**	**0.349**	0.355	0.358	0.346	0.361	0.372	0.378	0.339	0.357	0.341	0.357	0.344	0.364	0.348	0.366	0.345	0.359

Table 20: Full results for the long-term forecasting task compared with FilterNet [91], TimesNet [72], iTransformer [74], PatchTST [54], RLinear [141], DLinear [87] and TimeMixer [89]. (* means former, TNet is TimesNet, PTST is PatchTST, TMixer is TimeMixer) To ensure fairness in the comparison, we set the look-back window length of all models to **96**. The standard deviation is within 0.5%. **Red**: best, Blue: second best.

Methods		SymTime (Ours)		FilterNet [91]		Chronos [22]		TNet [72]		iTrans* [74]		PTST [54]		RLinear [141]		DLinear [87]		TMixer [89]	
Metrics		MSE	MAE	MSE	MAE	MSE	MAE	MSE	MAE	MSE	MAE	MSE	MAE	MSE	MAE	MSE	MAE	MSE	MAE
ETTm1	96	0.318	0.353	0.321	0.361	0.324	0.371	0.331	0.372	0.343	0.377	0.324	0.365	0.355	0.376	0.345	0.372	0.323	0.361
	192	0.362	0.380	0.367	0.387	0.381	0.400	0.397	0.402	0.381	0.395	0.367	0.389	0.387	0.392	0.382	0.391	0.362	0.383
	336	0.386	0.402	0.401	0.409	0.402	0.415	0.427	0.427	0.419	0.418	0.400	0.409	0.424	0.415	0.414	0.414	0.388	0.403
	720	0.419	0.423	0.477	0.448	0.428	0.435	0.493	0.463	0.487	0.457	0.460	0.445	0.487	0.450	0.473	0.450	0.454	0.442
	Avg	**0.371**	**0.390**	0.392	0.401	0.384	0.405	0.412	0.416	0.407	0.412	0.388	0.402	0.413	0.408	0.403	0.407	0.382	0.397
ETTm2	96	0.174	0.257	0.175	0.258	0.192	0.265	0.185	0.265	0.185	0.271	0.182	0.266	0.182	0.265	0.194	0.293	0.177	0.259
	192	0.238	0.299	0.240	0.301	0.268	0.320	0.256	0.310	0.254	0.314	0.250	0.311	0.246	0.304	0.283	0.360	0.245	0.306
	336	0.295	0.337	0.311	0.347	0.289	0.341	0.314	0.345	0.315	0.352	0.313	0.350	0.307	0.342	0.376	0.423	0.298	0.338
	720	0.390	0.392	0.414	0.405	0.392	0.410	0.424	0.412	0.413	0.407	0.417	0.412	0.407	0.398	0.529	0.509	0.395	0.396
	Avg	**0.274**	**0.321**	0.285	0.328	0.286	0.334	0.295	0.333	0.292	0.336	0.291	0.335	0.286	0.327	0.346	0.396	0.279	0.325
ETTh1	96	0.376	0.400	0.382	0.402	0.408	0.402	0.409	0.425	0.394	0.409	0.381	0.400	0.386	0.395	0.396	0.411	0.385	0.400
	192	0.428	0.431	0.430	0.429	0.459	0.450	0.469	0.460	0.447	0.440	0.429	0.433	0.437	0.424	0.446	0.441	0.441	0.431
	336	0.463	0.456	0.472	0.451	0.445	0.437	0.507	0.478	0.491	0.464	0.475	0.460	0.479	0.446	0.490	0.468	0.482	0.450
	720	0.450	0.458	0.481	0.473	0.482	0.485	0.521	0.497	0.517	0.501	0.517	0.502	0.481	0.470	0.514	0.511	0.504	0.482
	Avg	**0.430**	0.436	0.441	0.439	0.449	0.444	0.476	0.465	0.462	0.454	0.451	0.449	0.446	**0.434**	0.461	0.458	0.453	0.441
ETTh2	96	0.293	0.347	0.293	0.343	0.299	0.354	0.331	0.372	0.300	0.350	0.301	0.351	0.318	0.363	0.348	0.401	0.293	0.343
	192	0.364	0.397	0.374	0.396	0.356	0.390	0.429	0.423	0.380	0.399	0.374	0.398	0.401	0.412	0.473	0.474	0.376	0.396
	336	0.385	0.423	0.417	0.430	0.376	0.423	0.450	0.451	0.422	0.432	0.429	0.439	0.436	0.442	0.588	0.539	0.425	0.432
	720	0.420	0.441	0.449	0.460	0.439	0.467	0.459	0.466	0.429	0.447	0.443	0.461	0.442	0.454	0.829	0.656	0.457	0.459
	Avg	**0.365**	**0.402**	0.383	0.407	0.368	0.408	0.417	0.428	0.383	0.407	0.387	0.412	0.399	0.418	0.559	0.518	0.388	0.408
Weather	96	0.166	0.213	0.162	0.207	0.177	0.231	0.171	0.222	0.176	0.215	0.177	0.219	0.192	0.232	0.197	0.258	0.172	0.220
	192	0.212	0.254	0.210	0.250	0.221	0.263	0.234	0.273	0.226	0.258	0.222	0.258	0.240	0.271	0.237	0.296	0.227	0.259
	336	0.267	0.294	0.265	0.290	0.265	0.311	0.284	0.306	0.281	0.299	0.281	0.299	0.292	0.307	0.282	0.332	0.266	0.294
	720	0.342	0.344	0.342	0.340	0.339	0.347	0.358	0.352	0.359	0.350	0.356	0.348	0.364	0.353	0.347	0.385	0.346	0.347
	Avg	0.247	0.276	**0.245**	**0.272**	0.251	0.288	0.262	0.288	0.260	0.281	0.259	0.281	0.272	0.291	0.266	0.318	0.253	0.280
ECL	96	0.162	0.253	0.147	0.245	0.157	0.249	0.167	0.271	0.148	0.240	0.180	0.272	0.201	0.281	0.210	0.302	0.157	0.249
	192	0.173	0.264	0.160	0.250	0.193	0.288	0.186	0.288	0.165	0.256	0.188	0.279	0.201	0.283	0.210	0.305	0.170	0.261
	336	0.194	0.285	0.173	0.267	0.213	0.304	0.203	0.304	0.179	0.271	0.204	0.296	0.215	0.298	0.223	0.319	0.186	0.276
	720	0.220	0.304	0.210	0.309	0.255	0.336	0.227	0.322	0.209	0.298	0.246	0.328	0.257	0.331	0.258	0.350	0.227	0.311
	Avg	0.187	0.276	**0.173**	0.268	0.204	0.294	0.196	0.296	0.175	**0.267**	0.204	0.294	0.219	0.298	0.225	0.319	0.185	0.274
Traffic	96	0.432	0.280	0.430	0.294	0.420	0.294	0.589	0.316	0.393	0.268	0.461	0.298	0.649	0.389	0.696	0.429	0.479	0.299
	192	0.444	0.287	0.452	0.307	0.436	0.306	0.616	0.328	0.413	0.277	0.467	0.301	0.601	0.366	0.647	0.407	0.490	0.303
	336	0.458	0.293	0.470	0.316	0.491	0.315	0.628	0.333	0.424	0.283	0.483	0.308	0.609	0.369	0.653	0.410	0.493	0.304
	720	0.492	0.303	0.498	0.323	0.526	0.330	0.667	0.352	0.458	0.300	0.517	0.325	0.647	0.387	0.695	0.429	0.534	0.319
	Avg	0.457	0.291	0.463	0.310	0.468	0.312	0.625	0.332	**0.422**	**0.282**	0.482	0.308	0.627	0.378	0.673	0.419	0.499	0.306
Exchange	96	0.084	0.201	0.091	0.211	0.090	0.207	0.115	0.246	0.094	0.216	0.088	0.205	0.093	0.217	0.093	0.226	0.091	0.210
	192	0.174	0.295	0.186	0.305	0.190	0.316	0.213	0.335	0.185	0.307	0.189	0.309	0.184	0.307	0.184	0.324	0.185	0.304
	336	0.331	0.416	0.380	0.449	0.354	0.419	0.367	0.440	0.336	0.422	0.327	0.415	0.351	0.432	0.328	0.436	0.361	0.435
	720	0.847	0.694	0.896	0.712	0.892	0.716	0.978	0.753	0.893	0.716	0.886	0.706	0.886	0.714	0.880	0.705	0.974	0.741
	Avg	**0.359**	**0.401**	0.388	0.419	0.381	0.415	0.418	0.443	0.377	0.415	0.373	0.409	0.379	0.418	0.371	0.423	0.403	0.423
Average		**0.336**	**0.349**	0.346	0.356	0.349	0.363	0.388	0.375	0.347	0.357	0.354	0.361	0.380	0.371	0.413	0.407	0.355	0.357

Table 21: Full results for the long-term forecasting task compared with Autoformer [75], Crossformer [79], FEDformer [77], ETSforemr [76], Stationary [78], LightTS [88], Informer [80]. (Stationary means Nonstationary Transformer. * means former) To ensure fairness in the comparison, we set the look-back window length of all models to **96**. The standard deviation is within 0.5%. **Red**: best, Blue: second best.

Methods		SymTime (Ours)		Autoformer [75]		Cross* [79]		FED* [77]		ETS* [76]		Stationary [78]		LightTS [88]		In* [80]	
Metrics		MSE	MAE	MSE	MAE	MSE	MAE	MSE	MAE	MSE	MAE	MSE	MAE	MSE	MAE	MSE	MAE
ETTm1	96	0.318	0.353	0.501	0.479	0.360	0.399	0.378	0.418	0.375	0.398	0.418	0.415	0.390	0.411	0.619	0.549
	192	0.362	0.380	0.578	0.510	0.422	0.449	0.438	0.449	0.408	0.410	0.506	0.454	0.425	0.436	0.760	0.645
	336	0.386	0.402	0.668	0.552	0.589	0.557	0.456	0.462	0.435	0.428	0.530	0.482	0.463	0.464	1.093	0.812
	720	0.419	0.423	0.602	0.524	0.838	0.706	0.530	0.498	0.499	0.462	0.610	0.525	0.547	0.520	1.114	0.806
	Avg	**0.371**	**0.390**	0.587	0.516	0.552	0.528	0.450	0.457	0.429	0.425	0.516	0.469	0.456	0.458	0.896	0.703
ETTm1	96	0.174	0.257	0.245	0.323	0.274	0.268	0.196	0.284	0.189	0.280	0.240	0.308	0.226	0.323	0.467	0.533
	192	0.238	0.299	0.289	0.345	0.366	0.380	0.264	0.325	0.275	0.319	0.428	0.402	0.361	0.421	0.742	0.664
	336	0.295	0.337	0.342	0.378	0.437	0.453	0.324	0.363	0.314	0.357	0.521	0.449	0.474	0.488	1.184	0.825
	720	0.390	0.392	0.441	0.429	0.506	0.623	0.434	0.428	0.414	0.413	0.602	0.501	0.760	0.631	4.039	1.530
	Avg	**0.274**	**0.321**	0.329	0.369	0.396	0.431	0.305	0.350	0.298	0.342	0.448	0.415	0.455	0.466	1.608	0.888
ETTh1	96	0.376	0.400	0.453	0.459	0.462	0.473	0.376	0.417	0.494	0.479	0.550	0.503	0.448	0.450	0.926	0.741
	192	0.428	0.431	0.481	0.470	0.495	0.484	0.431	0.454	0.538	0.504	0.655	0.569	0.503	0.483	0.968	0.757
	336	0.463	0.456	0.519	0.495	0.693	0.626	0.461	0.469	0.574	0.521	0.791	0.639	0.554	0.513	1.144	0.849
	720	0.450	0.458	0.510	0.508	0.668	0.599	0.502	0.499	0.562	0.535	0.797	0.652	0.627	0.578	1.214	0.880
	Avg	**0.430**	**0.436**	0.491	0.483	0.580	0.545	0.442	0.460	0.542	0.510	0.698	0.591	0.533	0.506	1.063	0.807
ETTh2	96	0.293	0.347	0.383	0.416	0.367	0.347	0.346	0.390	0.340	0.391	0.417	0.432	0.417	0.448	3.132	1.425
	192	0.364	0.397	0.479	0.467	0.450	0.459	0.428	0.439	0.430	0.439	0.529	0.486	0.546	0.520	5.552	1.957
	336	0.385	0.423	0.476	0.481	0.532	0.521	0.469	0.474	0.485	0.479	0.591	0.517	0.619	0.554	4.926	1.873
	720	0.420	0.441	0.494	0.503	0.614	0.633	0.473	0.486	0.500	0.497	0.601	0.531	0.972	0.704	4.201	1.741
	Avg	**0.365**	**0.402**	0.458	0.467	0.491	0.490	0.429	0.447	0.439	0.452	0.534	0.491	0.639	0.556	4.453	1.749
Weather	96	0.166	0.213	0.276	0.343	0.174	0.243	0.218	0.299	0.197	0.281	0.184	0.233	0.174	0.235	0.357	0.415
	192	0.212	0.254	0.305	0.361	0.235	0.307	0.281	0.344	0.237	0.312	0.248	0.286	0.218	0.276	0.458	0.456
	336	0.267	0.294	0.372	0.405	0.277	0.342	0.337	0.375	0.298	0.353	0.337	0.349	0.267	0.316	0.520	0.501
	720	0.342	0.344	0.430	0.437	0.369	0.407	0.423	0.429	0.352	0.288	0.399	0.385	0.353	0.366	0.926	0.705
	Avg	**0.247**	**0.276**	0.346	0.387	0.264	0.325	0.315	0.362	0.271	0.309	0.292	0.313	0.253	0.298	0.565	0.519
ECL	96	0.162	0.253	0.198	0.313	0.146	0.249	0.202	0.314	0.187	0.304	0.167	0.270	0.211	0.313	0.342	0.423
	192	0.173	0.264	0.218	0.329	0.163	0.262	0.211	0.323	0.199	0.315	0.183	0.284	0.223	0.326	0.360	0.442
	336	0.194	0.285	0.253	0.352	0.198	0.296	0.222	0.335	0.212	0.329	0.194	0.295	0.243	0.346	0.365	0.445
	720	0.220	0.304	0.265	0.367	0.245	0.346	0.272	0.373	0.233	0.345	0.224	0.321	0.277	0.371	0.412	0.469
	Avg	**0.187**	**0.276**	0.233	0.340	0.188	0.288	0.227	0.337	0.208	0.323	0.192	0.292	0.239	0.339	0.370	0.445
Traffic	96	0.432	0.280	0.608	0.383	0.516	0.268	0.592	0.372	0.607	0.392	0.621	0.347	0.667	0.419	0.720	0.407
	192	0.444	0.287	0.630	0.397	0.541	0.283	0.598	0.371	0.621	0.399	0.643	0.355	0.662	0.425	0.738	0.414
	336	0.458	0.293	0.622	0.387	0.566	0.351	0.636	0.397	0.622	0.396	0.650	0.360	0.683	0.436	0.833	0.470
	720	0.492	0.303	0.689	0.396	0.610	0.403	0.639	0.395	0.632	0.396	0.670	0.365	0.700	0.455	0.854	0.491
	Avg	**0.457**	**0.291**	0.637	0.391	0.558	0.326	0.616	0.384	0.621	0.396	0.646	0.357	0.678	0.434	0.786	0.445
Exchange	96	0.084	0.201	0.191	0.318	0.276	0.383	0.162	0.291	0.085	0.204	0.132	0.254	0.128	0.266	0.896	0.761
	192	0.174	0.295	0.315	0.407	0.540	0.552	0.276	0.382	0.182	0.303	0.251	0.361	0.292	0.402	1.146	0.861
	336	0.331	0.416	0.480	0.519	1.229	0.873	0.442	0.488	0.348	0.428	0.467	0.507	0.500	0.536	1.628	1.017
	720	0.847	0.694	1.255	0.868	1.721	1.055	1.175	0.833	1.025	0.774	1.304	0.837	1.002	0.763	2.552	1.299
	Avg	**0.359**	**0.401**	0.560	0.528	0.942	0.716	0.514	0.498	0.410	0.427	0.538	0.490	0.480	0.492	1.555	0.984
Average		**0.336**	**0.349**	0.455	0.435	0.496	0.456	0.456	0.412	0.402	0.398	0.483	0.427	0.467	0.444	1.412	0.818

Table 22: Full results for the long-term forecasting task compared with PatchTST [54], TimeMixer [89], TimesNet [72], Autoformer [75], DLinear [87], iTransformer [74], TimeXer [62], FEDformer [77]. (* means former, PTST is PatchTST, TMixer is TimeMixer.) To ensure fairness in the comparison, we set the look-back window length of all models to **336**. The standard deviation is within 0.5%. **Red**: best, Blue: second best.

Methods		SymTime (Our)		PTST [54]		TMixer [89]		TimesNet [72]		Auto* [75]		DLinear [87]		iTrans* [74]		TimeXer [62]		FED* [77]	
Metrics		MSE	MAE	MSE	MAE	MSE	MAE	MSE	MAE	MSE	MAE	MSE	MAE	MSE	MAE	MSE	MAE	MSE	MAE
ETTm1	96	0.295	0.346	0.292	0.343	0.322	0.358	0.344	0.378	0.514	0.506	0.300	0.344	0.305	0.359	0.318	0.361	0.382	0.427
	192	0.328	0.365	0.331	0.369	0.342	0.375	0.456	0.426	0.576	0.520	0.335	0.365	0.345	0.382	0.354	0.383	0.393	0.434
	336	0.366	0.395	0.365	0.392	0.371	0.395	0.426	0.432	0.703	0.564	0.369	0.386	0.377	0.401	0.381	0.402	0.445	0.459
	720	0.411	0.422	0.420	0.425	0.437	0.440	0.459	0.455	0.678	0.568	0.425	0.420	0.444	0.439	0.434	0.433	0.543	0.490
	Avg	**0.350**	0.382	0.352	0.382	0.368	0.392	0.421	0.423	0.618	0.539	0.357	**0.379**	0.368	0.395	0.372	0.395	0.441	0.452
ETTm2	96	0.165	0.255	0.165	0.255	0.176	0.259	0.184	0.272	0.349	0.400	0.169	0.266	0.174	0.265	0.169	0.254	0.260	0.336
	192	0.221	0.293	0.220	0.292	0.232	0.298	0.243	0.309	0.507	0.474	0.235	0.316	0.247	0.313	0.237	0.302	0.291	0.354
	336	0.275	0.329	0.278	0.329	0.280	0.329	0.310	0.351	0.328	0.375	0.305	0.366	0.294	0.345	0.284	0.333	0.325	0.366
	720	0.365	0.387	0.368	0.385	0.359	0.387	0.393	0.405	0.418	0.433	0.457	0.463	0.374	0.394	0.360	0.381	0.423	0.451
	Avg	**0.256**	0.316	0.258	**0.315**	0.262	0.318	0.282	0.334	0.400	0.420	0.291	0.353	0.272	0.329	0.262	0.317	0.325	0.377
ETTh1	96	0.372	0.399	0.382	0.405	0.379	0.403	0.423	0.437	0.536	0.498	0.375	0.399	0.397	0.416	0.403	0.421	0.387	0.434
	192	0.409	0.427	0.414	0.421	0.415	0.423	0.481	0.481	0.562	0.533	0.413	0.424	0.442	0.448	0.440	0.440	0.431	0.458
	336	0.430	0.440	0.431	0.435	0.453	0.449	0.488	0.477	0.551	0.533	0.438	0.444	0.459	0.459	0.495	0.488	0.471	0.480
	720	0.440	0.463	0.449	0.466	0.473	0.473	0.548	0.523	0.670	0.590	0.475	0.495	0.503	0.506	0.633	0.583	0.512	0.516
	Avg	**0.413**	0.432	0.419	**0.432**	0.430	0.437	0.485	0.480	0.580	0.539	0.425	0.440	0.450	0.457	0.493	0.483	0.450	0.472
ETTh2	96	0.271	0.341	0.274	0.336	0.284	0.350	0.378	0.421	0.509	0.527	0.307	0.370	0.307	0.363	0.313	0.365	0.394	0.457
	192	0.334	0.378	0.339	0.379	0.359	0.397	0.409	0.439	0.711	0.641	0.402	0.431	0.393	0.413	0.375	0.404	0.426	0.456
	336	0.359	0.403	0.331	0.381	0.388	0.422	0.410	0.439	0.574	0.569	0.489	0.485	0.428	0.437	0.400	0.429	0.420	0.461
	720	0.398	0.436	0.379	0.422	0.555	0.534	0.440	0.461	0.856	0.679	0.761	0.620	0.433	0.452	0.412	0.443	0.478	0.495
	Avg	0.341	0.390	**0.331**	**0.379**	0.396	0.425	0.409	0.440	0.663	0.604	0.490	0.476	0.390	0.416	0.375	0.410	0.430	0.467
Weather	96	0.149	0.199	0.227	0.273	0.175	0.224	0.170	0.228	0.268	0.343	0.174	0.234	0.162	0.210	0.169	0.203	0.217	0.296
	192	0.192	0.239	0.200	0.245	0.196	0.243	0.214	0.263	0.431	0.465	0.217	0.276	0.207	0.251	0.243	0.265	0.288	0.342
	336	0.245	0.282	0.259	0.298	0.243	0.280	0.272	0.301	0.559	0.498	0.262	0.313	0.257	0.291	0.322	0.318	0.340	0.382
	720	0.321	0.337	0.346	0.353	0.325	0.346	0.343	0.353	0.506	0.495	0.328	0.370	0.327	0.337	0.414	0.373	0.405	0.430
	Avg	0.238	0.273	0.258	0.292	**0.235**	0.273	0.250	0.286	0.441	0.450	0.245	0.298	0.238	**0.272**	0.287	0.290	0.313	0.363
ECL	96	0.133	0.230	0.131	0.361	0.144	0.244	0.174	0.278	0.205	0.322	0.147	0.249	0.132	0.227	0.155	0.235	0.193	0.308
	192	0.150	0.244	0.154	0.251	0.152	0.242	0.192	0.292	0.219	0.333	0.160	0.261	0.153	0.248	0.161	0.281	0.201	0.315
	336	0.163	0.262	0.164	0.262	0.172	0.261	0.198	0.299	0.227	0.340	0.176	0.278	0.173	0.267	0.187	0.279	0.214	0.329
	720	0.208	0.298	0.210	0.301	0.207	0.293	0.222	0.318	0.294	0.390	0.196	0.288	0.194	0.287	0.183	0.273	0.246	0.355
	Avg	0.164	0.258	0.165	0.294	0.169	0.260	0.197	0.297	0.236	0.346	0.170	0.269	**0.163**	**0.257**	0.172	0.267	0.214	0.327
Traffic	96	0.361	0.257	0.365	0.256	0.371	0.256	0.589	0.321	0.675	0.414	0.431	0.307	0.367	0.278	0.422	0.268	0.587	0.366
	192	0.382	0.258	0.383	0.258	0.401	0.271	0.605	0.322	0.672	0.411	0.443	0.312	0.414	0.284	0.433	0.280	0.604	0.373
	336	0.395	0.271	0.398	0.271	0.408	0.267	0.621	0.338	0.667	0.408	0.456	0.319	0.399	0.280	0.454	0.278	0.621	0.383
	720	0.424	0.281	0.438	0.288	0.464	0.292	0.647	0.344	0.689	0.421	0.528	0.343	0.422	0.290	0.498	0.299	0.626	0.382
	Avg	**0.391**	**0.267**	0.396	0.268	0.411	0.271	0.615	0.331	0.676	0.413	0.465	0.320	0.401	0.283	0.452	0.281	0.610	0.376
Exchange	96	0.085	0.204	0.093	0.214	0.092	0.217	0.218	0.343	0.967	0.778	0.099	0.235	0.099	0.224	0.234	0.312	0.168	0.285
	192	0.180	0.301	0.200	0.321	0.235	0.345	0.299	0.411	0.931	0.750	0.195	0.335	0.215	0.338	0.283	0.402	0.186	0.296
	336	0.335	0.419	0.373	0.448	0.370	0.441	0.468	0.527	1.051	0.809	0.380	0.474	0.378	0.454	0.433	0.343	0.250	0.342
	720	0.869	0.700	0.875	0.695	0.963	0.750	1.208	0.847	1.261	0.893	1.120	0.805	0.876	0.690	0.688	0.942	0.899	0.784
	Avg	**0.367**	**0.406**	0.385	0.420	0.415	0.438	0.548	0.532	1.053	0.807	0.448	0.462	0.392	0.427	0.409	0.500	0.376	0.427
Average		**0.315**	**0.341**	0.320	0.348	0.336	0.352	0.401	0.390	0.583	0.515	0.361	0.375	0.347	0.355	0.353	0.368	0.395	0.408

Table 23: Full results for the long-term forecasting task compared with PatchTST [54], TimeMixer [89], TimesNet [72], Autoformer [75], DLinear [87], iTransformer [74], TimeXer [62], FITS [90]. (* means former, TMixer is TimeMixer.) To ensure fairness in the comparison, we set the look-back window length of all models to **512**. The standard deviation is within 0.5%. **Red**: best, Blue: second best.

Methods		`SymTime` **(Ours)**		PatchTST [54]		TMixer [89]		TimesNet [72]		Auto* [75]		DLinear [87]		iTrans* [74]		TimeXer [62]		FITS [90]	
Metrics		MSE	MAE	MSE	MAE	MSE	MAE	MSE	MAE	MSE	MAE	MSE	MAE	MSE	MAE	MSE	MAE	MSE	MAE
ETTm1	96	0.313	0.348	0.290	0.344	0.315	0.354	0.358	0.388	0.495	0.499	0.304	0.347	0.310	0.364	0.332	0.374	0.306	0.349
	192	0.326	0.363	0.333	0.371	0.344	0.376	0.457	0.439	0.549	0.514	0.337	0.368	0.349	0.387	0.364	0.392	0.338	0.367
	336	0.376	0.390	0.369	0.392	0.385	0.397	0.412	0.427	0.536	0.509	0.366	0.385	0.376	0.401	0.387	0.407	0.421	0.384
	720	0.409	0.420	0.416	0.420	0.441	0.440	0.473	0.467	0.645	0.550	0.424	0.422	0.434	0.436	0.430	0.432	0.432	0.437
	Avg	0.356	**0.380**	**0.352**	0.382	0.371	0.392	0.425	0.430	0.556	0.518	0.358	0.380	0.367	0.397	0.378	0.401	0.374	0.384
ETTm2	96	0.169	0.258	0.166	0.256	0.173	0.261	0.192	0.279	0.278	0.353	0.166	0.262	0.182	0.272	0.177	0.263	0.165	0.254
	192	0.232	0.301	0.223	0.296	0.223	0.298	0.264	0.325	0.318	0.383	0.225	0.304	0.242	0.312	0.241	0.312	0.219	0.291
	336	0.287	0.333	0.274	0.329	0.291	0.342	0.320	0.364	0.411	0.444	0.299	0.361	0.292	0.346	0.294	0.340	0.272	0.326
	720	0.372	0.387	0.362	0.385	0.366	0.391	0.402	0.410	0.476	0.484	0.412	0.432	0.378	0.396	0.382	0.399	0.359	0.391
	Avg	0.265	0.320	0.256	0.317	0.263	0.323	0.294	0.344	0.371	0.416	0.275	0.340	0.273	0.331	0.274	0.329	**0.254**	**0.313**
ETTh1	96	0.372	0.389	0.370	0.400	0.380	0.408	0.442	0.465	0.556	0.534	0.368	0.397	0.394	0.420	0.397	0.424	0.372	0.396
	192	0.402	0.424	0.413	0.429	0.431	0.444	0.473	0.475	0.568	0.538	0.400	0.417	0.430	0.444	0.438	0.452	0.405	0.415
	336	0.433	0.445	0.422	0.440	0.468	0.472	0.505	0.501	0.606	0.573	0.430	0.442	0.447	0.459	0.466	0.472	0.440	0.468
	720	0.448	0.469	0.447	0.468	0.435	0.453	0.505	0.504	0.777	0.669	0.476	0.497	0.514	0.516	0.597	0.566	0.453	0.485
	Avg	0.414	**0.432**	**0.413**	0.434	0.429	0.444	0.481	0.486	0.627	0.579	0.418	0.438	0.446	0.460	0.475	0.479	0.418	0.441
ETTh2	96	0.290	0.352	0.273	0.337	0.298	0.364	0.336	0.391	0.447	0.486	0.288	0.355	0.317	0.367	0.299	0.358	0.291	0.353
	192	0.376	0.409	0.341	0.382	0.361	0.399	0.393	0.425	0.587	0.568	0.394	0.427	0.388	0.411	0.370	0.408	0.350	0.395
	336	0.382	0.416	0.398	0.458	0.393	0.421	0.406	0.445	0.689	0.608	0.501	0.491	0.422	0.437	0.372	0.410	0.375	0.424
	720	0.414	0.442	0.416	0.458	0.442	0.458	0.451	0.466	1.027	0.772	0.813	0.638	0.424	0.454	0.376	0.424	0.437	0.459
	Avg	0.365	0.405	0.357	0.409	0.373	0.410	0.397	0.432	0.687	0.609	0.499	0.478	0.388	0.417	**0.354**	**0.400**	0.363	0.408
Weather	96	0.159	0.205	0.230	0.282	0.169	0.225	0.168	0.224	0.375	0.426	0.171	0.230	0.175	0.223	0.175	0.209	0.172	0.226
	192	0.203	0.260	0.194	0.242	0.191	0.242	0.217	0.266	0.471	0.491	0.213	0.269	0.213	0.256	0.246	0.267	0.216	0.262
	336	0.256	0.289	0.245	0.282	0.246	0.283	0.278	0.310	0.514	0.521	0.260	0.312	0.265	0.296	0.314	0.309	0.261	0.295
	720	0.319	0.339	0.312	0.332	0.316	0.333	0.342	0.352	0.596	0.506	0.320	0.358	0.342	0.347	0.391	0.353	0.326	0.342
	Avg	0.234	0.273	0.245	0.284	**0.231**	**0.271**	0.251	0.288	0.489	0.486	0.241	0.292	0.249	0.280	0.282	0.284	0.244	0.281
ECL	96	0.128	0.256	0.129	0.224	0.137	0.229	0.184	0.288	0.215	0.328	0.141	0.241	0.131	0.227	0.140	0.242	0.145	0.244
	192	0.149	0.244	0.158	0.258	0.152	0.250	0.187	0.291	0.224	0.333	0.154	0.254	0.155	0.250	0.157	0.256	0.153	0.250
	336	0.161	0.261	0.163	0.261	0.193	0.295	0.206	0.307	0.235	0.341	0.169	0.271	0.171	0.266	0.176	0.275	0.169	0.266
	720	0.216	0.308	0.225	0.331	0.228	0.324	0.226	0.323	0.738	0.570	0.204	0.304	0.191	0.285	0.211	0.306	0.208	0.298
	Avg	0.163	0.267	0.169	0.269	0.177	0.274	0.201	0.302	0.353	0.393	0.167	0.267	**0.162**	**0.257**	0.171	0.270	0.169	0.265
Traffic	96	0.365	0.257	0.369	0.262	0.368	0.254	0.600	0.321	0.697	0.428	0.412	0.294	0.351	0.257	0.428	0.271	0.398	0.277
	192	0.379	0.256	0.379	0.253	0.399	0.268	0.612	0.328	0.700	0.429	0.422	0.299	0.373	0.268	0.448	0.282	0.409	0.280
	336	0.401	0.275	0.410	0.280	0.404	0.264	0.631	0.338	0.707	0.437	0.431	0.304	0.386	0.274	0.473	0.289	0.418	0.285
	720	0.433	0.284	0.438	0.291	0.467	0.293	0.654	0.352	0.718	0.445	0.468	0.325	0.424	0.294	0.516	0.307	0.456	0.306
	Avg	0.395	**0.268**	0.399	0.272	0.410	0.270	0.624	0.334	0.705	0.435	0.433	0.305	**0.383**	0.273	0.466	0.287	0.420	0.287
Exchange	96	0.089	0.212	0.095	0.220	0.096	0.220	0.238	0.366	0.617	0.623	0.120	0.260	0.135	0.267	0.099	0.223	0.100	0.225
	192	0.176	0.298	0.215	0.336	0.197	0.318	0.439	0.497	0.810	0.739	0.241	0.376	0.322	0.417	0.207	0.331	0.201	0.326
	336	0.380	0.439	0.392	0.459	0.737	0.642	0.647	0.620	0.858	0.746	0.439	0.509	0.361	0.448	0.767	0.689	0.350	0.437
	720	0.893	0.698	0.890	0.680	1.038	0.808	1.550	0.948	1.491	0.965	1.199	0.831	0.888	0.736	0.984	0.780	0.920	0.728
	Avg	**0.384**	**0.412**	0.398	0.423	0.517	0.497	0.718	0.608	0.944	0.768	0.500	0.494	0.427	0.467	0.514	0.506	0.393	0.439
Average		**0.322**	**0.345**	0.324	0.349	0.346	0.360	0.424	0.403	0.591	0.525	0.361	0.374	0.337	0.360	0.364	0.369	0.329	0.352

Table 24: Full results for the short-term forecasting task in the M4 dataset compared with PerimidFormer [63], S^2IP-LLM(S-LLM) [82], Time-LLM(T-LLM) [17], GPT4TS [2], TimeMixer [89], PatchTST [54], iTransformer [74], TimesNet [72], DLinear [87], Informer [80]. (* means former.) The standard deviation is within 0.5%. **Red**: best, Blue: second best.

	Methods Metric	SymTime **(Ours)**	Peri-mid* [63]	S-LLM [82]	T-LLM [17]	GPT4TS [2]	TimeMixer [89]	PatchTST [54]	iTrans* [74]	TimesNet [72]	DLinear [87]	In* [80]
Yearly	SMAPE	**13.355**	13.483	14.931	13.450	14.847	13.369	13.677	13.724	13.463	14.340	14.698
	MASE	**2.997**	3.080	3.345	3.184	3.628	3.009	3.049	3.157	3.058	3.112	3.293
	OWA	**0.786**	0.800	0.878	0.819	0.911	0.787	0.802	0.817	0.797	0.830	0.864
Quarterly	SMAPE	10.060	**10.037**	10.655	10.671	10.389	10.131	10.922	13.473	10.069	10.510	16.172
	MASE	1.183	**1.170**	1.249	1.276	1.228	1.186	1.326	1.722	1.175	1.241	2.136
	OWA	**0.872**	0.882	0.939	0.950	0.919	0.893	0.979	1.240	0.886	0.930	1.513
Monthly	SMAPE	**12.608**	12.795	13.012	13.416	12.907	12.762	14.200	13.674	12.760	13.382	15.446
	MASE	**0.925**	0.948	0.973	1.045	0.954	0.940	1.111	1.068	0.947	1.007	1.247
	OWA	**0.872**	0.889	0.909	0.957	0.896	0.884	1.015	0.976	0.887	0.937	1.122
Others	SMAPE	4.941	**4.912**	5.540	4.973	5.266	5.085	5.658	5.598	4.995	5.122	6.839
	MASE	3.327	**3.260**	8.426	3.412	3.595	3.403	3.626	3.957	3.346	3.608	4.536
	OWA	1.045	**1.031**	3.792	1.059	1.121	1.072	1.167	1.213	1.053	1.108	1.435
Average	SMAPE	**11.785**	11.897	12.514	12.584	12.367	11.885	12.866	13.233	11.888	12.500	15.018
	MASE	**1.584**	1.607	1.726	1.763	1.767	1.598	1.734	1.850	1.607	1.678	2.096
	OWA	**0.849**	0.859	0.913	0.915	0.918	0.856	0.928	0.972	0.858	0.899	1.102

Table 25: Full results for the short-term forecasting task in the M4 dataset compared with LightTS [88], Autoformer [75], Crossformer [79], FEDformer [77], ETSformer [76], Nonstationary Transformer (Stationary) [78], FiLM [142], MICN [86], Reformer [143], Pyraformer [130]. The standard deviation is within 0.5%. (* means former.) **Red**: best, Blue: second best.

	Methods Metric	SymTime **(Ours)**	LightTS [88]	Auto* [75]	Cross* [79]	FED* [77]	ETS* [76]	Stationary [78]	FiLM [142]	MICN [86]	Re* [143]	Pyra* [130]
Yearly	SMAPE	**13.355**	13.444	17.764	79.308	13.508	18.009	13.717	14.076	14.557	13.752	14.594
	MASE	**2.997**	3.022	3.919	18.692	3.051	4.487	3.078	3.017	3.380	3.088	3.269
	OWA	**0.786**	0.792	1.037	4.778	0.797	1.115	0.807	0.810	0.871	0.809	0.858
Quarterly	SMAPE	**10.060**	10.252	13.968	74.943	10.706	13.376	10.958	10.711	11.408	10.900	11.654
	MASE	**1.183**	1.183	1.754	13.133	1.263	1.906	1.325	1.292	1.384	1.316	1.392
	OWA	**0.872**	0.897	1.274	8.191	0.947	1.302	0.981	0.957	1.022	0.975	1.037
Monthly	SMAPE	**12.608**	12.798	18.200	68.892	13.925	14.588	13.917	13.362	13.803	13.949	14.963
	MASE	**0.925**	0.957	1.574	11.199	1.062	1.368	1.097	1.016	1.078	1.096	1.165
	OWA	**0.872**	0.894	1.371	7.654	0.982	1.149	0.998	0.941	0.985	0.999	1.066
Others	SMAPE	4.941	5.324	6.738	176.164	**4.888**	7.267	6.302	5.387	6.090	6.611	5.605
	MASE	3.327	3.410	4.853	116.723	**3.244**	5.240	4.064	3.670	4.203	4.492	3.966
	OWA	1.045	1.098	1.474	36.941	**1.026**	1.591	1.304	1.146	1.304	1.404	1.215
Average	SMAPE	**11.785**	11.962	16.511	78.103	12.605	14.718	12.780	12.491	13.016	12.805	13.616
	MASE	**1.584**	1.609	2.321	18.663	1.677	2.408	1.756	1.675	1.837	1.777	1.843
	OWA	**0.849**	0.862	1.215	7.759	0.903	1.172	0.930	0.899	0.960	0.937	0.984

Table 26: Full results for time series classification task compared with (1) classical methods: DTW [144], XGBoost [145], Rocket [84]; (2) RNN-based methods: LSTM [146], LSTNet [104], LSSL [147]; (3) CNN-based methods: InceptionTime (InTime) [85], TCN [148], TimesNet [72], TSLANet [83]. We report the classification accuracy (%) as the result. **Red**: best, Blue: second best. The standard deviation is within 1%.

Datasets / Methods	Classical Methods			RNN-based			CNN-based				
	DTW [144]	XGBoost [145]	Rocket [84]	LSTM [146]	LSTNet [104]	LSSL [147]	InTime [85]	TCN [148]	TimesNet [72]	TSLANet [83]	`SymTime` (**Ours**)
EthanolConcentration	32.3	43.7	**45.2**	32.3	39.9	31.1	39.1	28.9	35.7	30.4	37.3
FaceDetection	52.9	63.3	64.7	57.7	65.7	66.7	65.4	52.8	68.6	66.7	**69.2**
Handwriting	28.6	15.8	**58.8**	15.2	25.8	24.6	46.9	53.3	32.1	57.9	36.7
Heartbeat	71.7	73.2	75.6	72.2	77.1	72.7	75.2	75.6	**78.0**	77.5	74.1
JapaneseVowels	94.9	86.5	96.2	79.7	98.1	98.4	95.1	**98.9**	98.4	95.1	98.1
PEMS-SF	71.1	**98.3**	75.1	39.9	86.7	86.1	79.6	68.8	89.6	83.8	97.1
SelfRegulationSCP1	77.7	84.6	90.8	68.9	84.0	90.8	87.2	84.6	**91.8**	**91.8**	89.8
SelfRegulationSCP2	53.9	48.9	53.3	46.6	52.8	52.2	53.6	55.6	57.2	53.3	**58.9**
SpokenArabicDigits	96.3	69.6	71.2	31.9	**100.0**	**100.0**	96.3	95.6	99.0	98.0	98.9
UWaveGestureLibrary	90.3	75.9	**94.4**	41.2	87.8	85.9	92.4	88.4	85.3	89.4	89.4
Average Accuracy	67.0	66.0	72.5	48.6	71.8	70.9	73.1	70.3	73.6	74.4	**74.9**

Table 27: Full reuslts for time series classification task compared with (1) Transformer-based methods: Autoformer [75], FEDformer [77], ETSformer [76], Informer [80], iTransformer [74], PatchTST (Patch) [54], GPT4TS (GPT) [2], UniTS [92], Peri-midformer [63] and (2) MLP-based methods: DLinear [87], LightTS [88]. We report the classification accuracy (%) as the results. (* means former.) **Red**: best, Blue: second best. The standard deviation is within 1%.

Datasets / Methods	Transformer-based									MLP-based		
	Auto* [75]	FED* [77]	ETS* [76]	In* [80]	iTrans* [74]	Patch [54]	GPT [2]	UniTS [92]	Peri-mid* [63]	DLinear [87]	LightTS [88]	`SymTime` (**Ours**)
EthanolConcentration	31.6	31.2	28.1	31.6	27.0	29.6	34.2	37.3	**47.3**	32.6	29.7	37.3
FaceDetection	68.4	66.0	66.3	67.0	67.0	67.8	**69.2**	67.5	68.7	68.0	67.5	**69.2**
Handwriting	**36.7**	28.0	32.5	32.8	27.2	23.2	32.7	27.0	31.5	27.0	26.1	**36.7**
Heartbeat	74.6	73.7	71.2	80.5	75.6	75.7	77.2	80.5	**86.3**	75.1	75.1	74.1
JapaneseVowels	96.2	98.4	95.9	**98.9**	97.6	94.0	98.6	97.8	96.8	96.2	96.2	98.1
PEMS-SF	82.7	80.9	86.0	81.5	85.5	80.9	87.9	93.1	88.2	75.1	88.4	**97.1**
SelfRegulationSCP1	84.0	88.7	89.6	90.1	**92.2**	82.2	87.2	89.6	87.4	87.3	89.8	89.8
SelfRegulationSCP2	50.6	54.4	55.0	53.3	54.4	53.6	59.4	**61.1**	55.4	50.5	51.1	58.9
SpokenArabicDigits	**100.0**	**100.0**	**100.0**	**100.0**	98.0	98.0	95.2	98.9	98.0	81.4	**100.0**	98.9
UWaveGestureLibrary	85.9	85.3	85.0	85.6	85.9	81.7	85.1	87.8	84.3	82.1	80.3	**89.4**

Table 28: Full results for time series imputation task, where we randomly mask {12.5%, 25%, 37.5%, 50%} time points of length-96 time series to compare the model performance under different missing degrees. We compare with GPT4TS [2], TimesNet [72], Peri-midFormer [63], Moment [93], iTransformer [74], PatchTST [54], DLinear [87] in this table. (* means former.) The standard deviation is within 0.5%. **Red**: best, Blue: second best.

Models		SymTime (**Ours**)		GPT4TS [2]		TimesNet [72]		Peri-mid* [63]		Moment [93]		iTrans* [74]		PatchTST [54]		DLinear [87]	
Mask Ratio		MSE	MAE	MSE	MAE	MSE	MAE	MSE	MAE	MSE	MAE	MSE	MAE	MSE	MAE	MSE	MAE
ETTm1	12.5%	0.032	0.110	0.018	0.090	0.019	0.091	0.032	0.109	0.069	0.170	0.046	0.147	0.045	0.137	0.056	0.162
	25%	0.034	0.113	0.024	0.102	0.024	0.101	0.034	0.112	0.071	0.169	0.060	0.171	0.046	0.139	0.077	0.191
	37.5%	0.037	0.118	0.029	0.111	0.029	0.112	0.037	0.117	0.069	0.163	0.077	0.195	0.049	0.143	0.100	0.218
	50%	0.041	0.126	0.042	0.132	0.036	0.124	0.042	0.126	0.086	0.169	0.104	0.228	0.055	0.152	0.129	0.247
	Avg	0.036	0.116	0.028	0.109	**0.027**	**0.107**	0.036	0.116	0.074	0.168	0.072	0.185	0.049	0.143	0.090	0.204
ETTm2	12.5%	0.024	0.084	0.018	0.081	0.019	0.081	0.023	0.081	0.032	0.108	0.052	0.151	0.026	0.094	0.067	0.171
	25%	0.024	0.086	0.021	0.082	0.021	0.086	0.024	0.084	0.029	0.105	0.070	0.179	0.028	0.099	0.089	0.200
	37.5%	0.027	0.089	0.023	0.090	0.023	0.091	0.026	0.089	0.032	0.109	0.091	0.204	0.031	0.104	0.112	0.226
	50%	0.030	0.093	0.027	0.098	0.026	0.098	0.030	0.095	0.031	0.110	0.117	0.232	0.034	0.109	0.140	0.253
	Avg	0.026	0.088	**0.022**	**0.088**	**0.022**	0.089	0.026	0.087	0.031	0.108	0.082	0.191	0.030	0.101	0.102	0.212
ETTh1	12.5%	0.074	0.179	0.063	0.171	0.062	0.169	0.069	0.173	0.160	0.239	0.098	0.220	0.097	0.203	0.111	0.232
	25%	0.082	0.190	0.080	0.190	0.081	0.191	0.079	0.185	0.142	0.238	0.125	0.249	0.115	0.221	0.149	0.269
	37.5%	0.100	0.205	0.107	0.218	0.098	0.210	0.096	0.202	0.121	0.228	0.156	0.278	0.134	0.239	0.187	0.301
	50%	0.123	0.230	0.121	0.221	0.116	0.227	0.122	0.226	0.132	0.231	0.213	0.327	0.160	0.260	0.229	0.332
	Avg	0.095	0.201	0.093	0.200	**0.089**	0.199	0.091	**0.196**	0.139	0.234	0.148	0.269	0.126	0.231	0.169	0.283
ETTh2	12.5%	0.051	0.138	0.041	0.129	0.040	0.132	0.051	0.139	0.051	0.150	0.095	0.210	0.058	0.153	0.109	0.223
	25%	0.055	0.146	0.046	0.138	0.047	0.144	0.054	0.142	0.079	0.177	0.120	0.239	0.063	0.160	0.146	0.260
	37.5%	0.059	0.152	0.060	0.160	0.054	0.154	0.058	0.148	0.056	0.155	0.149	0.266	0.068	0.167	0.180	0.290
	50%	0.064	0.157	0.061	0.160	0.061	0.164	0.064	0.159	0.056	0.154	0.192	0.302	0.074	0.175	0.217	0.319
	Avg	0.058	0.148	0.052	**0.147**	**0.050**	0.148	0.057	**0.147**	0.061	0.159	0.139	0.254	0.066	0.164	0.163	0.273
ECL	12.5%	0.037	0.122	0.080	0.195	0.088	0.203	0.047	0.140	0.095	0.211	0.073	0.190	0.061	0.170	0.084	0.206
	25%	0.046	0.139	0.089	0.205	0.092	0.208	0.053	0.162	0.093	0.211	0.090	0.214	0.072	0.185	0.113	0.243
	37.5%	0.060	0.160	0.094	0.217	0.096	0.214	0.067	0.179	0.094	0.211	0.107	0.235	0.082	0.198	0.141	0.273
	50%	0.075	0.181	0.108	0.231	0.102	0.221	0.085	0.195	0.092	0.210	0.127	0.257	0.097	0.216	0.173	0.303
	Avg	**0.054**	**0.151**	0.093	0.212	0.094	0.211	0.063	0.169	0.094	0.211	0.099	0.224	0.078	0.192	0.128	0.256
Weather	12.5%	0.025	0.035	0.026	0.047	0.026	0.049	0.025	0.037	0.033	0.073	0.038	0.087	0.028	0.049	0.039	0.091
	25%	0.027	0.037	0.030	0.055	0.030	0.056	0.026	0.037	0.036	0.078	0.046	0.106	0.032	0.055	0.049	0.112
	37.5%	0.029	0.039	0.033	0.061	0.032	0.058	0.029	0.041	0.034	0.075	0.055	0.122	0.035	0.059	0.057	0.125
	50%	0.032	0.042	0.039	0.070	0.034	0.062	0.034	0.048	0.035	0.075	0.068	0.142	0.039	0.064	0.067	0.139
	Avg	**0.028**	**0.038**	0.032	0.058	0.030	0.056	0.029	0.041	0.035	0.075	0.052	0.114	0.033	0.057	0.053	0.116
Average		**0.049**	**0.124**	0.053	0.136	0.052	0.135	**0.050**	0.126	0.072	0.159	0.099	0.206	0.064	0.148	0.118	0.224

Table 29: Full results for time series imputation task, where we randomly mask {12.5%, 25%, 37.5%, 50%} time points of length-96 time series to compare the model performance under different missing degrees. We compare with Stationary [78], LightTS [88], ETSformer [76], FEDformer [77], Informer [80], Reformer [143] and Pyraformer [130] in this table. (Stationary means Nonstationary Transformer.) The standard deviation is within 0.5%. **Red**: best, Blue: second best.

	Methods	SymTime (Ours)		Stationary [78]		LightTS [88]		ETSformer [76]		FEDformer [77]		Informer [80]		Reformer [143]		Pyraformer [130]	
	Mask Ratio	MSE	MAE	MSE	MAE	MSE	MAE	MSE	MAE	MSE	MAE	MSE	MAE	MSE	MAE	MSE	MAE
ETTm1	12.5%	0.032	0.110	0.026	0.107	0.054	0.158	0.034	0.130	0.068	0.188	0.027	0.115	0.032	0.126	0.670	0.541
	25%	0.034	0.113	0.032	0.119	0.061	0.173	0.053	0.162	0.097	0.230	0.040	0.140	0.042	0.146	0.689	0.553
	37.5%	0.037	0.118	0.039	0.131	0.073	0.189	0.082	0.201	0.134	0.287	0.071	0.189	0.063	0.182	0.737	0.581
	50%	0.041	0.126	0.047	0.145	0.086	0.207	0.130	0.257	0.188	0.323	0.091	0.208	0.082	0.208	0.770	0.605
	Avg	**0.036**	**0.116**	**0.036**	0.126	0.068	0.182	0.075	0.187	0.121	0.257	0.057	0.163	0.055	0.166	0.717	0.570
ETTm2	12.5%	0.024	0.084	0.021	0.088	0.051	0.150	0.061	0.169	0.109	0.239	0.196	0.326	0.108	0.228	0.394	0.470
	25%	0.024	0.086	0.024	0.096	0.069	0.176	0.093	0.214	0.166	0.295	0.295	0.414	0.136	0.262	0.421	0.482
	37.5%	0.027	0.089	0.027	0.103	0.074	0.185	0.137	0.253	0.237	0.356	0.155	0.293	0.175	0.300	0.478	0.521
	50%	0.030	0.093	0.030	0.108	0.078	0.192	0.237	0.332	0.323	0.412	0.214	0.325	0.211	0.329	0.568	0.560
	Avg	**0.026**	**0.088**	**0.026**	0.099	0.068	0.176	0.132	0.242	0.209	0.326	0.215	0.340	0.157	0.280	0.465	0.508
ETTh1	12.5%	0.074	0.179	0.060	0.165	0.119	0.239	0.073	0.195	0.126	0.265	0.068	0.187	0.074	0.194	0.857	0.609
	25%	0.082	0.190	0.080	0.189	0.144	0.266	0.105	0.234	0.169	0.305	0.096	0.220	0.102	0.227	0.829	0.672
	37.5%	0.100	0.205	0.102	0.212	0.171	0.292	0.144	0.276	0.220	0.348	0.128	0.253	0.135	0.261	0.830	0.675
	50%	0.123	0.230	0.133	0.240	0.201	0.317	0.200	0.327	0.298	0.403	0.166	0.287	0.179	0.298	0.854	0.691
	Avg	0.095	**0.201**	**0.094**	**0.201**	0.159	0.278	0.130	0.258	0.204	0.330	0.115	0.237	0.122	0.245	0.842	0.682
ETTh2	12.5%	0.051	0.138	0.042	0.133	0.094	0.208	0.134	0.251	0.187	0.319	0.271	0.384	0.163	0.289	0.976	0.754
	25%	0.055	0.146	0.049	0.147	0.140	0.255	0.180	0.294	0.279	0.396	0.362	0.450	0.206	0.331	1.037	0.774
	37.5%	0.059	0.152	0.056	0.158	0.159	0.274	0.243	0.341	0.402	0.465	0.401	0.469	0.252	0.370	1.107	0.800
	50%	0.064	0.157	0.065	0.170	0.180	0.293	0.353	0.408	0.604	0.504	0.437	0.487	0.316	0.419	1.193	0.838
	Avg	0.058	**0.148**	**0.053**	0.152	0.143	0.258	0.228	0.324	0.368	0.421	0.368	0.448	0.234	0.352	1.079	0.792
ECL	12.5%	0.037	0.122	0.093	0.210	0.077	0.198	0.185	0.323	0.197	0.324	0.152	0.279	0.190	0.308	0.297	0.383
	25%	0.046	0.139	0.097	0.214	0.099	0.228	0.207	0.340	0.208	0.345	0.166	0.290	0.197	0.312	0.294	0.380
	37.5%	0.060	0.160	0.102	0.220	0.120	0.252	0.226	0.355	0.219	0.337	0.178	0.297	0.203	0.315	0.296	0.381
	50%	0.075	0.181	0.108	0.228	0.138	0.272	0.251	0.372	0.235	0.357	0.189	0.305	0.210	0.319	0.299	0.383
	Avg	**0.049**	**0.151**	0.100	0.218	0.108	0.238	0.217	0.347	0.215	0.341	0.171	0.293	0.200	0.313	0.297	0.382
Weather	12.5%	0.025	0.035	0.027	0.051	0.039	0.092	0.042	0.103	0.057	0.141	0.040	0.108	0.031	0.076	0.140	0.220
	25%	0.027	0.037	0.029	0.056	0.045	0.105	0.056	0.131	0.066	0.155	0.045	0.130	0.035	0.082	0.147	0.229
	37.5%	0.029	0.039	0.033	0.062	0.049	0.110	0.081	0.180	0.083	0.180	0.049	0.101	0.040	0.091	0.156	0.240
	50%	0.032	0.042	0.037	0.068	0.054	0.117	0.102	0.207	0.103	0.207	0.054	0.114	0.046	0.099	0.164	0.249
	Avg	**0.028**	**0.038**	0.032	0.059	0.047	0.106	0.071	0.155	0.077	0.171	0.047	0.113	0.038	0.087	0.152	0.235
	Average	**0.049**	**0.124**	0.057	0.143	0.099	0.206	0.142	0.252	0.199	0.308	0.162	0.265	0.134	0.241	0.592	0.528

Table 30: Full reuslts for time series anomaly detection task, where P, R and F1 represent the precision, recall and F1-score (%) respectively. F1-score is the harmonic mean of precision and recall. A higher value of P, R and F1 indicates a better performance. We compare with: Transformer [127], Reformer [143], Informer [80], Autoformer [75], Crossformer [79], iTransformer [74], Anomaly [81], Stationary [78], DLinear [87], LightTS [88], ETSformer [76], FEDformer [77], PatchTST [54], TimesNet [72], GPT4TS [2], Peri-midFormer [63], UniTS [92], where Anomaly means the Anomaly Transformer and Stationary means the Non-stationary Transformer. The standard deviation is within 1%. **Red**: best, Blue: second best.

Datasets	SMD			MSL			SMAP			SWaT			PSM			Avg F1
Metircs	P	R	F1	P	R	F1	P	R	F1	P	R	F1	P	R	F1	(%)
LSTM [146]	78.52	65.47	71.41	78.04	86.22	81.93	91.06	57.49	70.48	78.06	91.72	84.34	69.24	99.53	81.67	77.97
LogTrans [127]	83.46	70.13	76.21	73.05	87.37	79.57	89.15	57.59	69.97	68.67	**97.32**	80.52	63.06	98.00	76.74	76.60
Transformer [127]	78.44	65.26	71.24	89.85	73.71	80.99	90.77	61.76	73.50	96.82	66.41	79.76	99.31	83.18	90.53	79.20
TCN [148]	84.06	79.07	81.49	75.11	82.44	78.60	86.90	59.23	70.45	76.59	95.71	85.09	54.59	**99.77**	70.57	77.24
LSSL [147]	78.51	65.32	71.31	77.55	**88.18**	82.53	89.43	53.43	66.90	79.05	93.72	85.76	66.02	92.93	77.20	76.74
Reformer [143]	72.50	84.19	77.90	90.24	73.78	81.18	90.63	62.48	73.97	99.94	66.75	80.04	99.73	83.03	90.62	80.74
Informer [80]	72.51	84.13	77.88	90.10	73.68	81.07	90.57	61.51	73.26	99.83	67.24	80.35	99.03	83.21	90.43	80.60
Autoformer [75]	78.46	65.11	71.17	90.59	75.26	82.22	90.84	62.39	73.97	**99.95**	65.57	79.19	**99.99**	78.96	88.24	78.96
Crossformer [79]	71.89	83.41	77.22	90.32	72.74	80.59	89.68	53.63	67.12	98.00	83.59	90.22	97.49	88.02	92.52	81.53
iTransformer [74]	76.13	84.70	80.19	86.15	62.54	72.47	90.68	52.78	66.72	92.23	93.05	92.64	97.92	92.03	94.88	81.38
Pyraformer [130]	85.61	80.61	83.04	83.81	85.93	84.86	92.54	57.71	71.09	87.92	96.00	91.78	71.67	96.02	82.08	82.57
Anomaly [81]	**88.91**	82.23	85.49	79.61	87.37	83.31	91.85	58.11	71.18	72.51	**97.32**	83.10	68.35	94.72	79.40	80.50
Stationary [78]	78.51	**87.98**	82.97	86.86	68.63	76.68	90.62	55.74	69.02	89.26	95.42	92.24	98.17	96.30	97.23	83.63
DLinear [87]	75.91	84.02	79.76	89.68	75.31	81.87	89.87	53.79	67.30	92.26	93.05	92.66	98.65	94.70	96.64	83.64
LightTS [88]	87.10	78.42	82.53	82.40	75.78	78.95	**92.58**	55.27	69.21	91.98	94.72	93.33	98.37	95.97	97.15	84.23
ETSformer [76]	87.44	79.23	83.13	85.13	84.93	**85.03**	92.25	55.75	69.50	90.02	80.36	84.91	99.31	85.28	91.76	82.87
FEDformer [77]	72.82	81.68	76.99	90.72	75.41	82.36	90.47	58.10	70.76	**99.95**	65.55	79.18	99.98	81.92	90.05	79.46
PatchTST [54]	87.26	82.14	84.62	88.34	70.96	78.70	90.64	55.46	68.82	91.10	80.94	85.72	98.84	93.47	96.08	82.79
TimesNet [72]	88.07	80.97	84.37	88.83	74.68	81.14	89.98	56.02	69.05	91.99	93.24	92.61	98.46	95.70	97.06	84.85
GPT4TS [2]	87.68	81.52	84.49	82.09	81.97	82.03	90.12	55.70	68.85	92.12	93.09	92.60	98.36	95.85	97.09	85.01
FedTADBench [149]	87.31	80.06	83.53	77.69	69.37	84.09	90.49	57.44	70.27	90.63	84.43	87.42	97.67	94.41	96.01	84.26
PeFAD [150]	88.64	82.05	85.22	73.42	87.31	78.94	89.89	62.39	73.66	88.71	89.78	88.73	96.93	95.94	96.43	84.60
InterFusion [151]	84.06	83.52	83.78	84.83	78.49	81.54	90.66	58.11	70.82	96.76	78.45	86.65	83.61	83.45	83.53	81.26
Peri-midFormer [63]	86.97	81.37	84.08	88.66	74.02	80.68	90.02	54.03	67.53	90.74	92.55	91.64	98.46	94.06	96.21	84.03
UniTS [92]	82.42	84.99	83.69	**91.32**	73.04	81.16	90.58	**62.55**	**74.00**	92.60	92.42	92.51	98.45	96.19	**97.31**	85.73
SymTime **(Ours)**	88.08	83.37	**85.66**	89.46	75.31	81.77	91.06	61.51	73.43	95.94	91.39	**93.61**	98.90	95.36	97.10	**86.31**

Table 31: The full fine-tuning results of the time series long-term forecasting task under different sizes of pre-training datasets. The brief results of this experiment are shown in Table 1. **Red**: best, Blue: second best.

Methods		0B		1B		10B		25B		50B	
Datasets \Horizon		MSE	MAE	MSE	MAE	MSE	MAE	MSE	MAE	MSE	MAE
ETTm1	96	0.335	0.376	0.324	0.355	0.319	0.353	0.321	0.358	0.318	0.353
	192	0.404	0.382	0.363	0.385	0.374	0.382	0.369	0.383	0.362	0.380
	336	0.419	0.443	0.392	0.410	0.391	0.412	0.394	0.407	0.386	0.402
	720	0.446	0.435	0.426	0.440	0.422	0.423	0.426	0.423	0.419	0.423
	Avg	0.401	0.409	0.376	0.398	0.376	0.393	0.378	0.393	**0.371**	**0.390**
ETTm2	96	0.181	0.271	0.195	0.257	0.183	0.265	0.177	0.264	0.174	0.257
	192	0.241	0.323	0.268	0.316	0.249	0.310	0.245	0.302	0.238	0.299
	336	0.334	0.361	0.310	0.350	0.295	0.346	0.297	0.338	0.295	0.337
	720	0.417	0.401	0.394	0.400	0.398	0.396	0.391	0.396	0.390	0.392
	Avg	0.293	0.339	0.292	0.331	0.281	0.329	0.278	0.325	**0.274**	**0.321**
ETTh1	96	0.422	0.428	0.402	0.411	0.386	0.404	0.384	0.402	0.376	0.400
	192	0.457	0.459	0.447	0.462	0.430	0.432	0.434	0.436	0.428	0.431
	336	0.523	0.494	0.489	0.467	0.473	0.463	0.468	0.457	0.463	0.456
	720	0.547	0.515	0.507	0.495	0.486	0.478	0.481	0.479	0.450	0.458
	Avg	0.487	0.474	0.461	0.459	0.444	0.444	0.434	0.438	**0.430**	**0.436**
ETTh2	96	0.298	0.350	0.302	0.355	0.295	0.357	0.301	0.352	0.293	0.348
	192	0.373	0.403	0.364	0.416	0.369	0.405	0.369	0.403	0.364	0.397
	336	0.401	0.434	0.458	0.442	0.387	0.424	0.389	0.426	0.385	0.423
	720	0.433	0.461	0.490	0.464	0.454	0.447	0.427	0.438	0.420	0.441
	Avg	0.376	0.412	0.403	0.419	0.376	0.408	0.371	0.405	**0.365**	**0.402**
Weather	96	0.185	0.221	0.173	0.219	0.170	0.218	0.175	0.217	0.166	0.213
	192	0.217	0.279	0.223	0.259	0.232	0.263	0.221	0.263	0.212	0.254
	336	0.276	0.304	0.285	0.294	0.266	0.296	0.271	0.297	0.267	0.294
	720	0.353	0.353	0.347	0.357	0.332	0.340	0.345	0.350	0.342	0.344
	Avg	0.257	0.289	0.257	0.282	0.250	0.279	0.253	0.282	**0.247**	**0.276**
ECL	96	0.162	0.254	0.168	0.263	0.166	0.262	0.175	0.272	0.162	0.253
	192	0.179	0.268	0.182	0.270	0.173	0.269	0.183	0.276	0.173	0.264
	336	0.217	0.288	0.196	0.286	0.209	0.300	0.205	0.295	0.194	0.285
	720	0.216	0.324	0.250	0.321	0.236	0.312	0.216	0.308	0.220	0.304
	Avg	0.193	0.284	0.199	0.285	0.196	0.286	0.195	0.288	**0.187**	**0.276**
Traffic	96	0.460	0.288	0.451	0.289	0.438	0.293	0.442	0.282	0.432	0.280
	192	0.452	0.287	0.461	0.291	0.450	0.292	0.452	0.289	0.444	0.287
	336	0.461	0.330	0.469	0.296	0.472	0.294	0.467	0.296	0.458	0.293
	720	0.510	0.336	0.510	0.336	0.508	0.314	0.502	0.309	0.492	0.303
	Avg	0.471	0.310	0.473	0.303	0.473	0.294	0.467	0.299	**0.457**	**0.291**
Exchange	96	0.120	0.235	0.087	0.203	0.098	0.208	0.087	0.205	0.084	0.201
	192	0.188	0.298	0.192	0.309	0.186	0.301	0.177	0.297	0.174	0.295
	336	0.346	0.428	0.341	0.423	0.337	0.420	0.326	0.414	0.331	0.416
	720	0.878	0.699	0.861	0.706	0.850	0.701	0.838	0.689	0.847	0.694
	Avg	0.383	0.415	0.370	0.410	0.368	0.407	**0.357**	**0.401**	0.359	**0.401**
Average		0.358	0.366	0.354	0.361	0.345	0.355	0.342	0.354	**0.336**	**0.349**

Table 32: The full fine-tuning results of the time series short-term forecasting task under different sizes of pre-training datasets. The brief results of this experiment are shown in Table 2. **Red**: best, Blue: second best.

Methods	Metric	0B	1B	10B	25B	50B
Yearly	SMAPE	**13.291**	13.341	13.332	13.380	13.355
	MASE	**2.981**	2.986	2.985	3.012	2.997
	OWA	**0.782**	0.784	0.783	0.788	0.786
Quartly	SMAPE	10.270	10.274	10.197	10.228	**10.060**
	MASE	1.224	1.218	1.212	1.219	**1.183**
	OWA	0.913	0.911	0.905	0.909	**0.872**
Monthly	SMAPE	13.545	12.811	12.833	12.662	**12.608**
	MASE	1.053	0.955	0.959	0.932	**0.925**
	OWA	0.964	0.893	0.896	0.877	**0.872**
Others	SMAPE	5.186	5.070	5.003	5.034	**4.941**
	MASE	3.498	3.479	3.350	3.372	**3.327**
	OWA	1.097	1.082	1.055	1.061	**1.045**
Avg.	SMAPE	12.283	11.937	11.924	11.862	**11.785**
	MASE	1.660	1.611	1.605	1.601	**1.584**
	OWA	0.887	0.861	0.859	0.856	**0.849**

Table 33: The full fine-tuning results of the time series classification task under different sizes of pre-training datasets. The brief results of this experiment are shown in Figure 7 (a). **Red**: best, Blue: second best.

Datasets	0B	1B	10B	25B	50B
EthanolConcentration	33.08	30.04	34.22	35.74	**37.30**
FaceDetection	51.31	58.12	58.12	58.12	**69.20**
Handwriting	35.76	36.24	36.24	36.00	**36.70**
Heartbeat	70.24	71.71	72.20	73.17	**74.15**
JapaneseVowels	94.86	95.95	94.86	96.76	**98.11**
PEMS-SF	86.71	88.44	88.44	92.49	**97.11**
SelfRegulationSCP1	86.69	85.67	87.71	88.05	**89.76**
SelfRegulationSCP2	56.11	57.78	57.78	58.89	**58.89**
SpokenArabicDigits	89.77	93.91	95.91	97.04	**98.86**
UWaveGestureLibrary	78.75	85.63	85.63	87.19	**89.38**
Average Accuracy	68.33	70.35	71.11	71.34	**74.90**

Table 34: The full fine-tuning results of the time series imputation task under different sizes of pre-training datasets. The brief results of this experiment are shown in Table 2. **Red**: best, Blue: second best.

Methods		0B		1B		10B		25B		50B	
Mask	Ratio	MSE	MAE	MSE	MAE	MSE	MAE	MSE	MAE	MSE	MAE
ETTm1	12.5%	0.034	0.111	0.034	0.112	0.032	0.111	0.033	0.110	0.032	0.110
	25%	0.050	0.125	0.042	0.116	0.041	0.118	0.036	0.116	0.034	0.113
	37.5%	0.040	0.122	0.037	0.119	0.039	0.118	0.036	0.118	0.037	0.118
	50%	0.044	0.128	0.042	0.129	0.042	0.128	0.042	0.126	0.041	0.126
	Avg	0.042	0.122	0.039	0.119	0.038	0.119	0.037	0.118	**0.036**	**0.117**
ETTm2	12.5%	0.030	0.088	0.027	0.087	0.028	0.087	0.026	0.086	0.024	0.084
	25%	0.038	0.101	0.029	0.087	0.029	0.087	0.028	0.088	0.024	0.086
	37.5%	0.040	0.120	0.032	0.107	0.028	0.096	0.027	0.091	0.027	0.089
	50%	0.045	0.114	0.036	0.109	0.034	0.110	0.032	0.106	0.030	0.093
	Avg	0.038	0.106	0.031	0.097	0.030	0.095	0.028	0.093	**0.026**	**0.088**
ETTh1	12.5%	0.100	0.208	0.085	0.185	0.087	0.186	0.080	0.180	0.074	0.179
	25%	0.120	0.238	0.116	0.222	0.106	0.221	0.103	0.207	0.082	0.190
	37.5%	0.118	0.234	0.118	0.227	0.100	0.206	0.103	0.209	0.100	0.205
	50%	0.140	0.241	0.133	0.235	0.137	0.240	0.130	0.232	0.123	0.230
	Avg	0.112	0.230	0.113	0.217	0.107	0.213	0.104	0.207	**0.095**	**0.201**
ETTh2	12.5%	0.061	0.158	0.061	0.158	0.057	0.151	0.054	0.146	0.051	0.138
	25%	0.066	0.161	0.058	0.153	0.059	0.155	0.058	0.154	0.055	0.146
	37.5%	0.065	0.158	0.070	0.164	0.067	0.160	0.059	0.155	0.059	0.152
	50%	0.068	0.164	0.073	0.167	0.068	0.166	0.066	0.161	0.064	0.157
	Avg	0.065	0.160	0.066	0.160	0.063	0.158	0.059	0.154	**0.057**	**0.148**
ECL	12.5%	0.046	0.123	0.039	0.123	0.039	0.123	0.038	0.123	0.037	0.122
	25%	0.046	0.148	0.049	0.140	0.048	0.139	0.047	0.139	0.046	0.139
	37.5%	0.062	0.168	0.063	0.163	0.062	0.161	0.060	0.161	0.060	0.160
	50%	0.076	0.181	0.076	0.182	0.075	0.182	0.076	0.183	0.075	0.181
	Avg	0.058	0.155	0.057	0.152	0.056	**0.151**	**0.055**	0.152	**0.055**	**0.151**
Weather	12.5%	0.029	0.044	0.030	0.046	0.025	0.036	0.026	0.038	0.025	0.035
	25%	0.038	0.054	0.030	0.044	0.036	0.052	0.029	0.042	0.027	0.037
	37.5%	0.038	0.058	0.037	0.057	0.034	0.052	0.032	0.045	0.029	0.039
	50%	0.040	0.057	0.036	0.054	0.036	0.052	0.034	0.046	0.032	0.042
	Avg	0.036	0.053	0.033	0.050	0.033	0.048	0.030	0.043	**0.028**	**0.038**
Average		0.058	0.138	0.057	0.132	0.055	0.131	0.052	0.128	**0.049**	**0.124**

Table 35: The full fine-tuning results of the time series classification task under different sizes of pre-training datasets. The brief results of this experiment are shown in Figure 7 (b). **Red**: best, Blue: second best.

Datasets	0B			1B			10B			25B			50B		
Metrics	P	R	F1	P	R	F1	P	R	F1	P	R	F1	P	R	F1
SMD	86.70	80.72	83.60	88.08	83.37	85.66	87.46	81.05	84.13	86.89	82.02	84.39	88.08	83.37	**85.66**
MSL	89.28	73.68	80.74	89.13	73.59	80.62	89.48	74.59	81.36	89.34	73.91	80.90	89.46	75.31	**81.77**
SMAP	89.97	54.16	67.61	90.06	53.56	67.17	90.08	54.51	67.92	90.11	54.63	68.02	91.06	61.51	**73.43**
SWaT	91.57	85.45	88.40	92.21	92.70	92.45	92.23	92.77	92.50	92.28	92.87	92.57	95.94	91.39	**93.61**
PSM	98.69	94.24	96.41	98.53	94.30	96.37	98.65	94.41	96.48	98.79	94.13	96.40	91.39	93.61	**98.90**
Avg.	91.24	77.65	83.40	91.60	79.50	84.45	91.58	79.47	84.48	91.48	79.51	84.46	95.36	97.10	**86.31**

NeurIPS Paper Checklist

1. **Claims**

   Question: Do the main claims made in the abstract and introduction accurately reflect the paper's contributions and scope?

   Answer: [Yes]

   Justification: We made our main claims in the abstract and introduction. We have clearly pointed out the problem to be solved and the method to be used in the abstract and introduction.

   Guidelines:

   - The answer NA means that the abstract and introduction do not include the claims made in the paper.
   - The abstract and/or introduction should clearly state the claims made, including the contributions made in the paper and important assumptions and limitations. A No or NA answer to this question will not be perceived well by the reviewers.
   - The claims made should match theoretical and experimental results, and reflect how much the results can be expected to generalize to other settings.
   - It is fine to include aspirational goals as motivation as long as it is clear that these goals are not attained by the paper.

2. **Limitations**

   Question: Does the paper discuss the limitations of the work performed by the authors?

   Answer: [Yes]

   Justification: The S^2 bimodal data generation mechanism is the core method and contribution of this paper. In Appendix B.9, we further explore the current limitations in this aspect and will try to improve it in subsequent work.

   Guidelines:

   - The answer NA means that the paper has no limitation while the answer No means that the paper has limitations, but those are not discussed in the paper.
   - The authors are encouraged to create a separate "Limitations" section in their paper.
   - The paper should point out any strong assumptions and how robust the results are to violations of these assumptions (e.g., independence assumptions, noiseless settings, model well-specification, asymptotic approximations only holding locally). The authors should reflect on how these assumptions might be violated in practice and what the implications would be.
   - The authors should reflect on the scope of the claims made, e.g., if the approach was only tested on a few datasets or with a few runs. In general, empirical results often depend on implicit assumptions, which should be articulated.
   - The authors should reflect on the factors that influence the performance of the approach. For example, a facial recognition algorithm may perform poorly when image resolution is low or images are taken in low lighting. Or a speech-to-text system might not be used reliably to provide closed captions for online lectures because it fails to handle technical jargon.
   - The authors should discuss the computational efficiency of the proposed algorithms and how they scale with dataset size.
   - If applicable, the authors should discuss possible limitations of their approach to address problems of privacy and fairness.
   - While the authors might fear that complete honesty about limitations might be used by reviewers as grounds for rejection, a worse outcome might be that reviewers discover limitations that aren't acknowledged in the paper. The authors should use their best judgment and recognize that individual actions in favor of transparency play an important role in developing norms that preserve the integrity of the community. Reviewers will be specifically instructed to not penalize honesty concerning limitations.

3. **Theory assumptions and proofs**

Question: For each theoretical result, does the paper provide the full set of assumptions and a complete (and correct) proof?

Answer: [Yes]

Justification: All the theorems, formulas, and proofs in the paper should be numbered and cross-referenced. The core ideas of this paper are further explained and proved by Takens's theorem and symbolic dynamics in the beginning Section 3.

Guidelines:

- The answer NA means that the paper does not include theoretical results.
- All the theorems, formulas, and proofs in the paper should be numbered and cross-referenced.
- All assumptions should be clearly stated or referenced in the statement of any theorems.
- The proofs can either appear in the main paper or the supplemental material, but if they appear in the supplemental material, the authors are encouraged to provide a short proof sketch to provide intuition.
- Inversely, any informal proof provided in the core of the paper should be complemented by formal proofs provided in appendix or supplemental material.
- Theorems and Lemmas that the proof relies upon should be properly referenced.

4. **Experimental result reproducibility**

   Question: Does the paper fully disclose all the information needed to reproduce the main experimental results of the paper to the extent that it affects the main claims and/or conclusions of the paper (regardless of whether the code and data are provided or not)?

   Answer: [Yes]

   Justification: We describe the proposed methodology in detail in Section 3 and provide further explanation in Appendix B. Experimental details are outlined in Appendix C. Additionally, all the code related to the proposed method is included in the supplementary material.

   Guidelines:

   - The answer NA means that the paper does not include experiments.
   - If the paper includes experiments, a No answer to this question will not be perceived well by the reviewers: Making the paper reproducible is important, regardless of whether the code and data are provided or not.
   - If the contribution is a dataset and/or model, the authors should describe the steps taken to make their results reproducible or verifiable.
   - Depending on the contribution, reproducibility can be accomplished in various ways. For example, if the contribution is a novel architecture, describing the architecture fully might suffice, or if the contribution is a specific model and empirical evaluation, it may be necessary to either make it possible for others to replicate the model with the same dataset, or provide access to the model. In general. releasing code and data is often one good way to accomplish this, but reproducibility can also be provided via detailed instructions for how to replicate the results, access to a hosted model (e.g., in the case of a large language model), releasing of a model checkpoint, or other means that are appropriate to the research performed.
   - While NeurIPS does not require releasing code, the conference does require all submissions to provide some reasonable avenue for reproducibility, which may depend on the nature of the contribution. For example
     (a) If the contribution is primarily a new algorithm, the paper should make it clear how to reproduce that algorithm.
     (b) If the contribution is primarily a new model architecture, the paper should describe the architecture clearly and fully.
     (c) If the contribution is a new model (e.g., a large language model), then there should either be a way to access this model for reproducing the results or a way to reproduce the model (e.g., with an open-source dataset or instructions for how to construct the dataset).

(d) We recognize that reproducibility may be tricky in some cases, in which case authors are welcome to describe the particular way they provide for reproducibility. In the case of closed-source models, it may be that access to the model is limited in some way (e.g., to registered users), but it should be possible for other researchers to have some path to reproducing or verifying the results.

5. **Open access to data and code**

   Question: Does the paper provide open access to the data and code, with sufficient instructions to faithfully reproduce the main experimental results, as described in supplemental material?

   Answer: [Yes]

   Justification: The code is available in the supplementary material.

   Guidelines:

   - The answer NA means that paper does not include experiments requiring code.
   - Please see the NeurIPS code and data submission guidelines (`https://nips.cc/public/guides/CodeSubmissionPolicy`) for more details.
   - While we encourage the release of code and data, we understand that this might not be possible, so "No" is an acceptable answer. Papers cannot be rejected simply for not including code, unless this is central to the contribution (e.g., for a new open-source benchmark).
   - The instructions should contain the exact command and environment needed to run to reproduce the results. See the NeurIPS code and data submission guidelines (`https://nips.cc/public/guides/CodeSubmissionPolicy`) for more details.
   - The authors should provide instructions on data access and preparation, including how to access the raw data, preprocessed data, intermediate data, and generated data, etc.
   - The authors should provide scripts to reproduce all experimental results for the new proposed method and baselines. If only a subset of experiments are reproducible, they should state which ones are omitted from the script and why.
   - At submission time, to preserve anonymity, the authors should release anonymized versions (if applicable).
   - Providing as much information as possible in supplemental material (appended to the paper) is recommended, but including URLs to data and code is permitted.

6. **Experimental setting/details**

   Question: Does the paper specify all the training and test details (e.g., data splits, hyperparameters, how they were chosen, type of optimizer, etc.) necessary to understand the results?

   Answer: [Yes]

   Justification: We describe the datasets used in detail in Appendix C.1, and further elaborate on the model pre-training and fine-tuning configurations for downstream tasks in Appendix C.4 and C.5.

   Guidelines:

   - The answer NA means that the paper does not include experiments.
   - The experimental setting should be presented in the core of the paper to a level of detail that is necessary to appreciate the results and make sense of them.
   - The full details can be provided either with the code, in appendix, or as supplemental material.

7. **Experiment statistical significance**

   Question: Does the paper report error bars suitably and correctly defined or other appropriate information about the statistical significance of the experiments?

   Answer: [Yes]

   Justification: In Section 4.4 we conducted multiple experiments in the ablation experiments and drew error bars in the bar graphs to further ensure the reliability of the ablation conclusions. However, due to the large number of experiments, detailed standard deviations are not shown. Instead, we uniformly present them in the headings of each table in Appendix F.

Guidelines:

- The answer NA means that the paper does not include experiments.
- The authors should answer "Yes" if the results are accompanied by error bars, confidence intervals, or statistical significance tests, at least for the experiments that support the main claims of the paper.
- The factors of variability that the error bars are capturing should be clearly stated (for example, train/test split, initialization, random drawing of some parameter, or overall run with given experimental conditions).
- The method for calculating the error bars should be explained (closed form formula, call to a library function, bootstrap, etc.)
- The assumptions made should be given (e.g., Normally distributed errors).
- It should be clear whether the error bar is the standard deviation or the standard error of the mean.
- It is OK to report 1-sigma error bars, but one should state it. The authors should preferably report a 2-sigma error bar than state that they have a 96% CI, if the hypothesis of Normality of errors is not verified.
- For asymmetric distributions, the authors should be careful not to show in tables or figures symmetric error bars that would yield results that are out of range (e.g. negative error rates).
- If error bars are reported in tables or plots, The authors should explain in the text how they were calculated and reference the corresponding figures or tables in the text.

8. **Experiments compute resources**

   Question: For each experiment, does the paper provide sufficient information on the computer resources (type of compute workers, memory, time of execution) needed to reproduce the experiments?

   Answer: [Yes]

   Justification: In Appendix C we describe the hardware environment in detail. Using the pre-trained configuration in Appendix C.4 on our eight A6000s is enough to fill the memory of all devices. The computing resources and memory required for fine-tuning the model are shown in Figure 5 (**right**).

   Guidelines:

   - The answer NA means that the paper does not include experiments.
   - The paper should indicate the type of compute workers CPU or GPU, internal cluster, or cloud provider, including relevant memory and storage.
   - The paper should provide the amount of compute required for each of the individual experimental runs as well as estimate the total compute.
   - The paper should disclose whether the full research project required more compute than the experiments reported in the paper (e.g., preliminary or failed experiments that didn't make it into the paper).

9. **Code of ethics**

   Question: Does the research conducted in the paper conform, in every respect, with the NeurIPS Code of Ethics `https://neurips.cc/public/EthicsGuidelines`?

   Answer: [Yes]

   Justification: We have read the NeurIPS Code of Ethics and conducted it in the paper conform in every respect.

   Guidelines:

   - The answer NA means that the authors have not reviewed the NeurIPS Code of Ethics.
   - If the authors answer No, they should explain the special circumstances that require a deviation from the Code of Ethics.
   - The authors should make sure to preserve anonymity (e.g., if there is a special consideration due to laws or regulations in their jurisdiction).

10. **Broader impacts**

Question: Does the paper discuss both potential positive societal impacts and negative societal impacts of the work performed?

Answer: [Yes]

Justification: We illustrate broader impacts of our research in Appendix G.

Guidelines:

- The answer NA means that there is no societal impact of the work performed.
- If the authors answer NA or No, they should explain why their work has no societal impact or why the paper does not address societal impact.
- Examples of negative societal impacts include potential malicious or unintended uses (e.g., disinformation, generating fake profiles, surveillance), fairness considerations (e.g., deployment of technologies that could make decisions that unfairly impact specific groups), privacy considerations, and security considerations.
- The conference expects that many papers will be foundational research and not tied to particular applications, let alone deployments. However, if there is a direct path to any negative applications, the authors should point it out. For example, it is legitimate to point out that an improvement in the quality of generative models could be used to generate deepfakes for disinformation. On the other hand, it is not needed to point out that a generic algorithm for optimizing neural networks could enable people to train models that generate Deepfakes faster.
- The authors should consider possible harms that could arise when the technology is being used as intended and functioning correctly, harms that could arise when the technology is being used as intended but gives incorrect results, and harms following from (intentional or unintentional) misuse of the technology.
- If there are negative societal impacts, the authors could also discuss possible mitigation strategies (e.g., gated release of models, providing defenses in addition to attacks, mechanisms for monitoring misuse, mechanisms to monitor how a system learns from feedback over time, improving the efficiency and accessibility of ML).

11. **Safeguards**

Question: Does the paper describe safeguards that have been put in place for responsible release of data or models that have a high risk for misuse (e.g., pretrained language models, image generators, or scraped datasets)?

Answer: [NA]

Justification: The paper poses no such risks.

Guidelines:

- The answer NA means that the paper poses no such risks.
- Released models that have a high risk for misuse or dual-use should be released with necessary safeguards to allow for controlled use of the model, for example by requiring that users adhere to usage guidelines or restrictions to access the model or implementing safety filters.
- Datasets that have been scraped from the Internet could pose safety risks. The authors should describe how they avoided releasing unsafe images.
- We recognize that providing effective safeguards is challenging, and many papers do not require this, but we encourage authors to take this into account and make a best faith effort.

12. **Licenses for existing assets**

Question: Are the creators or original owners of assets (e.g., code, data, models), used in the paper, properly credited and are the license and terms of use explicitly mentioned and properly respected?

Answer: [Yes]

Justification: The models compared and the datasets used in this article are open source, and the corresponding papers or web pages are cited.

Guidelines:

- The answer NA means that the paper does not use existing assets.
- The authors should cite the original paper that produced the code package or dataset.
- The authors should state which version of the asset is used and, if possible, include a URL.
- The name of the license (e.g., CC-BY 4.0) should be included for each asset.
- For scraped data from a particular source (e.g., website), the copyright and terms of service of that source should be provided.
- If assets are released, the license, copyright information, and terms of use in the package should be provided. For popular datasets, `paperswithcode.com/datasets` has curated licenses for some datasets. Their licensing guide can help determine the license of a dataset.
- For existing datasets that are re-packaged, both the original license and the license of the derived asset (if it has changed) should be provided.
- If this information is not available online, the authors are encouraged to reach out to the asset's creators.

13. **New assets**

    Question: Are new assets introduced in the paper well documented and is the documentation provided alongside the assets?

    Answer: [Yes]

    Justification: We provide the code for the proposed methodology in the supplementary material and will make it publicly available at an appropriate time.

    Guidelines:

    - The answer NA means that the paper does not release new assets.
    - Researchers should communicate the details of the dataset/code/model as part of their submissions via structured templates. This includes details about training, license, limitations, etc.
    - The paper should discuss whether and how consent was obtained from people whose asset is used.
    - At submission time, remember to anonymize your assets (if applicable). You can either create an anonymized URL or include an anonymized zip file.

14. **Crowdsourcing and research with human subjects**

    Question: For crowdsourcing experiments and research with human subjects, does the paper include the full text of instructions given to participants and screenshots, if applicable, as well as details about compensation (if any)?

    Answer: [NA]

    Justification: The paper does not involve crowdsourcing nor research with human subjects.

    Guidelines:

    - The answer NA means that the paper does not involve crowdsourcing nor research with human subjects.
    - Including this information in the supplemental material is fine, but if the main contribution of the paper involves human subjects, then as much detail as possible should be included in the main paper.
    - According to the NeurIPS Code of Ethics, workers involved in data collection, curation, or other labor should be paid at least the minimum wage in the country of the data collector.

15. **Institutional review board (IRB) approvals or equivalent for research with human subjects**

    Question: Does the paper describe potential risks incurred by study participants, whether such risks were disclosed to the subjects, and whether Institutional Review Board (IRB) approvals (or an equivalent approval/review based on the requirements of your country or institution) were obtained?

    Answer: [NA]

Justification: The paper does not involve crowdsourcing nor research with human subjects.

Guidelines:

- The answer NA means that the paper does not involve crowdsourcing nor research with human subjects.
- Depending on the country in which research is conducted, IRB approval (or equivalent) may be required for any human subjects research. If you obtained IRB approval, you should clearly state this in the paper.
- We recognize that the procedures for this may vary significantly between institutions and locations, and we expect authors to adhere to the NeurIPS Code of Ethics and the guidelines for their institution.
- For initial submissions, do not include any information that would break anonymity (if applicable), such as the institution conducting the review.

16. **Declaration of LLM usage**

Question: Does the paper describe the usage of LLMs if it is an important, original, or non-standard component of the core methods in this research? Note that if the LLM is used only for writing, editing, or formatting purposes and does not impact the core methodology, scientific rigorousness, or originality of the research, declaration is not required.

Answer: [NA]

Justification: The LLM does not affect the core methodology, scientific rigor or originality of the research.

Guidelines:

- The answer NA means that the core method development in this research does not involve LLMs as any important, original, or non-standard components.
- Please refer to our LLM policy (`https://neurips.cc/Conferences/2025/LLM`) for what should or should not be described.